Application of Factor Analysis in the Identification of a Geochemical Signature of Buried Kimberlites in Near-Surface Groundwaters in the Attawapiskat Area of the James Bay Lowlands of Northern Ontario, Canada

Marc Drouin, B.A.Sc.

A thesis submitted to the
Faculty of Graduate and Postdoctoral Studies
in partial fulfillment of the requirements for the
Master of Science Degree, in Earth Sciences

Ottawa-Carleton Geoscience Centre
Faculty of Science
University of Ottawa

Abstract

In the James Bay Lowlands of northern Ontario, kimberlite pipes are concealed by peat, thick layers of till, and Tyrell sea sediments. Studies have shown that buried ore bodies produce geochemical signatures in surface media. This thesis explores the geochemistry of near-surface groundwater above concealed kimberlite pipes using factor analysis to determine whether (1) a factor analysis can reveal an underlying structure (factors) in a multivariate groundwater geochemical dataset, and whether (2) those factors are related to the presence of concealed kimberlite. Factor analysis was performed on two datasets of near-surface groundwater, collected at 0.2 m and 1.1 m below ground surface in peat. Results revealed that (1) there is a significant difference in the behaviour of elements in groundwater near the surface compared to those in deeper groundwater, which is sheltered from the effects of the atmosphere; (2) for both datasets, the first factor is dominated by elements known to be enriched in kimberlite, notably rare earth elements (REE), U, Th, Ti – the composition of factor one is consistent with their derivation from kimberlite in a limestone background where such elements are in very low concentration; (3) high-valence and low-valence kimberlite indicator elements (KIE) are found separated into distinct factors suggesting that once released from the kimberlite after weathering, KIE are subjected to various geochemical processes to be differentiated as they migrate upward to the surface; and (4) Fe and Mn load on a factor distinct from other metals, suggesting that in this environment Fe-Mn-O-OH is not a significant controller of metal mobility in groundwater. Overall, this research has further highlighted the multivariate nature of geochemical processes in groundwater. Compared with previous work in geochemical exploration where often only univariate or bivariate statistics or single element profiles over concealed ore

bodies were used, this thesis has shown that factor analysis, as a multivariate data analysis technique, is a robust exploration tool, able to shed light on relevant geochemical processes hidden within geochemical datasets. This thesis shows that high-valence KIE, notably U,V, Th, Ti and the REE, as a group, are better indicators of the presence of kimberlites than other well-known KIE. Single element concentration profiles such as Ni or Cr (known KIE) show similar anomalies over a concealed kimberlite as a factor score profile for factor one (U, V, Th, Ti, REE, Ni) would; however, it is the peculiar assemblage of elements in factor one that makes it unique to kimberlites, a feature that can be used in future exploration work for concealed kimberlites in similar surficial environments, such as the Siberian wetlands. The results suggest that future geochemical exploration work involving groundwater should focus on the more stable groundwater located below the zone of oxidation, sheltered from the effects of the atmosphere.

Résumé

Les cheminées de kimberlite présentes dans la région des basses terres de la Baie James du nord de l'Ontario se trouvent enfouies sous d'épais dépôts de tourbe, de till et de sédiments de la mer de Tyrell. Des études antérieures ont démontré que les gisements enfouis génèrent une signature géochimique en surface. Dans le cadre de ce projet la composition géochimique de l'eau souterraine située près de la surface a été étudiée à l'aide de l'analyse factorielle afin de déterminer si, dans un premier temps, l'analyse factorielle pouvait identifier une structure latente (des facteurs) à l'intérieur des données géochimiques et deuxièmement, si ces facteurs pouvaient être associés à la présence de kimberlite enfouie. Une analyse factorielle a été réalisée sur deux séries de données géochimiques issues de l'analyse d'échantillons d'eau souterraine prélevés à 0.2m et 1.1m de profondeur dans la tourbe. Les résultats de l'analyse factorielle révèlent que 1) il existe une différence significative du comportement des éléments dans l'eau souterraine située près de la surface comparativement à l'eau plus profonde, située à l'abri des effets de l'atmosphère; 2) que pour les deux séries de données, le premier facteur est dominé principalement par des éléments connus comme étant enrichis dans la kimberlite, notamment les terres rares, l'uranium, le thorium, le titane. Une telle composition du premier facteur est cohérente avec une anomalie géochimique générée par une inclusion de kimberlite dans la roche mère composé de calcaire; que 3) les éléments indicateurs de kimberlite (EIK) de valence élevée sont séparés des EIK de valence moindre. Ce phénomène suggère que des processus géochimiques agissent pour séparer les éléments lors de leur migration vers la surface; et que 4) le fer et le manganèse apparaissent dans des facteurs distincts des autres métaux suggérant

que les oxyhydroxydes de fer ou de manganèse ne sont pas des contrôles significatifs de la mobilité des métaux dans cet environnement. De façon générale les travaux de cette recherche soulèvent la nature multivariée des processus géochimiques existant dans l'eau souterraine. Contrairement aux travaux antérieurs en exploration géochimique où seulement une analyse uni-variée, bi-variée ou la superposition de profils de concentration au-dessus des gisements ont été utilisés, les travaux de cette recherche ont démontré que l'analyse factorielle, un outil d'analyse multivariée, est beaucoup plus robuste pour mettre à jours les processus sous-jacents les données géochimiques. Concrètement, les résultats de cette recherche démontrent que, en tant que groupe, les EIK de valence élevée comme l'uranium, le vanadium, le thorium, le titane et les terres rares sont de meilleurs indicateurs de kimberlite relativement aux autre EIK. Même si des profils de concentration en nickel ou en chrome au-dessus d'une kimberlite enfouie montrent des anomalies similaires à celles démontrées par le profil des scores du premier facteur, c'est la combinaison des éléments du premier facteur qui la rend unique à la kimberlite et qui en fait une signature propre utile lors de travaux d'exploration géochimique dans des contextes similaires tel que les terres humides de Sibérie. Les travaux de recherche suggèrent qu'à l'avenir, lors de travaux d'exploration géochimique impliquant l'eau souterraine comme média, l'eau plus profonde, sous la zone d'oxydation et à l'abri des effets de l'atmosphère soit privilègiée.

Table of Contents

List of Figures

List of Tables

Acknowledgements

I would like to thank Dr Keiko Hatori and Dr Bahram Daneshfar for giving me the opportunity to work on this project. Thank you for your support and patience throughout this lengthy project. Not only have you been supportive and understanding, you have opened my eyes to a whole new field of interest.

This project would not have been possible without the field work carried out by others. Thanks to Kirsten Brauneder and Jamil Sader, Ph.D.

I also wish to thank my employer for giving me the time and latitude to pursue this endeavour.

Finally, I wish to extend very special thanks to my wife Kim who has been by my side throughout this lengthy process. You have tolerated me through the highs and the lows but have always been supportive of my decisions. Thank you.

1. Introduction

1.1 Diamond exploration in Canada

In Canada, before 1980, diamond exploration techniques consisted mainly of indicator mineral surveys, while geophysical methods were relegated to regional surveys of geophysical anomalies indicative of generalized kimberlite potential (Richardson, 1996).

Indicator mineral surveys utilize the distinctive mineralogy of kimberlites. These surveys involve identification of heavy minerals in streams and tills, determination of the chemistry of selected mineral grains (for example, garnet and ilmenite), and mapping of the concentration of those mineral grains over the survey area. For example, garnet with high Cr, Cr-rich clinopyroxene, and low-Ca and high-Mg ilmenite are associated with diamonds (McClenaghan, 1996; McClenaghan et al., 1999). By examining the trail of these minerals in till one can infer the location of the source kimberlite: the higher the concentration, the closer the kimberlite.

However, indicator mineral surveys have significant limitations, not the least of which is that dispersal trains can reach 1000 kilometres in length. Furthermore, indicator mineral surveys, which were initially developed in non-glaciated terrains, have proven to be subject to error in glaciated terrains, where surface sediments have been altered by multiple glacial flows (multiple directions) over the years, making it difficult to trace back to the source of indicator minerals (Kjarsgaard, 1996; Hattori, 2009; DiLabio, 1996).

Geophysical methods rely on the unusual geophysical signature of kimberlite (Keating, 1996). In Canada, after 1980, and more extensively after 1990 during the diamond rush, airborne magnetic and electro-magnetic methods have been successfully used for diamond exploration (Kjarsgaard, 1996). However, as with indicator mineral surveys, many

rocks, like ultramafic rocks and granites with a high content of magnetite, show similar geophysical signatures as kimberlite (Power et al., 2004).

In northern Ontario these issues in mineral prospecting are exacerbated by the concealment of kimberlite under thick layers of till, marine sediments and peat.

1.2 Geochemical exploration of buried ore bodies

There is ample evidence in the literature showing that buried ore bodies form geochemical anomalies at the surface (Levinson, 1980; Goldberg, 1997). To that effect, researchers have devised geochemical exploration techniques combined with sophisticated analysis techniques that enable explorers to detect anomalies in surface media (soil, sediments, peat, near-surface groundwater) that can reveal buried ore bodies (Cameron et al., 2004; Hamilton et al., 2004, and other authors referenced therein; Leybourne, 2007).

These exploration techniques rely on specialized leaching techniques to extract mobile phases of elements that are thought to have originated from the ore body and migrated to the surface (Goldberg, 1997). Such specialized leach techniques and improvements in inductively coupled plasma mass spectrometry technology allow geochemists to attain lower and lower detection limits, thus enabling the detection of anomalous concentrations of elements not previously possible. These advances also have increased the number of elements that can be included in the investigation (Cameron et al., 2004; Leybourne, 2007).

Field methodology generally consists of sampling surface media in a grid pattern over an area known to harbour a possible zone of mineralization. This approach presupposes that a zone of mineralization has been detected by a more general type of survey, such as a stream sediment survey (watershed) or an aerial geophysical survey (Levinson, 1980).

For example, studies conducted on B-horizon soil samples have shown anomalies of REE, Y, Ni and high field strength elements (HFSE) over the known sites of concealed kimberlites (Hattori et al., 2009). Similar studies conducted on peat have also shown anomalies of kimberlite pathfinder elements over concealed kimberlites (Hattori and Hamilton, 2008). More recently, studies by Sader and others (2010) on shallow groundwater (peat interstitial water) confirmed previous results of a kimberlite geochemical signature in surface media by Brauneder (2007).

1.3 The problem

Studies of surface media geochemistry for the purpose of exploration often rely solely on univariate or bivariate statistics (correlation of pairs of elements, relationship of elements with pH or Eh, etc.) or single element profiles to infer relationships with ore bodies. Furthermore, some studies have assumed an *a priori* knowledge of the geochemical processes occurring at the site and only explored the behaviour of those elements known to be associated with either the geochemical processes thought to occur at the site or the ore body.

Although the above described methodology gives insight into the behaviour of a particular element (or pairs of elements, or a ratio of two elements), in a given geochemical context (case-specific) they are seldom able to provide an overall, "big picture" view of the mechanisms governing the geochemistry in surface media in relation to the ore body.

1.4 The purpose

The purpose of this thesis is to explore the geochemistry of near-surface groundwater above concealed kimberlite using factor analysis in order to identify a geochemical signature associated with the presence of concealed kimberlite.

The hypothesis underlying this thesis is that (1) a factor analysis will reveal an underlying structure (factors) in a multivariate groundwater geochemical dataset, and that (2) the factors can be related to geochemical processes indicative of the presence of concealed kimberlite.

1.5 Factor analysis in geochemistry

Originally developed in the field of psychology, factor analysis is a computational technique that examines correlation between variables to identify an underlying structure (patterns of correlation) within a multivariate dataset. It also reduces the dataset to a set of factors fewer than the original number of variables that explain the overall behaviour of the dataset (Rummel, 1970; Jöreskog et al., 1976; Reimann et al., 2002).

The study of geological processes relies more often than not on multivariate datasets. Since it is impossible to efficiently study more than three variables simultaneously, geologists have developed and relied on multivariate analysis tools to study large multivariate datasets (Jöreskog et al., 1976).

With factor analysis, there is no *a priori* judgement as to what elements may be relevant. Instead, it is based solely on the information hidden within the datasets. Also, the methodology is insensitive to the geochemical context and therefore widely applicable.

In geochemistry, factor analysis has been used either to reduce large datasets into a more manageable and usable set of factors or to find hidden relationships between groups of elements within the data and their association with geological and environmental features, geochemical processes or human activity (anthropogenic contamination) (Berg et al., 1993; Buckley et al., 1995; Borovec, 1996; Davies, 1997; Kumru and Bakaç, 2002; Reimann et al.,

2002; Cameron and Hattori, 2003; Boruvka et al., 2005; Mil-Homens et al., 2009; Chen et al., 2010; Cheng and Chen, 2010; Prasanna et al., 2010;).

In exploration geochemistry, factor analysis has been used to evaluate the association of elements, or group of elements, with an area of mineralization or a geochemical process known to be associated with a mineralization. Closs and Nichol (1975) investigated the combined use of factor and regression analysis as a means of identifying the parameters contributing to the geochemical data of stream sediments in the Halls Bay area of east-central Newfoundland, Canada. Data exploration by univariate methods revealed some correlation between the stream sediment data and the regional geology. However, it was also observed that the geochemistry of the stream sediments was of mixed origin, i.e., from bedrock geology or areas of mineralization. In the study, factor analysis combined with regression analysis was not only able to identify relationships between elements that could be associated with regional geologic features but was also better able to identify areas of mineralization that were not apparent when examining the data with univariate methods (single element mapping) or factor analysis alone. Reis et al. (2009) used principal component analysis (PCA), a multivariate data reduction technique similar to factor analysis, to identify relationships between elements within a soil geochemical dataset collected in an area known to host a gold-tungsten mineralization in northwestern Portugal. When mapped, PCA results showed distinct association with known areas of mineralization and enabled the selection of a subset of the initial elements analyzed as a geochemical signature of the deposit. Mapping also revealed new areas favourable for future exploration work. In a study by Huelin et al. (2006), the composition of Fe-Mn oxide coatings on stream pebbles collected in four distinct stream environments (two near copper mines, one in an urban

setting and one in carbonate geology) in Newfoundland and Labrador, Canada, was investigated. Factor analysis performed on trace metal concentration adsorbed on the Fe-Mn oxide coatings show the relationships of elements with geologic environments and anthropogenic contamination, thus suggesting the potential of Fe-Mn coatings on pebbles as an exploration or environmental monitoring tool.

1.6 The rationale

The Attawapiskat area of the James Bay Lowlands offers an ideal backdrop against which to investigate the use of factor analysis in geochemical exploration of buried kimberlite, due to the geological environment offered by the relatively uniform background of the Attawapiskat limestone formation combined with the vast and undisturbed state of the surface wetlands (Hattori and Hamilton, 2008). Kimberlite are rocks rich in alkali metals, light rare earth elements, and incompatible and compatible elements, while in limestone, these elements appear in very low concentrations. In the uniform background of the limestone host rock, kimberlite pipes will present themselves as local geochemical anomalies. It is hoped that the factor analysis will reveal a multivariate structure representing the contrast between enriched and background levels.

2. Study Area

2.1 Site location

This study centres on a group of concealed kimberlite pipes known as Alpha, Golf, Yankee, and Zulu which are part of a cluster of 19 kimberlite pipes found approximately 100 km west of the village of Attawapiskat in the Hudson Bay Lowlands of northern Ontario, Canada (Figure 1, Figure 2). These kimberlites pipes are located on the same property as the Victor Mine (De Beers) currently in production.

The Hudson Bay Lowlands consists of a vast area of continuous flat-lying peatlands (wetlands) located south of Hudson Bay and southwest of James Bay in northern Ontario, Canada. The lowlands extend along the coast of James Bay and Hudson Bay from the Harricana and Nottaway rivers in Quebec to the east, to Churchill in Manitoba to the west. The lowlands extend inland for a distance of approximately 320 km at the widest extent (Sjörs, 1959).The Hudson Bay Lowlands are characterized by vast expanses of flat-lying and poorly drained peatlands: the world's third largest peatlands, after the West Siberian Lowlands and the Amazon River (Keddy, 2000).

Peatlands are peat-forming ecosystems where at least 30 cm of peat have accumulated (Shotyk, 1988). The topography, the climate made it possible for peat to accumulate in great thickness over the years.

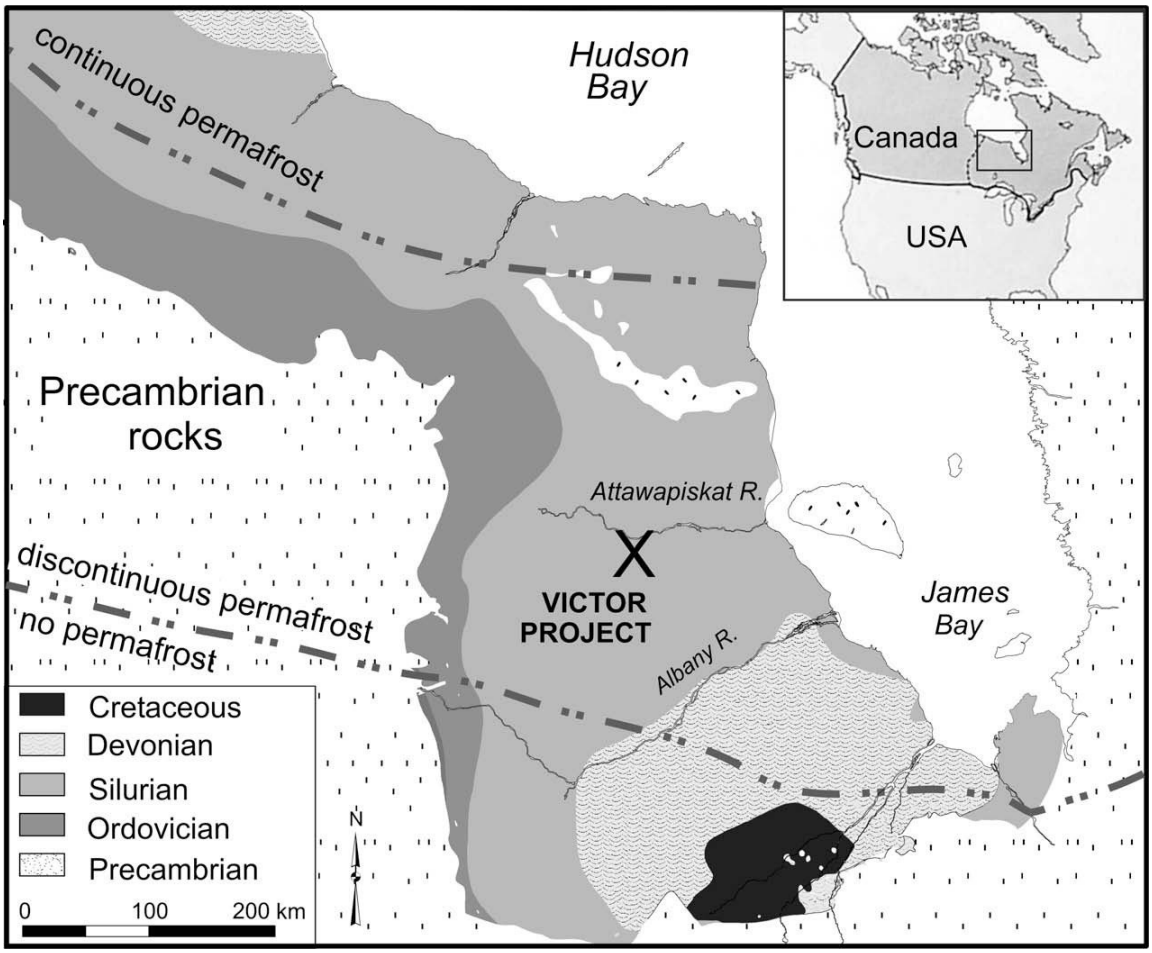

Figure 1: The location of the study area and geology of the James Bay Lowlands., 2004. Thick dash-dot lines show the boundaries between continuous permafrost, discontinuous permafrost, and no-permafrost areas. From Hattori and Hamilton, 2008, based on the Geological Map of Canada (Map 1860A), and maps in Fowler et al., 2001, and Webb et al., 2004. Victor Project indicates the area where the kimberlite pipes of this study are found.

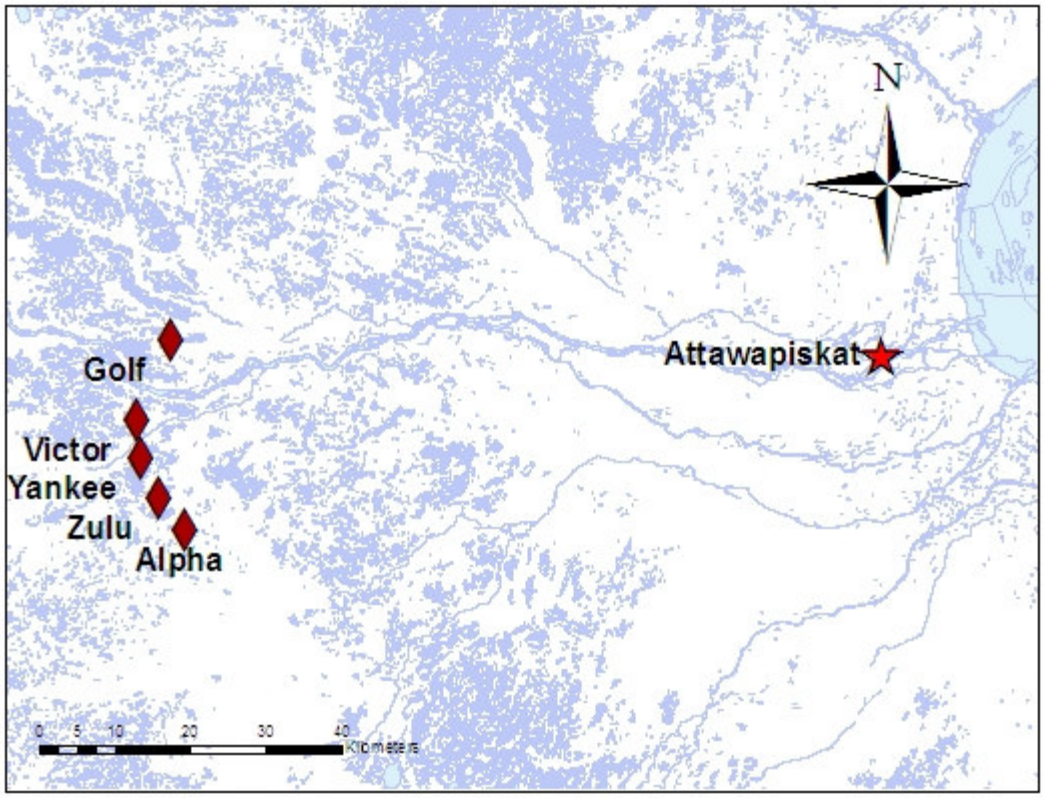

Figure 2: Location of Alpha, Golf, Yankee, Victor and Zulu, approximately 100 km west of the village of Attawapiskat, Ontario. Based on CanVec digital vector data (hydrography and city), Natural Resources Canada.

2.2 Topography and population

The topography of the area is extremely flat. Sjörs (1959) reported that the average slope of the lowlands is "4 feet to the mile" (less than 1:1000). The area is drained by four major rivers: the Albany, the Attawapiskat, the Winisk and the Severn. Between the rivers, the land is poorly drained and gives way to bogs and fens, characteristics of the lowlands.

There is little or no human activity in the lowlands. In the Kenora district the population density is approximately 0.2 persons/km. Economic activities are limited to the primary sector activities of mining and logging (Ontario Ministry of Northern Development, Mines and Forestry, 2011).

2.3 Climate

The study area lies within the zone of discontinuous permafrost. From the Canadian Climate Normals for 1971 to 2000 (Environment Canada 2010), the mean annual temperature recorded at Moosonee (World Meteorological Organization ID: 71836, 51° 16' 0.0''N, 80° 39' 0.0'') is -1.1°C. The coldest month is the month of January, with an average daily temperature of -20.7°C, and the warmest month is July, with an average daily temperature of 15.4°C. The annual average precipitation is 681.6 mm (493.9 mm rainfall, 212.9 mm snowfall).

2.4 Geology

The Hudson Bay Lowlands peatland lies in an extremely flat plain above the Attawapiskat limestone formation, a bioclastic limestone of the Middle Silurian. Along major rivers, the limestone formation exposes karst features (Cowell, 1983).

Approximately 170 Ma, kimberlite intruded the Ordovician and Silurian limestone (Webb et al., 2004) before being covered by quaternary deposits of glacial till reaching 30 m in thickness (Hattori and Hamilton, 2008).

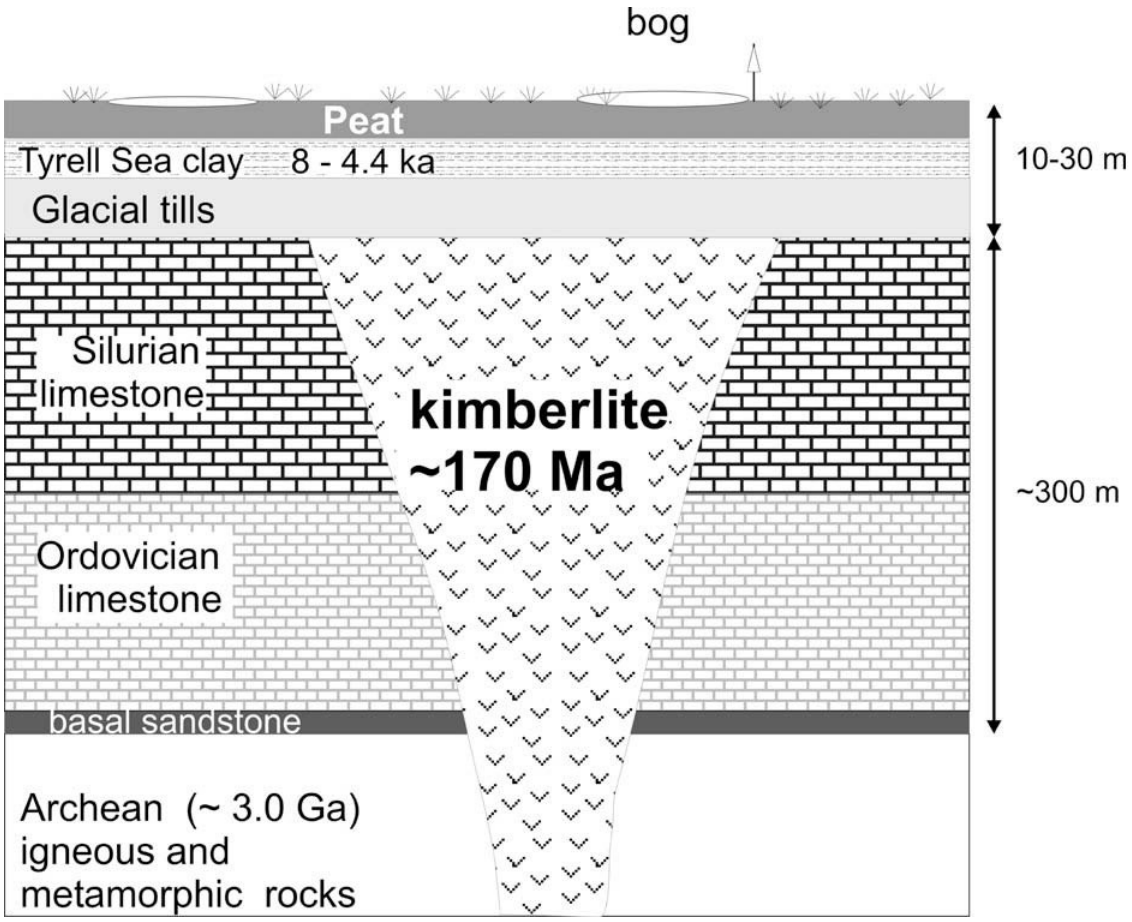

Figure 3: Diagram showing the vertical section of rocks hosting kimberlites and overburden in the study area. Kimberlites intruded Archean rocks and Paleozoic limestone beds at circa 170 Ma. The kimberlites are covered by Quaternary sediments, including tills and Tyrell Sea clayey sediments, the latter deposited 8–4.4 ka ago. From Hattori and Hamilton (2008), modified after Webb et al. (2004).

2.5 Kimberlite

Kimberlite is a rare ultramafic igneous rock originating from the upper mantle. It appears as dykes, sills and diatrems relatively small in size (Mitchell, 1986).

Geochemically, kimberlite is highly enriched with alkali metals, Zr, Hf, Ti, Sr, Ba, Pb, Nb, Ta, U, Th and light rare earth elements (LREE) compared to other rock. Kimberlite is also enriched in Cl, B, Mo, Y, B, Bi compared to ultramafic rock, but to a lesser extent (Dawson, 1980; McClenaghan and Kjarsgaard, 2007).

2.6 Data

The data used in this thesis are subsets of the data collected during a broad geochemical surface media study undertaken in 2006 and 2007 to investigate the geochemistry of surface media over concealed kimberlite (Brauneder, 2007; Hattori and Hamilton, 2008; Sader et al., 2010).

The datasets consist of composition data of groundwater samples collected approximately 0.2 and 1.1 metres below ground surface (BGS) along transects over concealed kimberlite pipes (Figures 4-7). For purposes of clarity these datasets will be referred to as the 0.2m BGS and the 1.1m BGS datasets throughout the rest of the text. The 0.2m BGS dataset consists of 53 samples of near-surface groundwater collected in the summer and fall of 2006 over Alpha (21 samples), Golf (17 samples) and Yankee (15 samples). The 1.1m BGS dataset is a collection of 37 groundwater samples, of which 16 samples were collected over Yankee and 21 over Zulu in 2007.

Groundwater samples were collected in small-diameter monitoring wells constructed of 19 mm inside-diameter polyvinyl chloride (PVC) tubing. The field procedure, sampling methodology and analytical programs are detailed in Brauneder (2007) and Sader et al. (2010). The analytical parameters selected to be included in the datasets are Al, Ba, Ca, Cd, Ce, Co, Cr, Cs, Fe, Ga, Li, Mg, Mn, Mo, Ni, Pb, Rb, Sb, Sn, Th, Ti, Tl, U, V, Y, Zn, Na, Si, K, pH, Eh. These parameters were selected because they were available for each site. Although all rare earth elements (REE) were available for all sites, Ce was chosen as a proxy variable to represent REE. The reason that Ce was selected as a proxy element for all REE will be described in detail in section 3.6.

The 0.2 m BGS and 1.1m BGS datasets are presented in Appendix A and Appendix B respectively.

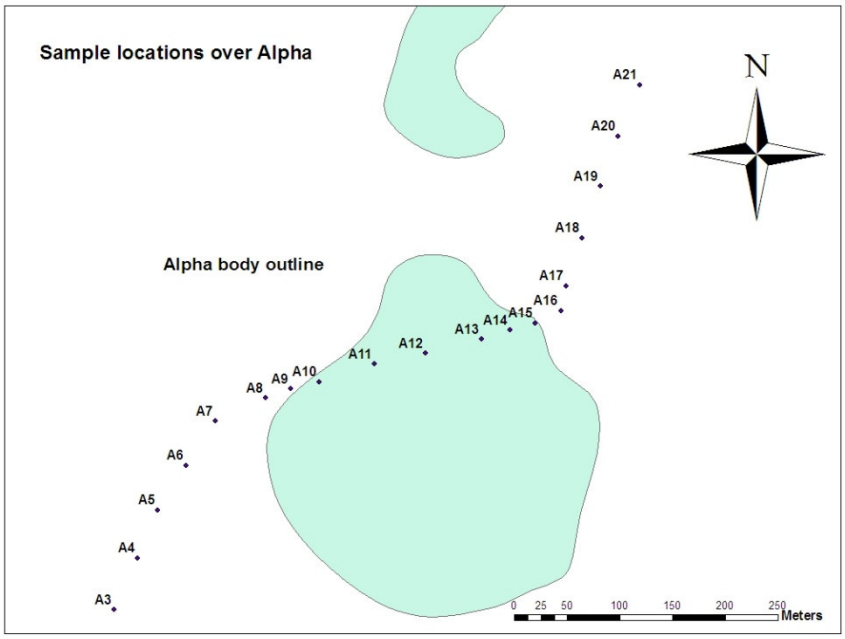

Figure 4: Groundwater sample locations over Alpha.

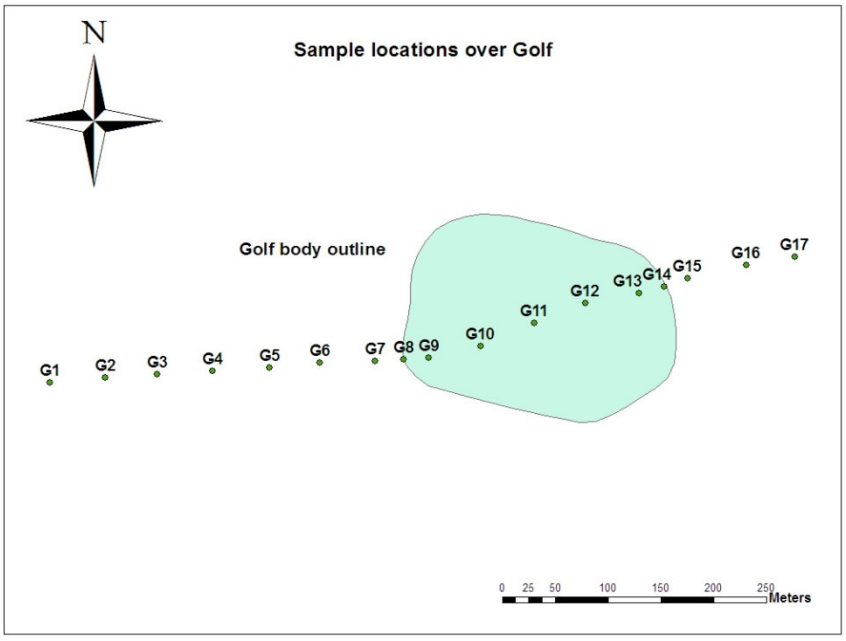

Figure 5: Groundwater sample locations over Golf.

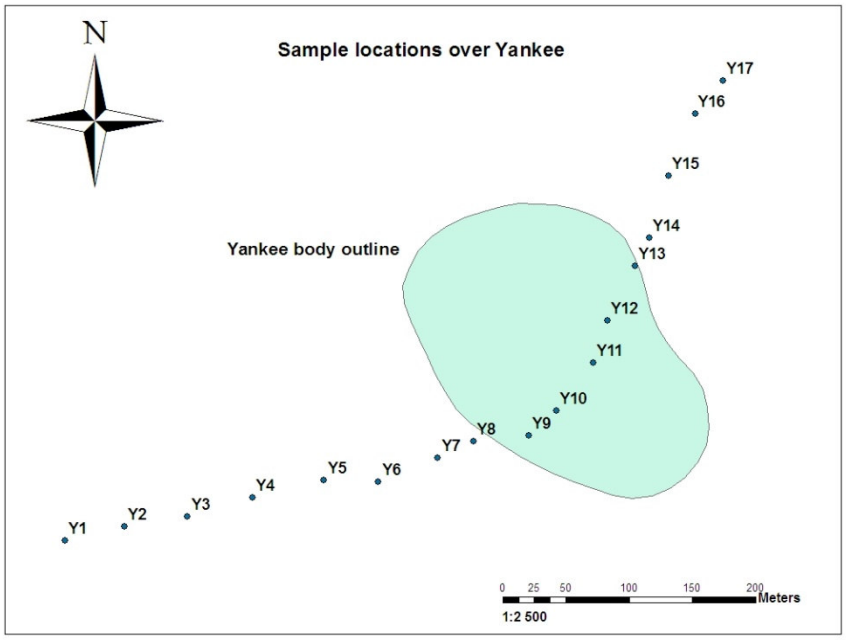

Figure 6: Groundwater sample locations over Yankee.

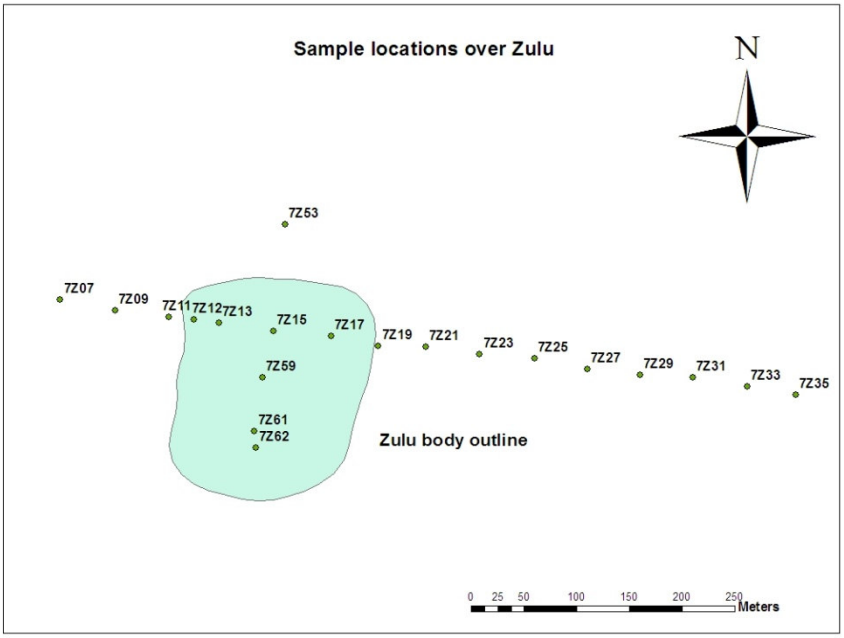

Figure 7: Groundwater sample locations over Zulu.

3. Data Exploration and Preparation

3.1 Introduction

Prior to any multivariate data analysis, the data should be examined for "defects" or any issues that might prevent the data lending itself to the multivariate data analysis technique. The issues surrounding the use of factor analysis in geochemistry have been discussed by Reimann et al. (2002).

Factor analysis makes several assumptions, not the least of which is that a certain amount of correlation between variables of the dataset must exist. Also, data "quality" issues must be addressed and meet minimum prerequisites prior to undertaking a factor analysis (i.e., treatment of compositional data, treatment of data with large differences in the amount of variation, non–normally distributed data, existence of outliers, data homogeneity, low sample-to-variable ratio, etc.) as they have the potential to affect the correlations between variables, a fundamental of factor analysis.

Although one should strive to attain the best dataset possible, a full data exploration as described in Reimann et al. (2002) is beyond the scope of this thesis. The data exploration and subsequent treatment process are detailed in the sections that follow.

3.2 Distribution and transformation

Several techniques exist to evaluate the distribution of a dataset. Methods like chi-square, Kolmogorov-Smirnov and Shapiro-Wilkes tests test the significance of the fit of the dataset to a normal distribution (Swan and Sandilands, 1995; Reimann and Filzmoser, 1999). Graphical methods like the normal probability plot (Normal QQ plot) are simple yet powerful techniques to subjectively evaluate the distribution of a variable (Swan and

Sandilands, 1995). A Normal QQ plot shows the quantiles of the observed values of a variable against the quantiles of the normal distribution. In this thesis the distribution of the data was evaluated using Normal QQ plots.

Normal QQ plots for each variable of the raw datasets are presented in Appendix C (0.2m BGS) and Appendix D (1.1m BGS).

The shape of the curve of the Normal QQ plots can reveal much about the distribution of the dataset. Normally distributed data would lie along the oblique line while positively skewed data would appear on the Normal QQ plot as a sharp steep slope transitioning to a flatter slope moving right. The flattening of the plot is attributed to the presence of extreme values at the right tail of the distribution. The sharpness in the transition from a steep to a flat section is also an indication of the degree of skewness in the data (Murdoch University, 2009).

The variables were generally found to be moderately to highly positively skewed with a few variables approaching normality. Sample Normal QQ plots are shown in Figures 8-10.

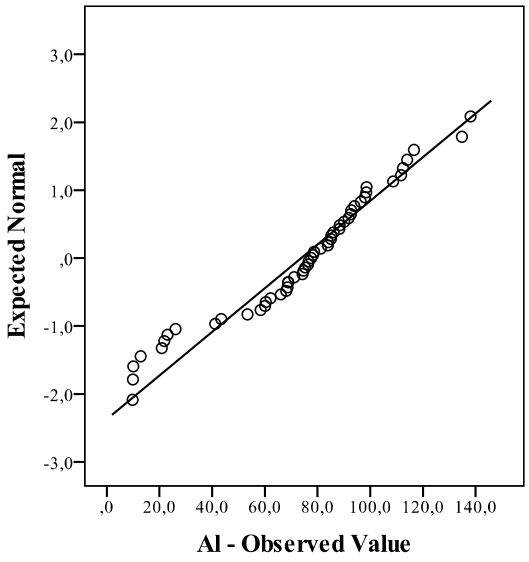

Figure 8: Example of an almost normally distributed variable – QQ plot Al (0.2m BGS).

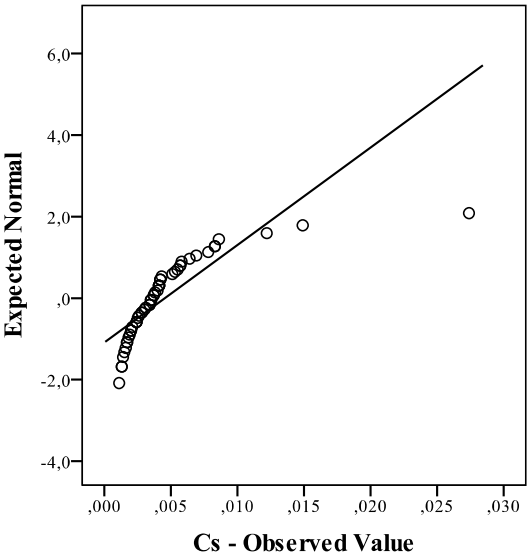

Figure 9: Example of a moderately positively skewed variable – QQ plot Cs (0.2m BGS).

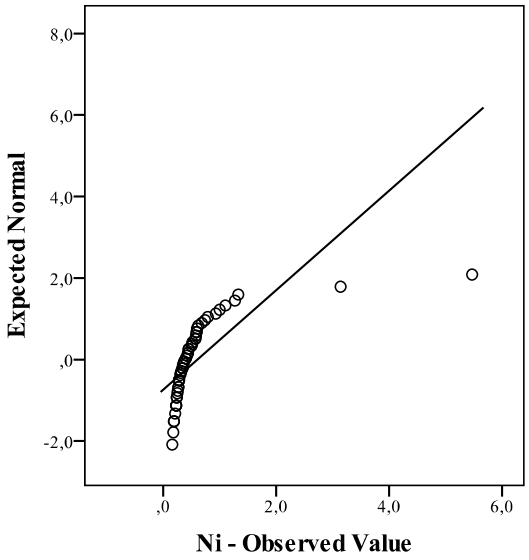

Figure 10: Example of a highly positively skewed variable with outlier – QQ plot Cs (0.2m BGS).

Geochemical and environmental data are seldom, if ever, normally distributed (Stanley, 2006). It has been the general consensus that a log transformation be applied to geochemical data to bring it as close as possible to a normal distribution.

From Figure 11, one can see the effects of log transformation on the variable Ni of the 0.2m BGS dataset. Although the transformed data does not lie perfectly on the oblique line as would a normally distributed variable there is a marked improvement, suggesting that Ni is near log-normally distributed. However one should note the presence of possible outliers at the extreme right affecting the distribution of the variable.

Some would argue that the outright application of the log transformation is not necessarily correct and call for a much more detailed study of the distribution and subsequent transformation (Reimann and Filzmoser, 1999). The plots shown in Figures 8-10 highlight the disparity in the distribution of geochemical data, almost normally distributed data in the case of Al (Figure 8), moderately skewed for Cs (Figure 9) and highly skewed for

Ni (Figure 10). When transforming variables, moderately skewed dataset may be over-transformed by a log transformation and may benefit from a softer transformation like the square root transformation, while a highly skewed dataset may benefit from an inverse transformation. That being said, a rigorous application of an alternative method of transformation such as Box-Cox is beyond the scope of this thesis. The log transformation was therefore applied to the datasets.

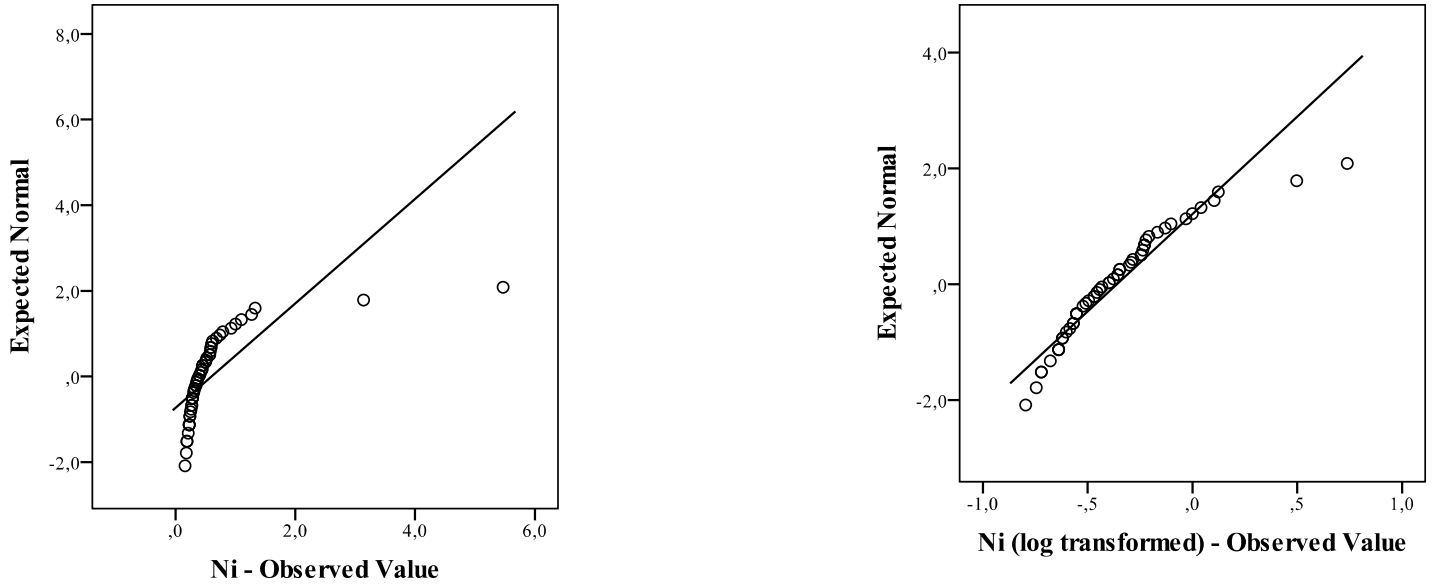

Figure 11: Example of QQ plots of Ni (0.2m BGS dataset) – raw and log-transformed.

3.3 Outlier detection and treatment

Outliers and extreme values are defined as statistical observations that are markedly different in value from the others of the sample (Merriam-Webster). Outliers are of concern in factor analysis in that they may unduly influence the correlation between variables, the fundamental concept behind factor analysis (Reimann et al., 2002; Hair et al., 2010).

Although in a multivariate setting one can revert to sophisticated techniques like the calculation of Mahalanobis distance to identify multivariate outliers, these techniques are beyond the scope of this thesis. Instead, the z-score values of the individual cases were used. For a sample size of less than 80, a z-score beyond ±2.5 is considered an outlier.

Because each site, i.e. kimberlite, is an independent sub-population of the data, z-scores were calculated from the log-transformed data for each site individually. Cases with z-scores above and below ±2.5 were identified as outliers. A sample is deemed a multivariate outlier if it registered as an outlier in a significant number of variables. As a supplementary check, the outliers were confirmed graphically by examining the normal QQ plots.

Table 1: Outliers

Site	Case	Variables
Alpha (0.2m BGS)	A14	Cd
	A18	Cr
	A16	Ni
	A9	Zn
Golf (0.2m BGS)	G5	Ba, Cs, Zn
	G8	Ni
	G16	Rb
	G17	Rb
Yankee (0.2m BGS)	Y9	Cr, Y, Zn
	Y11	Mg
	Y12	Mn
Yankee (1.1m BGS)	Y8	Ba, Ce, Co, Cr, Mn, Ni, Th, Ti, U, V, Y
	Y4	Cs
Zulu (1.1m BGS)	Z12C	Ba, Ni, U, V
	Z35	Cs

The second column of Table 1 lists all the cases that were determined as being outliers irrespective of the variable. The third column lists the variables where that particular case was determined as being an outlier.

Table 1 shows that samples Y8 (1.1m BGS) and Z12C (1.1m BGS) are outliers in 11 and 4 out of 25 variables respectively. The frequency of occurrence is such that these two variables are deemed outliers. The same can be said of samples Y9 (0.2m BGS) and G5 (0.2m BGS), but to a lesser extent. Other samples have been recorded as being outliers in only one variable.

After being identified as outliers, cases Y8 (1.1m BGS), Z12C (1.1m BGS), Y9 (0.2m BGS) and G5 (0.2m BGS) were removed from the dataset.

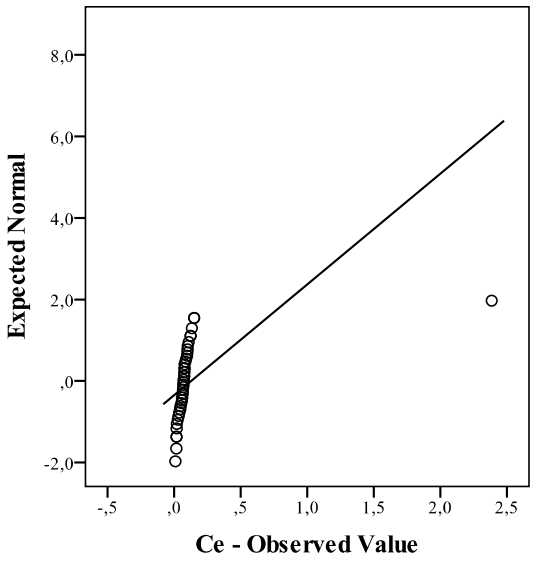

a)

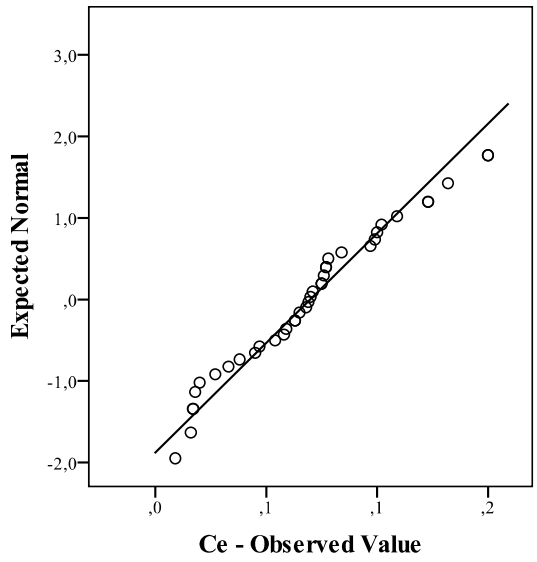

b)

Figure 12: QQ plots of Ce (1.1m BGS): a) raw data b) outlier removed.

3.4 Correlation and standardization

Scatter plots were examined to graphically assess the correlation between variables. The examination of scatter plots revealed possible multimodality in the datasets, a probable artifact of the sampling scheme. Multimodality can affect the correlation between variables by inducing spurious correlations (Davies, 1997).

Groundwater samples were collected over widely dispersed kimberlite pipes, giving rise to multiple sub-populations that, when combined in a single dataset of groundwater collected at a set depth, may have resulted in spurious correlations between variables.

The datasets were therefore standardized on a site-specific basis for each dataset. In Figure 13, a scatter plot of U vs Ce of the 0.2m BGS dataset shows the effects of having multiple sub-populations in a dataset. In the scatter plot of the raw data (Figure 13a), one can observe that the data from Alpha denoted by the circle symbol are grouped together near the upper right corner of the graph, whereas data from Golf and Yankee, denoted by crosses and boxes, are spread along the diagonal. In the scatter plots of the standardized data (Figure 13b) all the symbols are spread throughout the graph. After standardization the correlation coefficient (r) between U and Ce was reduced from 0.85, significant at the 0.01 level ($r=0.85$, $p<0.01$) to 0.72 significant at the 0.01 level ($r=0.72$, $p<0.01$).

The peculiar behaviour of the data from Alpha compared to the data from Golf and Yankee may also be the result of the sampling scheme over Alpha. Whereas the transect over Yankee and Golf extends some distance outside the boundary of the kimberlite (Figure 5 and Figure 6), the transect over Alpha does not terminate as far away from the boundary of the kimberlite body due to the two lobes of Alpha.

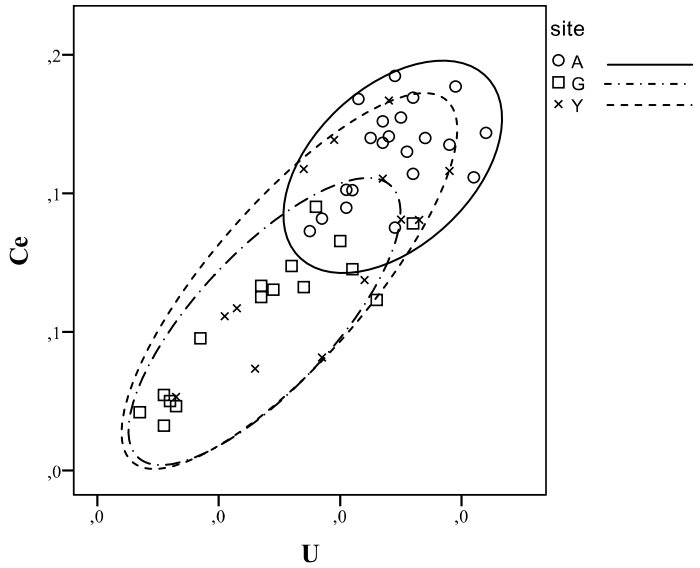

a) r=0.85; p< 0.01

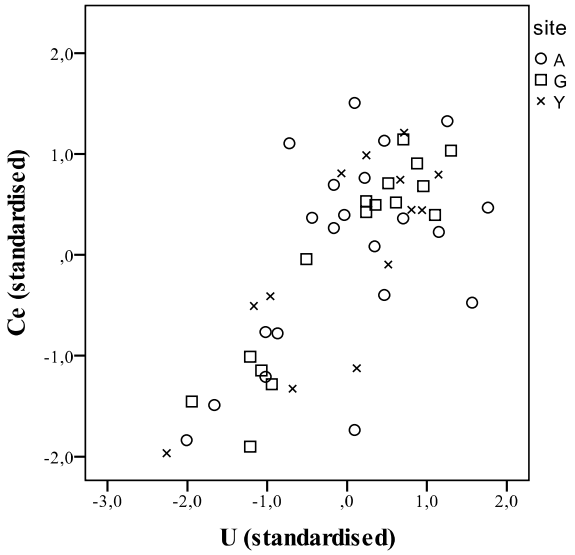

b) r=0.720; p<0.01

Figure 13: Scatter plot of U and Ce showing effects of multimodality on correlation. In figure a), data from Alpha is grouped together near the upper right corner of the graph (solid ellipse), whereas data from Golf and Yankee are spread wider along the diagonal (dash-dot and dash ellipse respectively). In figure b) the standardized data from each kimberlite are spread evenly along the scale.

3.5 Non-detected values

Non-detected (ND) values are typical in geochemical datasets. One recognized practice is to transform the ND values to one-half the analytical method detection limit. The dataset was examined for ND values. In the 0.2m BGS dataset, K has 22 non-detected values out of 53 samples and 5 out of 53 for Rb. Similarly, in the 1.1m BGS dataset, K has 14 non-detected values out of 37, 6 for Ni and 2 for Ti.

A high number of non-detected values in a dataset can greatly affect the correlation between variables by inducing spurious correlations (Swan and Sandilands, 1995). Authors have observed that variables with more than 25% of non-detected values should be removed from the analysis (Reimann and Filzmoser, 1999; Reimann et al., 2002). Potassium with 42% non-detected values, was therefore removed from both datasets.

3.6 Multicollinearity

During the data exploration process it was found that all rare earth elements (REE) correlated strongly which translated itself into issues of multicollinearity in the correlation matrix (too much correlation, since 15 of a total of 46 variables were highly correlated) overshadowing (hiding) other relevant correlations. Furthermore, in the initial factor analysis trials, all REE were found to fall into factor one. To resolve this issue of multicollnearity, Ce was chosen as a proxy to represent all REE.

3.7 Discussion and conclusion

Early in the study it was found that the datasets were less than ideal for a factor analysis. However, as will be discussed in later chapters, the datasets still presented with data qualities that could lend themselves to a factor analysis (significant correlation between some variables). Furthermore, in this project, factor analysis was used as a way of examining

a multivariate dataset for hidden meaning that could not be found by univariate methods. It was not to disprove or prove any specific theories, but to find hidden meaning and guide further investigations.

That being said, some steps were taken to ensure that the dataset still met some minimum requirements. Outliers were removed so as to not cause spurious correlation. Because the (kimberlite) sites are widely dispersed, they have the potential to induce multimodality in the datasets. The data from the individual sites were therefore standardized. Furthermore, variables with large numbers of non-detected values were removed from the dataset. The resulting normal QQ plots for the processed 0.2m BGS and 1.1m BGS datasets are presented in Appendix E and Appendix F.

4. Results and Discussion

This section presents and discusses the results of the factor analysis in terms of the factoring process and its limitations. In the second part of this section, the factor solutions for both datasets are interpreted and discussed in terms of geochemical processes occurring in near-surface groundwater in the context of geochemical exploration for buried kimberlite.

4.1 Factor analysis

Factor analysis was performed using IBM™ SPSS Statistics 18 software package. The correlation coefficient matrix of the processed datasets was used as the input for the factor analysis. Principal component analysis was used to extract factors and the Kaiser criterion was used as the factor retention criterion (eigenvalue greater than 1.0). The number of extracted factors was corroborated by examination of the scree plot. The factor solution was rotated using the Varimax method to enhance the factor solution prior to interpretation (Davis, 2002; Hair, 2010)

Because of the different units involved in the input data (log-ppm for metal concentration, pH units and mV for Eh), the correlation matrix was used instead of the covariance. The correlation matrix has the effect of standardizing the data into "unitless" variables.

4.1.1Correlation

Factor analysis is based on the fundamental concept that there exists a certain amount of correlation between pairs of variables in a large multivariate dataset (Jöreskog et al., 1976; Davis, 2002; Reimann et al., 2002).

Upon entering into a factor analysis one has to examine the correlation matrix for the presence of sufficient intercorrelations between variables to warrant proceeding with the analysis. The correlation matrices, which contain the Pearson's correlation coefficient for each pair of variables of both datasets, are presented in Tables 2 and 4. The one-tailed significance matrices of the correlation coefficients are presented in Tables 3 and 5.

Table 2: Correlation Matrix – 0.2m BGS dataset

	pH	Eh	Al	Ba	Ca	Ce	Co	Cr	Cs	Fe	Mg	Mn	Ni	Pb	Rb	Sr	Th	Ti	U	V	Y	Zn
pH	1.00																					
Eh	**-.88**	1.00																				
Al	**-.62**	**.55**	1.00																			
Ba	**-.35**	**.38**	**.47**	1.00																		
Ca	**.64**	**-.63**	**-.54**	-.14	1.00																	
Ce	**-.58**	**.55**	**.81**	**.52**	**-.58**	1.00																
Co	.02	-.07	.02	.23	.31	.08	1.00															
Cr	.00	.05	.06	**.72**	.21	.24	**.34**	1.00														
Cs	-.31	**.39**	**.44**	.25	-.24	**.46**	.22	.03	1.00													
Fe	.11	-.29	-.03	.10	**.44**	-.09	**.44**	.16	-.09	1.00												
Mg	**.47**	**-.51**	-.31	-.11	**.77**	**-.36**	**.40**	.22	**-.37**	**.59**	1.00											
Mn	.28	**-.30**	**-.38**	-.19	.24	-.21	.28	-.15	.07	.12	.16	1.00										
Ni	-.01	.05	.11	.04	.14	.22	**.43**	.13	**.59**	.15	.19	.26	1.00									
Pb	-.09	.11	.20	.24	.00	**.49**	.09	.13	.28	.01	-.02	.07	**.48**	1.00								
Rb	**-.47**	**.45**	**.70**	**.37**	**-.38**	**.66**	.15	.07	**.58**	-.03	-.27	-.11	**.34**	**.48**	1.00							
Sr	**.58**	**-.55**	**-.40**	.10	**.88**	**-.37**	**.38**	**.40**	-.28	**.42**	**.73**	.22	.06	.04	-.28	1.00						
Th	**-.60**	**.58**	**.79**	**.30**	**-.68**	**.71**	-.08	-.08	**.50**	-.28	**-.58**	**-.34**	.05	.20	**.66**	**-.61**	1.00					
Ti	**-.59**	**.57**	**.90**	**.35**	**-.50**	**.67**	.06	.03	**.54**	-.09	-.32	**-.39**	.15	.07	**.65**	**-.43**	**.76**	1.00				
U	**-.56**	**.58**	**.80**	**.45**	**-.56**	**.72**	.11	.11	**.50**	-.28	**-.46**	-.30	.11	.21	**.66**	**-.40**	**.87**	**.81**	1.00			
V	**-.56**	**.56**	**.60**	**.45**	**-.55**	**.74**	.08	.21	**.40**	-.02	**-.37**	-.16	.18	**.43**	**.64**	**-.46**	**.57**	**.50**	**.59**	1.00		
Y	**-.53**	**.53**	**.67**	**.82**	**-.38**	**.84**	.25	**.56**	**.39**	.09	-.22	-.16	.20	**.39**	**.56**	-.14	**.47**	**.53**	**.58**	**.72**	1.00	
Zn	.06	.02	.14	**.68**	.18	.13	**.34**	**.61**	-.05	.08	.11	-.03	-.07	.03	.05	**.49**	-.01	.05	.26	-.06	.39	1.00

Note: Significant correlations are in bold.

Table 3: Significance Matrix (single-tailed) – 0.2m BGS dataset

	pH	Eh	Al	Ba	Ca	Ce	Co	Cr	Cs	Fe	Mg	Mn	Ni	Pb	Rb	Sr	Th	Ti	U	V	Y	Zn
pH																						
Eh	.000																					
Al	.000	.000																				
Ba	.006	.003	.000																			
Ca	.000	.000	.000	.170																		
Ce	.000	.000	.000	.000	.000																	
Co	.447	.307	.453	.053	.013	.297																
Cr	.500	.354	.328	.000	.070	.049	.007															
Cs	.014	.003	.001	.040	.045	.000	.061	.431														
Fe	.218	.022	.429	.242	.001	.268	.001	.140	.272													
Mg	.000	.000	.015	.216	.000	.005	.002	.063	.004	.000												
Mn	.025	.017	.004	.092	.049	.073	.023	.149	.303	.210	.139											
Ni	.482	.355	.231	.397	.161	.059	.001	.187	.000	.148	.098	.036										
Pb	.270	.214	.081	.048	.495	.000	.271	.184	.025	.478	.443	.303	.000									
Rb	.000	.001	.000	.004	.003	.000	.146	.315	.000	.418	.029	.222	.008	.000								
Sr	.000	.000	.002	.236	.000	.004	.003	.002	.023	.001	.000	.062	.334	.395	.023							
Th	.000	.000	.000	.017	.000	.000	.297	.284	.000	.024	.000	.007	.356	.083	.000	.000						
Ti	.000	.000	.000	.007	.000	.000	.349	.429	.000	.260	.012	.003	.145	.322	.000	.001	.000					
U	.000	.000	.000	.000	.000	.000	.228	.221	.000	.023	.000	.017	.216	.071	.000	.002	.000	.000				
V	.000	.000	.000	.000	.000	.000	.286	.073	.002	.435	.004	.141	.105	.001	.000	.000	.000	.000	.000			
Y	.000	.000	.000	.000	.003	.000	.039	.000	.002	.259	.063	.136	.085	.002	.000	.158	.000	.000	.000	.000		
Zn	.348	.449	.161	.000	.106	.179	.008	.000	.357	.282	.224	.421	.304	.430	.362	.000	.478	.363	.035	.350	.003	

Table 4: Correlation Matrix – 1.1m BGS dataset

.

	pH	Eh	Al	Ba	Ca	Ce	Co	Cr	Cs	Fe	Mg	Mn	Ni	Pb	Rb	Sr	Th	Ti	U	V	Y	Zn
pH	1.00																					
Eh	-.25	1.00																				
Al	**-.50**	**.65**	1.00																			
Ba	**.47**	**-.67**	**-.60**	1.00																		
Ca	.23	-.35	-.34	.36	1.00																	
Ce	-.17	.30	**.72**	-.26	-.23	1.00																
Co	**.43**	-.37	**-.55**	**.68**	.19	-.32	1.00															
Cr	-.37	.27	**.60**	-.28	-.27	**.57**	**-.58**	1.00														
Cs	-.16	.09	.07	.02	.06	-.10	-.07	.31	1.00													
Fe	.29	-.36	**-.58**	.34	**.57**	**-.47**	.26	**-.41**	.01	1.00												
Mg	.10	-.33	-.31	.34	**.82**	-.24	.12	-.18	-.03	**.54**	1.00											
Mn	.29	-.26	**-.53**	**.40**	**.74**	-.42	.23	-.34	-.08	**.65**	**.64**	1.00										
Ni	-.05	.13	**.40**	.01	-.19	**.74**	-.13	**.47**	-.03	-.25	-.07	-.37	1.00									
Pb	-.30	**.56**	**.67**	-.25	-.24	**.59**	-.23	**.58**	.23	-.38	-.19	-.35	**.50**	1.00								
Rb	.23	-.30	-.27	.36	.20	-.23	.33	-.02	**.70**	.36	.07	.06	-.19	-.11	1.00							
Sr	**.62**	**-.65**	**-.76**	**.79**	**.44**	-.30	**.74**	**-.65**	-.19	**.51**	.33	**.50**	-.11	**-.53**	.30	1.00						
Th	-.10	.05	**.41**	-.02	-.17	**.65**	-.35	**.61**	-.13	**-.41**	-.30	-.23	**.53**	.34	-.30	-.23	1.00					
Ti	-.23	.25	**.65**	-.20	-.29	**.73**	-.34	**.60**	.00	**-.51**	**-.42**	**-.42**	**.51**	.36	-.21	-.33	**.79**	1.00				
U	-.06	.11	**.46**	-.06	-.31	**.81**	-.19	**.53**	-.17	**-.49**	-.28	**-.47**	**.74**	.38	-.23	-.17	**.79**	**.71**	1.00			
V	-.19	.20	**.59**	-.23	-.23	**.84**	**-.42**	**.55**	-.20	**-.41**	-.22	-.35	**.69**	.35	-.36	-.30	**.69**	**.72**	**.78**	1.00		
Y	-.08	.28	**.54**	-.20	-.27	**.90**	-.20	**.43**	-.24	**-.40**	-.28	**-.41**	**.75**	**.48**	-.30	-.16	**.67**	**.70**	**.84**	**.83**	1.00	
Zn	-.21	.24	.30	-.06	-.26	.28	-.13	**.61**	**.44**	-.31	-.11	-.33	.25	**.60**	.21	**-.44**	.19	.10	.23	.09	.18	1.00

Note: Significant correlations are in bold.

Table 5: Significance Matrix (single -tailed) – 1.1m BGS dataset

	pH	Eh	Al	Ba	Ca	Ce	Co	Cr	Cs	Fe	Mg	Mn	Ni	Pb	Rb	Sr	Th	Ti	U	V	Y	Zn
pH																						
Eh	.074																					
Al	.001	.000																				
Ba	.002	.000	.000																			
Ca	.093	.019	.020	.015																		
Ce	.165	.035	.000	.060	.090																	
Co	.005	.012	.000	.000	.130	.029																
Cr	.013	.057	.000	.051	.059	.000	.000															
Cs	.183	.308	.332	.461	.366	.279	.335	.031														
Fe	.046	.015	.000	.021	.000	.002	.063	.006	.487													
Mg	.276	.025	.031	.020	.000	.082	.238	.143	.430	.000												
Mn	.045	.063	.000	.008	.000	.005	.086	.023	.328	.000	.000											
Ni	.393	.222	.008	.485	.131	.000	.228	.002	.426	.070	.346	.014										
Pb	.040	.000	.000	.072	.075	.000	.086	.000	.088	.011	.127	.020	.001									
Rb	.085	.039	.059	.015	.117	.090	.025	.458	.000	.015	.333	.369	.130	.266								
Sr	.000	.000	.000	.000	.003	.036	.000	.000	.133	.001	.026	.001	.270	.001	.037							
Th	.282	.376	.006	.464	.156	.000	.018	.000	.218	.007	.039	.091	.000	.022	.040	.086						
Ti	.084	.074	.000	.117	.043	.000	.020	.000	.489	.001	.006	.006	.001	.015	.108	.026	.000					
U	.368	.270	.002	.374	.033	.000	.129	.000	.165	.001	.051	.002	.000	.012	.087	.165	.000	.000				
V	.136	.122	.000	.084	.089	.000	.006	.000	.122	.006	.096	.018	.000	.018	.016	.036	.000	.000	.000			
Y	.332	.052	.000	.117	.056	.000	.127	.005	.078	.008	.047	.007	.000	.001	.035	.170	.000	.000	.000	.000		
Zn	.115	.081	.039	.365	.065	.049	.228	.000	.004	.035	.263	.023	.075	.000	.113	.004	.138	.273	.087	.301	.152	

Visual examination of the correlation and significance matrices shows that there are a number of significant correlations at the 0.01 level (in bold) (Hair et al., 2010).

The Kaiser-Meyer-Olkin (KMO) measure of sampling adequacy and Bartlett's test of sphericity were also performed on the correlation matrix to test for the amount of intercorrelations between variables.

The first method is a measure of the amount of intercorrelation between variables. KMO values range from 0 to 1.0, with 1.0 being the case where each variable can be represented by a linear combination of all the other variables. A value of 0.5 is the minimum acceptable value suitable for factor analysis (Hair et al., 2010).

The second method is a statistical test to determine whether the correlation matrix is significantly different from an identity matrix (ones on the diagonal and zeros elsewhere); that is, a matrix where each variable is perfectly correlated with itself and the other pairs of variables are uncorrelated. If the test fails, there exists some correlation amongst some pairs of variables (Hair et al., 2010).

Table 6: KMO measure of sampling adequacy

Dataset	KMO
0.2m BGS	0.743
1.1m BGS	0.639

Table 7: Bartlett's test of sphericity

Dataset	Chi square	Degree of freedom	Significance
0.2m BGS	1089.898	231	0.000
1.1m BGS	782.570	231	0.000

KMO values of 0.743 for the 0.2m BGS dataset and 0.639 for the 1.1m BGS dataset are qualitatively considered middling and mediocre (as opposed to meritorious for KMO values greater than 0.8). At these levels, one should expect a fair amount of variance to be accounted for after factor analysis, but not a substantial amount (Hair et al., 2010).

The results of Bartlett's test of sphericity show that the test failed at the 0.05 level of significance for both datasets. The correlation matrices are therefore significantly different from an identity matrix; i.e., there exists some correlation between pairs of variables.

These preliminary results indicate that there was enough correlation among variables to warrant proceeding with the factor analysis.

4.1.2 Factor extraction results

Tables 8-11 show the number of factors extracted from the 0.2m BGS and 1.1m BGS datasets (initial and rotated solutions), respectively.

For the 1.1m BGS dataset (rotated solution), five factors account for 80% of the total variance, with 28.2% for factor one, 17.6% for factor two, 14.7% for factor three, 10.5% for factor four and 9.2% for factor five. Although five factors were extracted, the first three account for the bulk (approximately 60%) of the variance in the dataset. For the 0.2m BGS dataset (rotated solution), six factors account for 83% of the total variance, with 23% for factor one, 18% for factor two, 14.4% for factor three, 10.3% for factor four, 8.8% for factor five and 8.6% for factor six. Although six factors were extracted, the first three account for the bulk (approximately 55%) of the variance in the dataset.

The extraction results based on the Kaiser criterion were corroborated with the scree plots of each factor extraction results. The scree plots are presented in Figure 14 and Figure 15.

Overall, the factor solutions are able to reproduce a significant amount of the variance in the datasets. With five or six factors, the solutions were able to extract more than 80% of the variance in the system. Furthermore, in both solutions the first few factors account, by themselves, for more than 50% of the variance.

Table 8: Extracted components for the 1.1m BGS dataset

Total Variance Explained

	Initial Eigenvalues			Extraction Sums of Squared Loadings		
Component	Total	% of Variance	Cumulative %	Total	% of Variance	Cumulative %
1	8.96	40.72	40.7	8.96	40.72	40.7
2	3.30	14.99	55.7	3.30	14.99	55.7
3	2.29	10.39	66.1	2.39	10.39	66.1
4	1.94	8.81	74.9	1.94	8.81	74.9
5	1.14	5.18	80.1	1.14	5.18	80.1
6	.86	3.93	84.0			
7	.72	3.26	87.3			
8	.64	2.89	90.2			
9	.46	2.09	92.2			
10	.34	1.56	93.8			
11	.27	1.24	95.0			
12	.24	1.07	96.1			
13	.22	.98	97.1			
14	.15	.68	97.8			
15	.13	.59	98.4			
16	.12	.54	98.9			
17	.09	.40	99.3			
18	.06	.27	99.6			
19	.04	.20	99.8			
20	.02	.11	99.9			
21	.02	.07	99.9			
22	.01	.04	100.000			

Table 9: Extracted components for the 1.1m BGS dataset – Rotated solution (Varimax)

Total Variance Explained

	Rotation Sums of Squared Loadings		
Component	Total	% of Variance	Cumulative %
1	6.19	28.16	28.16
2	3.87	17.61	45.76
3	3.23	14.68	60.44
4	2.30	10.47	70.91
5	2.02	9.18	80.08

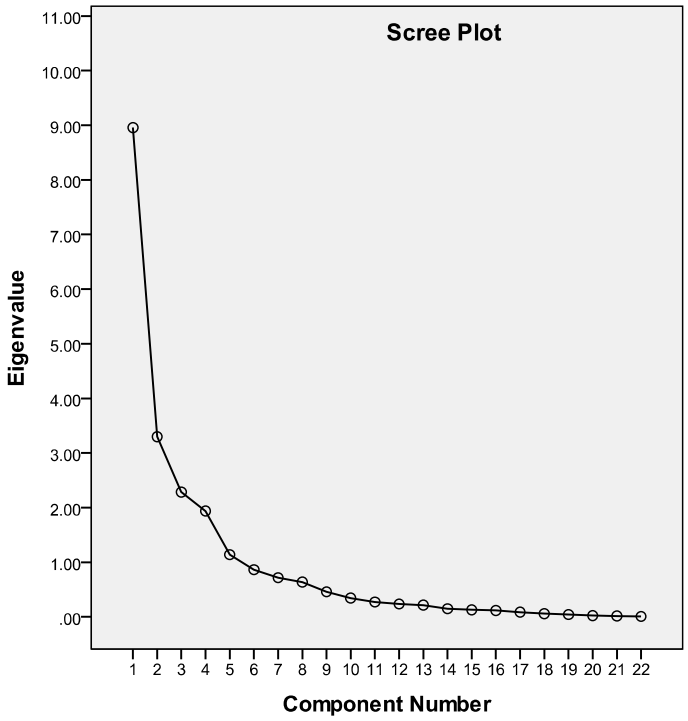

Figure 14: Scree plot for the 1.1m BGS dataset. Components to the right of component 5 (below eigenvalue of 1.0) do not account for a significant portion of variance in the dataset.

Table 10: Extracted components for the 0.2m BGS dataset

Total Variance Explained

	Initial Eigenvalues			Extraction Sums of Squared Loadings		
Component	Total	% of Variance	Cumulative %	Total	% of Variance	Cumulative %
1	8.82	40.07	40.1	8.82	40.07	40.1
2	3.90	17.73	57.8	3.9	17.73	57.8
3	2.17	9.86	67.7	2.17	9.86	67.7
4	1.29	5.87	73.5	1.29	5.87	73.5
5	1.10	4.99	78.5	1.10	4.99	78.5
6	1.02	4.65	83.2	1.02	4.65	83.2
7	.75	3.43	86.6			
8	.56	2.53	89.1			
9	.48	2.17	91.3			
10	.39	1.77	93.1			
11	.34	1.56	94.6			
12	.25	1.14	95.8			
13	.20	.90	96.7			
14	.18	.82	97.5			
15	.14	.62	98.1			
16	.12	.54	98.7			
17	.09	.40	99.1			
18	.06	.29	99.4			
19	.06	.27	99.6			
20	.04	.17	99.8			
21	.03	.13	99.9			
22	.02	.07	100.0			

Table 11: Extracted components for the 0.2m BGS dataset – Rotated solution (Varimax)

Total Variance Explained

	Rotation Sums of Squared Loadings		
Component	Total	% of Variance	Cumulative %
1	5.07	23.04	23.04
2	3.95	17.97	41.01
3	3.16	14.37	55.38
4	2.28	10.36	65.74
5	1.94	8.82	74.56
6	1.90	8.62	83.17

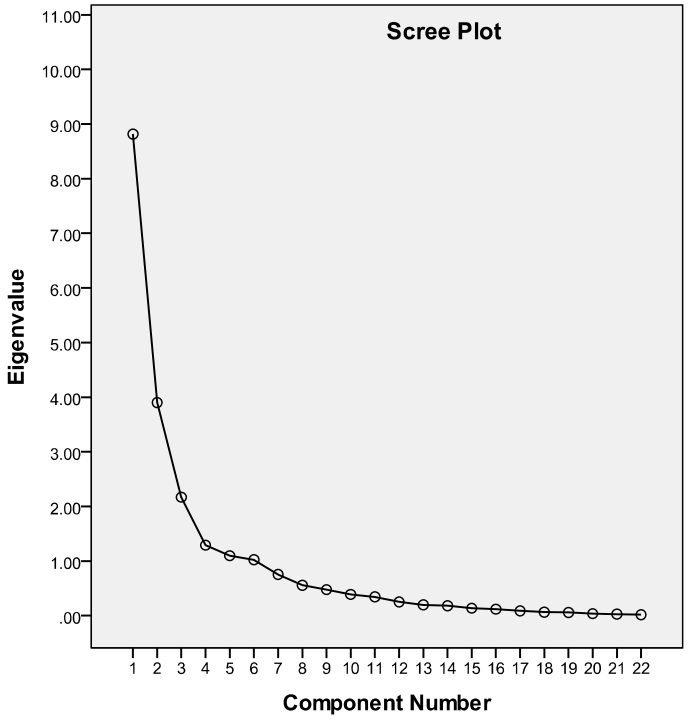

Figure 15: Scree plot for the 0.2m BGS dataset. Components to the right of component 6 (below eigenvalue of 1.0) do not account for a significant portion of the variance in the dataset.

4.1.3 Communalities

Communalities are measures of how the extracted factors are able to reproduce the variance of the individual variables. Tables 12 and 13 show the communalities obtained after factor

extraction for both datasets. There are no statistical guidelines to qualify a communality as being large or small (Hair et al., 2010). However, for logical reasons, one should strive for communalities greater than 0.5, which indicates that at least 50% of the variance of the variable is reproduced by the linear combination of the extracted factor (Hair et al., 2010).

Based on this guideline, the communalities are relatively "high," the lowest being that of pH in the 1.1 m BGS dataset with a communality of 0.52. At that level the communality is just above the threshold value of 0.5 but the extracted factors are still able to reproduce more than 50% of the variance in pH.

Table 12: Communalities for 1.1m BGS groundwater dataset

Communalities

	Initial	Extraction
pH	1.000	.51
Eh	1.000	.78
Al	1.000	.83
Ba	1.000	.81
Ca	1.000	.85
Ce	1.000	.89
Co	1.000	.81
Cr	1.000	.86
Cs	1.000	.81
Fe	1.000	.64
Mg	1.000	.84
Mn	1.000	.78
Ni	1.000	.74
Pb	1.000	.84
Rb	1.000	.78
Sr	1.000	.95
Th	1.000	.80
Ti	1.000	.78
U	1.000	.88
V	1.000	.84
Y	1.000	.89
Zn	1.000	.70

Table 13: Communalities for 0.2m BGS groundwater dataset

Communalities		
	Initial	**Extraction**
pH	1.000	.83
Eh	1.000	.76
Al	1.000	.91
Ba	1.000	.89
Ca	1.000	.87
Ce	1.000	.85
Co	1.000	.77
Cr	1.000	.79
Cs	1.000	.77
Fe	1.000	.81
Mg	1.000	.85
Mn	1.000	.67
Ni	1.000	.76
Pb	1.000	.87
Rb	1.000	.75
Sr	1.000	.89
Th	1.000	.87
Ti	1.000	.91
U	1.000	.88
V	1.000	.80
Y	1.000	.92
Zn	1.000	.86

4.1.4 Discussion

This thesis has relied on limited datasets of 53 and 37 samples (0.2m BGS and 1.1m BGS datasets respectively), analyzed for 32 variables. Ideally, for a factor analysis to be effective, a sample-to-variable ratio greater than 5:1 is recommended with a minimum of 100 samples (Hair et al., 2010). Care was taken to properly process the data to remove any defects that could hamper the factoring process; namely, removing outliers, transforming the data, and standardizing the data to remove multimodality which can induce spurious correlations between variables. After the data exploration and processing phase of the analysis was completed, the sample-to-variable ratio was below 2:1 (1.6:1 for the 0.2m BGS dataset and 1.1:1 for the 1.1m BGS dataset). At those ratios an analysis should not be carried out (Hair et al., 2010). However, an examination of the correlation matrix, and the results of the Kaiser-Meyer-Olkin (KMO) and Bartlett's test of sphericity conducted on the correlation matrix, indicated that there was a reasonable amount of correlation between variables – enough to proceed with the factor analysis.

In this thesis, the "strength" of the factor analysis, as highlighted by the strong loadings and communalities (Costello and Osborne, 2005) may be artificially high due to the low number of samples (Hair et al., 2010). Factor analysis will always produce factors. In a geochemical exploration context, the interpretation and subsequent association of factors with geochemical processes need to be carefully weighed against the quality of the data and respect for the fundamentals of factor analysis.

This thesis has shown that even when forgoing minimum data quality prerequisites, factor analysis can still be very useful as a data exploration tool to give insight into the hidden structure underlying large datasets. It may also serve to highlight yet unknown latent

geochemical processes expressed by the data (Reimann et al., 2002) and hence guide exploration geochemists in further investigation work.

4.2 Factor solution and interpretation

The rotated factor solutions are presented in Table 14 (1.1 m BGS groundwater) and Table 15 (0.2m BGS groundwater). Varimax rotation was used for the rotation in this study. The rotation enhances a factor solution for ease of interpretation. The end result of a factor rotation is a factor solution where each factor contains a few variables with high loadings (the degree to which a variable belongs to a certain factor) and the remaining loadings tending towards 0. For each factor, the composing variables are sorted into decreasing loading values. Loadings less than 0.4 are not shown. The value of 0.4 is an arbitrary threshold value below which loadings are not considered significant (Hair et al., 2010). For the purpose of discussion the valence states of elements have been added to the table.

Table 14: 1.1 m BGS groundwater dataset (2007) – Rotated Component Matrix

	Component				
Element (valence)	1	2	3	4	5
U (+4/+6)	.90				
Ce (+3/+4)	.87				
Y (+3)	.87				
V (+5, variable)	.86				
Th (+4)	.85				
Ni (+2)	.80				
Ti (+4)	.79				
Cr (+3)	.59	-.52		.47	
Co (+2)		.87			
Sr (+2)		.85			
Ba (+2)		.76			
pH		.70			
Al (+3)	.47	-.59			.44
Mg (+2)			.90		
Ca (+2)			.90		
Mn (+2, variable, +4,+6)			.79		
Fe (+2/+3)			.65		
Cs (+1)				.88	
Rb (+1)				.77	
Zn (+2)				.68	.41
Pb (+2)	.41				.72
Eh		-.45			.71

Table 15: 0.2m BGS groundwater dataset (2006) – Rotated Component

	Component					
Element (valence)	1	2	3	4	5	6
Ti (+4)	.90					
Al (+3)	.86					
U (+4/+6)	.82					
Th (+4)	.80					
Rb (+1)	.68				.43	
Ce (+3/+4)	.59	.46			.47	
pH		-.82				
Eh		.76				
Ca (+2)		-.71		.46		
Sr (+2)		-.67	.43	.41		
V (+5, variable)		.63			.50	
Zn (+2)			.88			
Cr (+3)			.86			
Ba (+2)			.85			
Y (+3)		.50	.61			
Fe (+2/+3)				.89		
Mg (+2)		-.50		.74		
Pb (+2)					.90	
Ni (+2)					.41	.72
Mn (+2, variable, +4,+6)	-.45					.68
Cs (+1)	.52					.64
Co (+2)				.50		.61

A factor is considered significant if it contains more than two significantly loading variables. Factors with only two or less significantly loading variables do not contribute to the factor solution nor add much to the understanding of the underlying structure within the datasets (Rummel, 1970; Jöreskog et al., 1976; Hair et al., 2010). Generally both factor solutions show a significant number of variables with loadings greater than 0.7. In both factor solutions, the first three factors contain more than two significantly loading variables.

In the 1.1m BGS dataset, the fourth and fifth factors do meet the criteria; however, the loadings are middling. In the 0.2m BGS, factors four, five and six do not meet the criteria.

In the 0.2m BGS dataset (Table 15), 11 out of 22 variables (Rb, Ce, Ca, Sr, V, Y, Mg, Mn, Cs, Co) cross-load on multiple factors, whereas only 5 out of 22 variables (Cr, Al, Zn. Eh, Pb, Eh) cross-load on multiple factors in the 1.1m BGS dataset (Table 14). The factor solution for the 0.2m BGS dataset appears to be less defined than that of the 1.1m BGS dataset.

The factor solutions have also been reproduced in three-dimensional loading plots. In Figure 16 (1.1m BGS water samples) clusters of elements such as those of factor one (cluster on the right) are easily distinguishable from other clusters (Sr, Ba, pH, Co, Rb in the upper middle cluster). For the 0.2m BGS dataset (Figure 17), clusters of elements are much less distinguishable; only a broad trend can be observed.

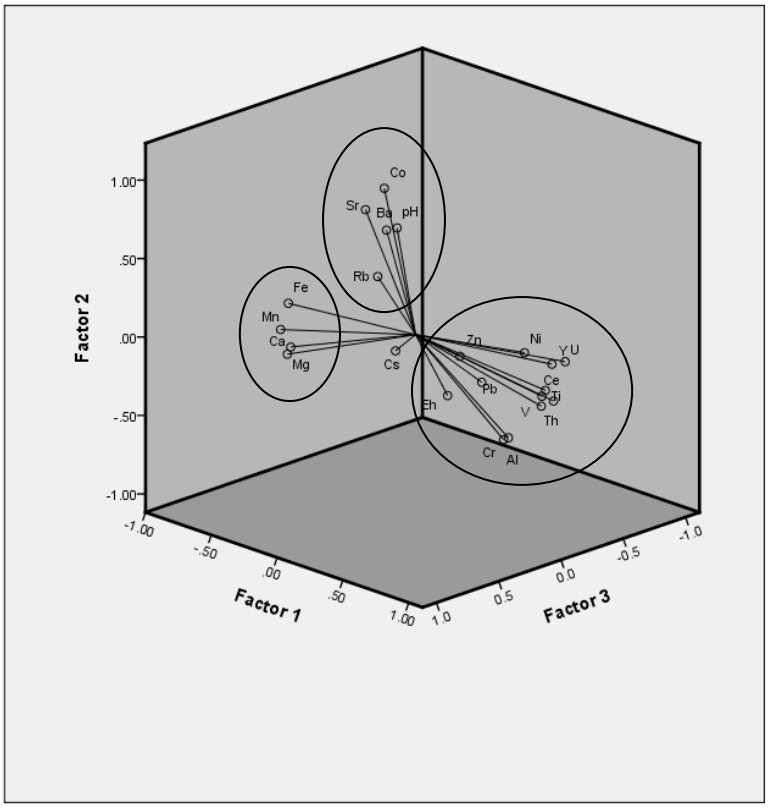

Figure 16: Loadings plot for factors one, two and three – 1.1m BGS dataset. Elements making up factors one, two and three can be seen clustering together in three distinguishable groups.

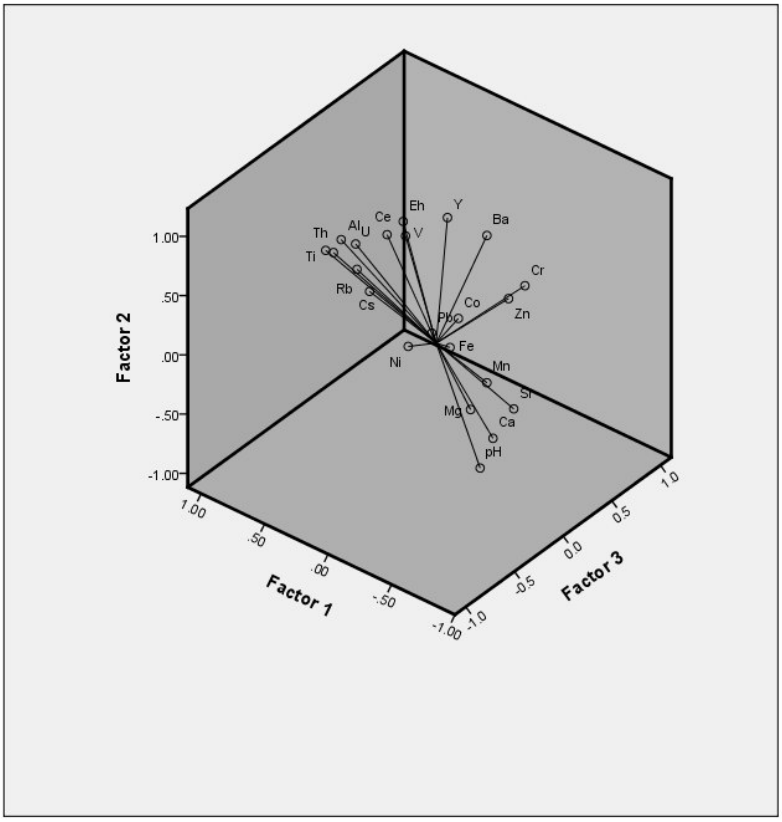

Figure 17: Loadings plot for factors one, two and three – 0.2m BGS groundwater samples. In this loading plot, clusters of elements are much less defined.

4.2.1 Element separation with depth

The 0.2m BGS is characterized by a greater number of cross-loading variables and a lower number of high-loading variables in each factor compared to the 1.1m BGS dataset, indicating a significant difference in the behaviour of elements at the two sampled depths.

The ambivalence in the behaviour of elements near the surface can also be observed in the factor loading plots (Figures 16 and 17). In Figure 16 (1.1m BGS dataset) one can observe the separation of elements in three distinct clusters, whereas such clustering of elements is not present in Figure 17 (0.2m BGS dataset).

The lack of coherent behaviour of metals in near-surface groundwater may be the result of the influence of the atmosphere on groundwater. At shallow depths, at or near the groundwater-atmosphere interface, pH and Eh vary drastically due to rainfall/snowfall, freezing and thawing, respiration and photosynthesis of plants, and the availability of oxygen from the atmosphere. Respiration and photosynthesis of plants releases CO_2 and lowers pH, which may lead to the dissolution of carbonates. Photosynthesis takes CO_2 and releases O_2, which may cause the precipitation of oxides. Decay of plants produces humic acids and lowers the pH.

Furthermore, the difference between the two factor solutions suggests that elements are not simply transferred upward from the underlying kimberlites. The difference in depth between the two datasets being 0.9 m suggests that the processes controlling the concentrations of elements change within short distances.

4.2.2 Factors and kimberlite indicator elements (KIE)

In the factor solution of the 1.1m BGS dataset (Table 14), factor one is composed of U, Ce, Y, V, Th, Ni, Ti, Cr, Al and Pb. Uranium, Ce, Y, V, Th, Ni and Ti have high loadings (>0.79) whereas Cr, Al and Pb load marginally (<0.60) on factor one and cross-load on other factors. Similarly, in Figure 18, Ni, U, Y, Ce, Th, V and Ti cluster together at the extreme end of factor one with high loadings whereas Al, Cr and Pb are set away from the main cluster of factor one.

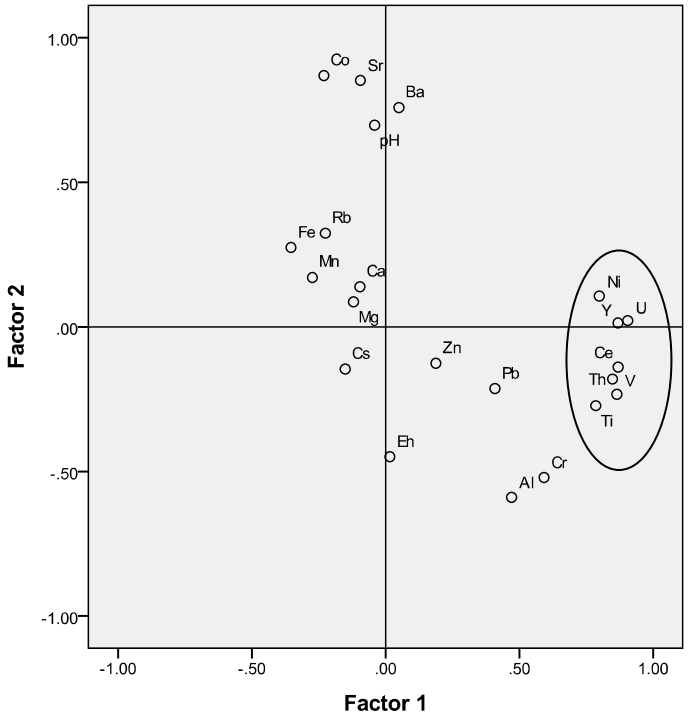

Figure 18: Loadings plot of factor one and factor two – 1.1m BGS dataset.

The elements U, Ce, Y, V, Th, Ti and Ni in factor one are known to be enriched in kimberlite (kimberlite indicator elements or KIE), whereas these elements are found in low to very low concentrations in crustal rock and limestone. For example, Ce has an average concentration of 200 ppm in kimberlite (Mitchell, 1986), whereas the average upper continental crust contains 64 ppm (Taylor and McLennan, 1985, 1995, cited in Rudnick and Gao, 2003). Nickel, U and Th have average concentrations of 710-1600 ppm (Dawson, 1980), 3.1 ppm (Mitchell, 1986) and 17 ppm (Mitchell, 1986) in kimberlites compared to 44, 2.8 and 10.7 ppm in the upper continental crust, respectively (Taylor and McLennan, 1985, 1995, cited in Rudnick and Gao, 2003). These elements are also elements of the high field strength group of elements (U, Th, Ce, Y, Ti).

In a factor analysis, the first factor accounts for the greatest variability in the dataset, with the subsequent factors accounting for successively less variability. In the context of this

study, the first factor would group together the correlating elements that show the greatest contrast between zones of enrichment (near a kimberlite pipe) compared to background levels (over the limestone host rock).

The dominance of U, Ce, V, Y, Th, Ti and Ni in the first factor suggests the influence of buried kimberlites in surface media. The elemental assemblage is a geochemical signature of kimberlites and none of the elements are associated with the surrounding limestones. If these elements form a factor because of their specific geochemical characters in natural environments, they should be found in lesser factors (factors of lesser variance like factor 4 or 5), because U, Th, REE, V, Y, Ti and Ni are usually found in trace concentrations in most rocks and in many surface waters. Conversely, this may explain why Sr, a well-known KIE, is found in a lesser factor (factor two) due to the contribution of the underlying limestone or the carbonate-rich marine silts.

Although there is a difference in the overall composition of factor one between the two depths (Tables 14 and 15), KIE remain the significant component of the first factor even though, as discussed in the previous section, elements near the surface are subject to greater influence from atmospheric conditions and precipitation.

Scores for factor one (Yankee) were plotted in relation to the known position of the kimberlite pipe (Figure 19). Factor scores can be construed as the "concentration" of the new factors (Jöreskog et al., 1976) in each sample and were calculated by multiplying the concentration values of all the samples, including outliers that were removed during the data exploration process, by the factor score coefficients obtained from the factor analysis.

Figure 19 shows three local high scores at Y4, Y8 and Y11. Peaks of factor one scores are located over or close to the kimberlite pipe, suggesting an association between

high concentrations of U, Ce, V, Y, Th, Ti and Ni (as a group) and the underlying kimberlite, again consistant with a geochemical signature of a concealed kimberlite. It should be noted that control data was not available for comparison. Control data only exists for the 0.2m BGS dataset. Furthermore, the observed concentrations of high valence elements were mostly below detection limit at the control site.

The peak observed at Y4 corresponds to the location of an outcropping bioherm where Sader (2010) observed upwelling groundwater.

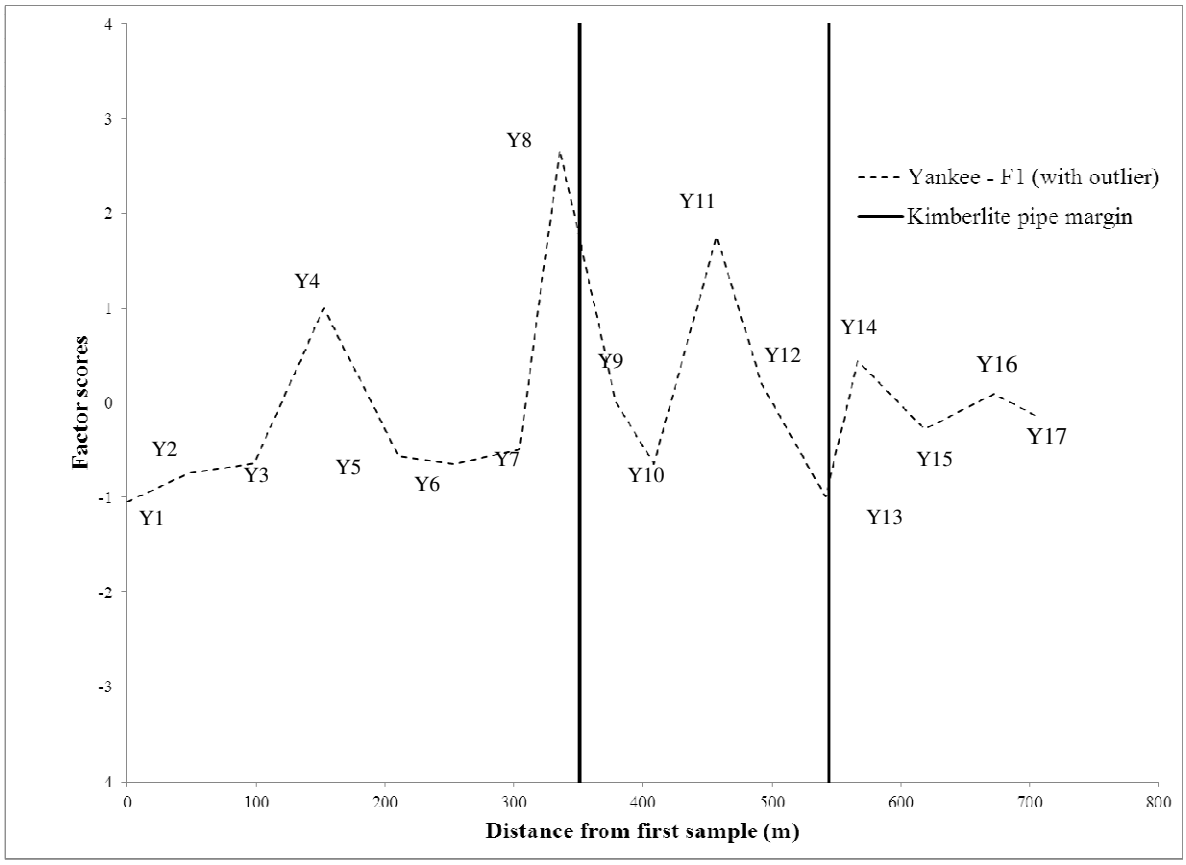

Figure 19: Factor score plot for factor one over Yankee, 1.1m BGS dataset. The two vertical lines at approximately 350m and 540m correspond to the margins of the kimberlite pipe.

Factors resulting from factor analysis are assemblages of co-varying elements that give insight as to what is contributing to the composition of the groundwater. Factor score plot of factor one generates a picture of the behaviour of, in this case, seven elements (U, Ce, V, Y, Th, Ti and Ni) simultaneously (Figure 19). However, to obtain the same results using univariate concentration plots one would have to generate concentration profiles for all elements, then identify anomalies and anomalous elements. This process is time-consuming and anomalous elements may not be unique to the mineralization investigated. Figure 20 shows concentration profiles of Ni and Cr over Yankee for the 1.1m BGS dataset where a strong anomaly can be observed near the margin of the kimberlite. Even though ordinary rocks do not contain high concentration of these elements, and limestone, which underlies the study area, do not contain Ni or Cr, an anomaly of these elements by themselves cannot justify an association with kimberlites because any ultramafic and mafic rocks contain high Ni and Cr. For example, a dyke of ultramafic or mafic rock would produce anomalies of Ni and Cr. It is the peculiar combination of U, Ce, V, Y, Th, Ti and Ni in factor one that makes this assemblage of elements unique to kimberlites and constitutes a geochemical anomaly of kimberlite in near-surface groundwaters.

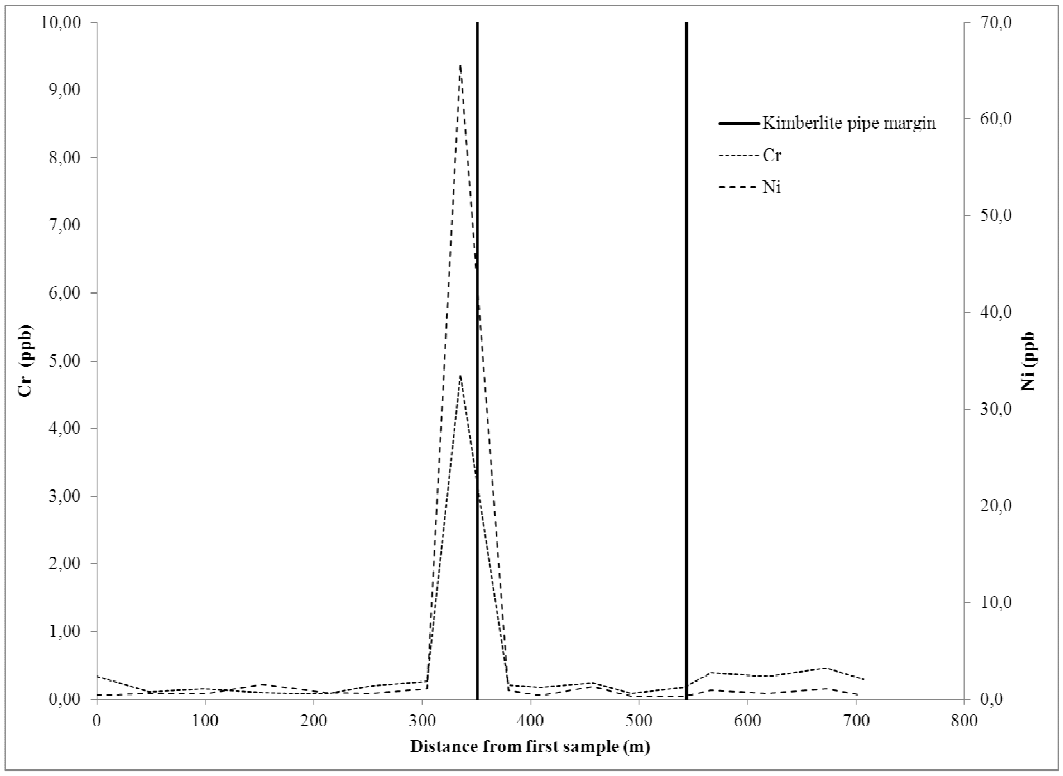

Figure 20: Concentration profile for Ni and Cr over Yankee, 1.1m BGS dataset. The two vertical lines at approximately 350m and 540m correspond to the margins of the kimberlite pipe.

4.2.3 Separation of kimberlite indicator elements

In the 1.1m BGS dataset, the kimberlite indicator elements U, Ce, Y, V, Th, Ni, Ti are found in factor one while other well-known KIE like Sr and Ba are found in factor two, and Cs and Rb are found in factor four. At this depth, it appears that the high-valence KIE (U, Th, Ti, REE, V) are separated from the low-valence KIE (Rb, Cs, Sr, Ba).

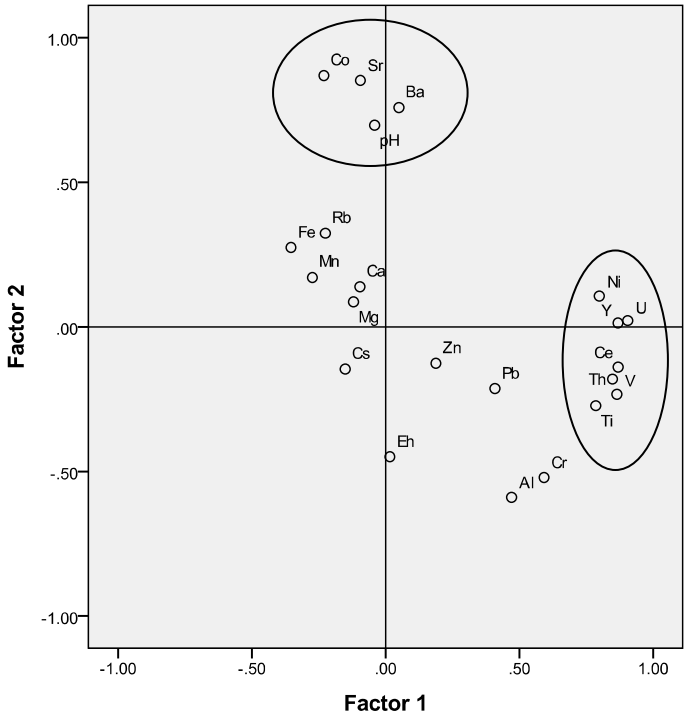

Figure 21: Loadings plot for factors one and two – 1.1m BGS groundwater samples. High-valence KIE (U, V, Ce, Th, Ti, Y) and Ni are clustered to the extreme right, loading strongly on factor one, while Sr and Ba, low-valence KIE, are clustered together, loading strongly on factor two.

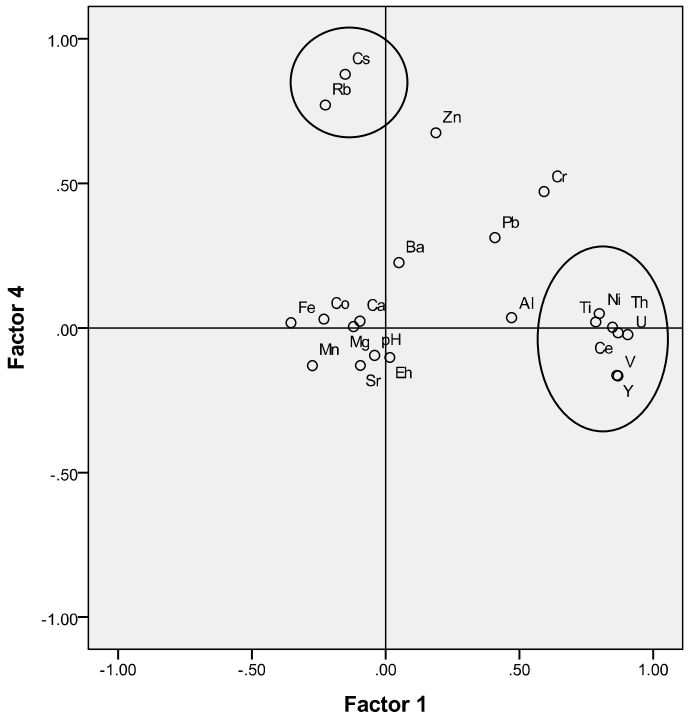

Figure 22: Loadings plot for factors one and four – 1.1m BGS groundwater samples. High-valence KIE (U, V, Ce, Th, Ti, Y) and Ni are clustered to the extreme right, loading strongly on factor one, while Cs and Rb, low-valence KIE, are clustered together, loading strongly on factor four.

The separation of KIE in terms of valence can still be observed in the 0.2m BGS but to a lesser extent (Table 15). High-valence KIE like U, Th and Ti are still found with high loadings in factor one. Low-valence KIE like Rb and Cs, although found in factor one, cross-load on other factors. Barium is found in factor three, and Sr cross-loads on factors two, three and four.

Considering that the KIE originate from a single source, a separation of KIE in terms of valence is an unexpected result, especially since the factors are independent of one another. Alkalis are highly soluble in water and they are very high in kimberlites compared to any other rocks. Therefore, it is surprising that alkalis are not loading on factor one with the other KIE. As before, it also suggests that elements released from kimberlites at depths are not directly transported to the surface. Reactions in the sediments and peat play an important role in the behaviour of elements.

The separation of the low-valence KIE from the high-valence KIE may be the result of the difference in mobility of these groups of elements. The high-valence elements of factor one are considered to be less mobile and therefore less prone to dispersion in the secondary environment than the low-valence elements. These high-valence elements generally have low solubilities in water and they are easily adsorbed on the negatively charged surface of clays and Fe-O-OH and Mn-O-OH in soil. Over time the low-mobility KIE will tend to stay concentrated over a smaller area, producing a zone of enrichment, whereas the high-mobility/low-valence KIE will tend to disperse over larger areas (disperse into the background) and therefore offer less contrast between zone of enrichment and background levels, as suggested by their presence in the lesser factors.

Kimberlite indicator element separation into different factors may also be the result of mixing of waters of different origins: one type of water that extensively interacted with kimberlites and therefore became enriched in KIE, and another water very similar to groundwaters in the regionally abundant limestones.

4.2.4 Relationship with Fe-Mn-Al-O-OH

In the 1.1m BGS dataset factor solution, factor three is composed of Mg, Ca, Mn and Fe, all major elements. Calcium and Mg load high on factor three (> 0.90), compared to Fe and Mn, with loadings of 0.65 and 0.79 respectively. The strong loading of Ca and Mg suggest the control of the hosting limestone which is composed of calcite, $CaCO_3$, with minor dolomite, $(Ca,Mg)CO_3$. Manganese, Fe, and Sr commonly substitute Ca in carbonate.

Adsorption of elements onto Fe, Mn and Al oxy-hydroxides together with carbonate co-precipitation are some of the most important controls on the mobility of trace metals in groundwater (Levinson, 1980; Drever, 1997). The presence of Fe and Mn in factor three separated from KIE of factor one suggests that adsorption onto Fe-Mn-O-OH is not a major governing factor at that depth (Figure 21).

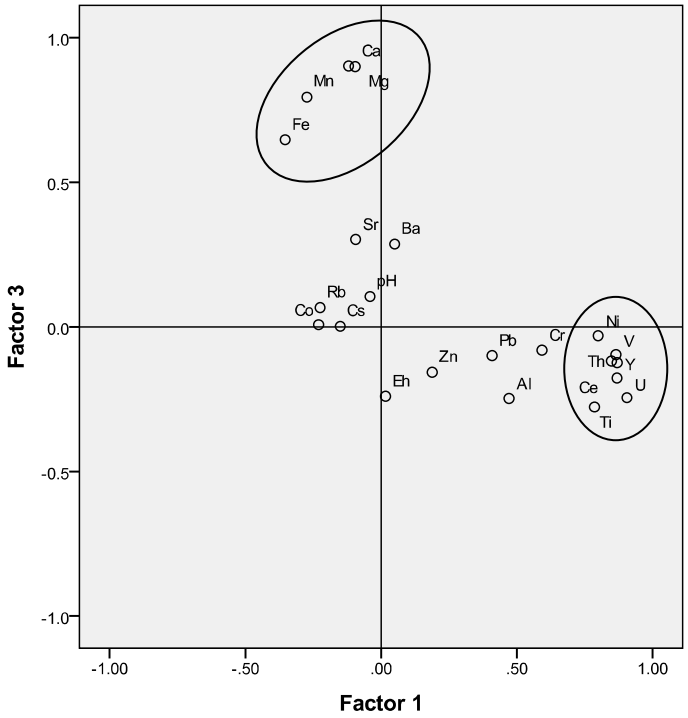

Figure 23: Loadings plot for factors one and three – 1.1m BGS groundwater samples. High-valence KIE (U, V, Ce, Th, Ti, Y) and Ni are clustered to the extreme right, loading strongly on factor one, while Ca, Mg, Mn and Fe are clustered together, loading strongly on factor three.

In natural waters, Fe, Al and Mn can precipitate as oxy-hydroxides and scavenge dissolved metals. The adsorption capacity, and hence the co-precipitation capabilities, of Fe, Al and Mn are dependent on pH and Eh conditions. Iron will precipitate as ferrihydrite or schwertmannite according to the pH and redox conditions, followed by Al at pH around 5 for all Eh and Mn at pH around 8 (Lee et al., 2002). These oxy-hydroxides have negatively charged surface to adsorb and scavenge large quantity of positively charged metals from water.

While Fe and Mn oxy-hydroxides do not appear to control the solubility of KIE in this dataset, the presence of Al cross-loading on factor one (loading of 0.47), factor two (loading of -0.59) and factor five (loading of 0.44) suggest that adsorption onto Al-O-OH

may be a significant process, although a middling one. In Figure 21, Al is not part of the high valence KIE but close enough to suggest a possible relationship.

Sader et al. (2010) provide a possible explanation for the absence of correlation between Fe-O-OH and the KIE. It was shown that dissolved organic matter (DOM) may contribute to the solubility of KIE. Metals are bound to dissolve organic acids to form neutral metal-DOM complexes, thus preventing these metals from adsorbing onto Fe-O-OH.

4.2.5 Discussion

Investigation methods relying on indicator elements suppose an *a priori* knowledge of the geochemical context of the study area, and consequently may limit or bias the investigation. In factor analysis there is no *a priori* judgement made about the geochemical context of a study and therefore the results (factors) are based solely on the data itself, independent of the researchers' bias and of the geological context.

The use of factor analysis in geochemistry has been deemed by some researchers as controversial due to past misuses of the method by inexperienced analysts who factor analyzed datasets until desired results are achieved (i.e. forcing factor solutions to match desired outcomes), or misuse simply due to a lack of understanding of the fundamentals of factor analysis; for example, a sufficient amount of correlation between variables in a given dataset. However, factor analysis remains a useful tool to help identify hidden controlling structures in large multivariate datasets (Reiman et al., 2002).

The findings of this research further highlight the multivariate nature of geochemical processes in groundwater. Although some of the findings of this thesis could have been deduced using a simple single-element concentration profile along a transect over a

kimberlite, the factor analysis found other unforeseen geochemical processes that shed light on unexpected metal behaviours. For example, the erratic behaviour of metals in near-surface groundwater compared to the deeper sheltered groundwater, the separation of high-valence and low-valence kimberlite indicator elements or the absence of relationship between Fe and Mn oxy-hydroxides would not have been as easily identified using bivariate element analysis.

Compared to previous work in geochemical exploration, where often only univariate or bivariate statistics, or single elements profiles over concealed ore bodies were used, this thesis has shown that factor analysis, as a multivariate data analysis technique, is a much more robust, holistic exploration tool able to shed light on relevant geochemical processes hidden within large datasets.

Also, the findings of this thesis are further demonstrations that concealed ore bodies form geochemical signatures in surface media. The presence of kimberlite indicator elements in factor one suggests that elements weathered from kimberlite migrate upward to the surface to form a geochemical signature. Elements grouped in factor one are those elements correlating together that show the greatest contrast between zones of enrichment near the kimberlite, the sole source of KIE in the area, with background level (away from the kimberlite body, above the limestone formation). However, the findings of this thesis also suggest that geochemical processes act on elements as they migrate upwards, as indicated by the differences between the factor solution of the 0.2m BGS and 1.1m BGS datasets and the separation of KIE in terms of valence.

Combined, these findings have practical applications for future diamond exploration work in similar surficial environments where concealed kimberlites are present. For

example, northwestern Canada, Siberia and the northern Fenno-Scandinavian countries host numerous diamondiferous kimberlites in vast areas covered by wetalnds.. The findings of this thesis are readily applicable to these areas. One should sample stable groundwater located below the zone of oxidation, sheltered from the effects of the atmosphere. Secondly, the high-valence KIE, notably the REE, U, Th, Ti, V and Y, by their strong presence in factor one may be the better indicators of concealed kimberlite than other well-known KIE.

5. Summary and Final Thoughts

In surficial geochemical exploration, researchers have often relied on simple statistical means or single-element concentration profiles to investigate the relationship between elements in surface media and buried ore bodies. In this thesis, factor analysis, a multivariate data analysis technique, was used to explore the geochemistry of near-surface groundwater overlying buried kimberlite pipes.

The factor analysis performed on two groundwater geochemistry datasets uncovered complex factors influencing the mobility of elements in near-surface groundwater. Elements released from kimberlites are not reaching the near-surface environments in similar manners. As elements migrate upwards they are subject to various geochemical processes acting to separate them. Furthermore, well-known processes like adsorption onto Fe-O-OH or Mn-O-OH are found not to be governing processes in this environment. These relationships between elements or groups of elements would have been very difficult, if possible at all, to identify without a multivariate approach.

Although this thesis is based on limited datasets, the rationale and methodology employed are sound. The findings of this thesis open the door to further research in geochemical exploration of surficial media and multivariate analysis techniques, while also guiding future kimberlite exploration work.

5.1 Recommendation for future research

This thesis highlights possible use of factor analysis in geochemical exploration for concealed ore bodies. The thesis relied on a limited dataset. Future work is therefore

recommended with larger datasets to ensure a sufficient sample-to-variable ratio. With regards to sampling strategies, future research should increase the number of samples to meet a minimum sampling-to-variable ratio of 3, ideally of 5. Considering the 32 elements used in this thesis, a dataset of a minimum of 100 samples is recommended. Furthermore, the datasets used were collections of data collected at four different sites during two distinct yearly sampling periods (Alpha, Golf and Yankee in 2006, and Yankee and Zulu in 2007). Future sampling should ensure that samples are collected during a single season to eliminate possible seasonal variations of groundwater geochemistry.

With regard to analytical parameters, Sader et al. (2010) suggested that dissolved organic matter forms soluble complexes with metals and may play a significant role in the mobility of elements in near-surface groundwater. Further research that would include dissolved organic matter (DOM) data is recommended to explore the relationship between DOM and dissolved metals.

Also, because the Attawapiskat area offers such an ideal setting, future research should be conducted at other locales, in other geological settings, to test the replicability of these findings, especially in terms of the group of elements being considered as the geochemical signature of kimberlite in near-surface groundwater.

References

Berg, T., Royset, O., Steinnes, E and Vadset, M. 1993, Atmospheric trace elements deposition: principal component analysis of ICP-MS data from moss sample. *Environmental Pollution*, 88: 67-77.

Bogle, E. W., and Nichol, I. 1981. Metal transport, partition and fixation in drainage waters and sediments in carbonate terrain in South-eastern Ontario. *Journal of Geochemical Exploration,* 15: 405-422.

Borovec, Z. 1996. Evaluation of the concentrations of trace elements in stream sediments by factor and cluster analysis and the sequential extraction procedure. *The Science of the Total Environment,* 177: 237-250.

Boruvka, L., Vacek, O., and Jehlicka, J. 2005. Principal component analysis as a tool to indicate the origin of potentially toxic elements in soils. *Geoderma,* 128: 289-300.

Brauneder, K. 2007. *Characterization of Peatland Waters Overlying Concealed Kimberlites in the Attawapiskat Region, Northern Ontario.* (Unpublished B.Sc. thesis at the University of Ottawa, 70 p.

Buckley, D. E., Smith, J. N., and Winters, G. V. 1995. Accumulation of contaminant metals in marine sediments of Halifax harbour, Nova Scotia: Environmental factors and historical trends. *Applied Geochemistry,* 10: 175-195.

Cameron, E. M., Hamilton, S. M., Leybourne, M. I., Hall, G.E.M., and McClenaghan, M. B. 2004. Finding deeply buried deposits using geochemistry. *Geochemistry: Exploration, Environment, Analysis,* 4: 7-32.

Cameron, E. M., and Hattori, K. H. 2003. Mobility of palladium in the surface environment: Data from a regional lake sediment survey in northwestern Ontario. *Geochemistry: Exploration, Environment, Analysis,* 3: 299-311.

Chague-Goff, C., and Fyfe, W. S. 1997. Effect of permafrost on geochemistry in a Canadian peat plateau bog. *Applied Geochemistry,* 12: 465-472. Cowell, D. W. 1983. Karst hydrogeology within a subarctic peatland: Attawapiskat River, Hudson Bay lowland, Canada. *Journal of Hydrology,* 61: 169-175.

Chen, M., Price, R.M., Yamashita, Y. and Jaffé, R. 2010. Comparative study of dissolved organic matter from groundwater and surface water in the Florida coastal Everglades using multi-dimensional spectrofluorometry combined with multivariate statistics. *Applied Geochemistry*, 25:872-880.

Cheng, M.-C.and Chen, C.-F. 2010. Sources of major ions and heavy metals in rainwater associated with typhoon events in southwestern Taiwan. *Journal of Geochemical Exploration*, 105:106-116.

Closs, L.G. and Nichol, I. 1975. The role of factor and regression analysis in the interpretation of geochemical reconnaissance data. *Canadian Journal of Earth Sciences*, 12:1316-1330.

Costello, Anna B., and Jason Osborne (2005). Best practices in exploratory factor analysis: Four recommendations for getting the most from your analysis. *Practical Assessment Research & Evaluatio*n, 10(7). From http://pareonline.net/pdf/v10n7.pdf

Davies, B. E. 1997. Heavy metal contaminated soils in an old industrial area of Wales, Great Britain: Source identification through statistical data interpretation. *Water, Air and Soil Pollution,* 94: 85-98.

Davis, John C. 2002. *Statistics and Data Analysis in Geology* (3rd ed.).: Wiley, NY., 638 p.

Dawson, John B. 1980. *Kimberlites and their Xenoliths*.: Springer-Verlag, New York, 252 p.

DiLabio, R.N.W. 1996. Partie 2: Exploration du diamant dans les terrains englacés. In A. N. LeCheminant, D. G. Richardson, R.N.W. DiLabio and K. A. Richardson (eds.), *La recherche de diamants au Canada* (pp. 193-195). Comission géologique du Canada, Ottawa.

Drever, James I. 1997. *The geochemistry of Natural Waters: Surface and Groundwater Environments* (3rd ed.).: Prentice Hall, Upper Saddle River, NJ, 436 p.

Environment Canada. 2011. *National Climate Data and Information Archive*. Retrieved November 21, 2011, from http://www.climate.weatheroffice.gc.ca

Fowler, J. A., Grutter, H. S., Kong, J. M., and Wood, B. D. 2001. Diamond exploration in northern Ontario with reference to the Victor kimberlite, near Attawapiskat. *Exploration and Mining Geology,* 10: 67-75.

Goldberg, I. S. 1998. Vertical migration of elements from mineral deposits. *Journal of Geochemical Exploration,* 61(1-3): 191-202.

Grant, A. 1990. Multivariate statistical analyses of sediment geochemistry. *Marine Pollution Bulletin,* 21(6): 297-299.

Hair, J. F., Black, W. C., Babin, B. J., and Anderson, R. E. 2010. *Multivariate Data Analysis* (7th ed.).: Prentice Hall, New Jersey, 786 p.

Hamilton, S. M., Cameron, E. M., McClenaghan, M. B., and Hall, G.E.M. 2004. Redox, pH and SP variation over mineralization in thick glacial overburden. Part I: Methodology and field investigation at the Marsh Zone gold property. *Geochemistry: Exploration, Environment, Analysis,* 4: 33-44.

Hamilton, S. M., Cameron, E. M., McClenaghan, M. B., and Hall, G.E.M. 2004. Redox, pH and SP variation over mineralization in thick glacial overburden. Part II: Field investigation at Cross Lake VMS property. *Geochemistry: Exploration, Environment, Analysis,* 4: 45-58.

Hattori, K. H., Hamilton, S., Kong, J., and Gravel, J. 2009. Soil geochemical survey over concealed kimberlites in the Attawapiskat area in northern Canada. *Geochemistry: Exploration, Environment, Analysis,* 9: 1-13.

Hattori, K. H., and Hamilton, S. 2008. Geochemistry of peat over kimberlites in the Attawapiskat area, James Bay Lowlands, northern Canada. *Applied Geochemistry,* 23: 3767-3782.

Hawkes, H. E., Rose, Arthur W., and Webb, John Stuart. 1979. *Geochemistry in Mineral Exploration* (2d ed.).: Academic Press, NY., 657 p.

Howarth, R J. 1983. *Statistics and Data Analysis in Geochemical Prospecting*.: Elsevier Scientific Publishing, Amsterdam, 437 p.

Huelin, S.R., Longerich, H.P., Wilton, D.H.C. and Fryer, B.J. 2006. The determination of trace elements in Fe-Mn oxide coatings on pebbles using LA-ICP-MS. *Journal of Geochemical Exploration*, 91:110-124.

Jones, J. M., and Hao, J. 1993. Ombrotrophic peat as a medium for historical monitoring of heavy metal pollution. *Environmental Geochemistry and Health,* 15: 67-74.

Jöreskog, K. G., Klovan, J. E, and Reyment, R A. 1976. *Geological Factor Analysis*.: Elsevier Scientific Publications, Amsterdam, 178 p.

Keating, P. 1996. Kimberlites et données aéromagnétiques. In A. N. LeCheminant, D. G. Richardson, R.N.W. DiLabio, and K. A. Richardson (eds.), *La recherche de diamants au Canada* (pp. 239-242). Comission géologique du Canada.

Keddy, P. A. 2000. *Wetland Ecology: Principles and Conservation*. Cambridge, UK: Cambridge University Press.

Kjarsgaard, B. A. 1996. Les kimberlites. In A. N. LeCheminant, D. G. Richardson, R.N.W. DiLabio, and K. A. Richardson (eds.), *La recherche de diamants au Canada* (pp. 29-38). Comission géologique du Canada.

Kumru, M.N. and Bakaç, M. 2003. R-mode factor analysis applied to the distribution of elements in soils from the Aydin basin, Turkey. *Journal of Geochemical exploration*, 77:81-91.

Lee, G., Bigham, J. M., and Faure, G. 2002. Removal of trace metals by coprecipitation with Fe, Al and Mn from natural waters contaminated with acid mine drainage in the Ducktown mining district, Tennessee. *Applied Geochemistry,* 17: 569-581.

Lesaffre, E. 1983. Normality tests and transformations. *Pattern Recognition Letters,* 1: 187-199.

Levinson, A. A. 1980. *Introduction to Exploration Geochemistry* (2d ed.).: Applied Publishing, Wilmette, Illinois, 924 p.

Leybourne, M. I. 2007. Aqueous geochemistry in mineral exploration. In W. D. Goodfellow (ed.), *Mineral deposits of Canada: A synthesis of major deposit-types, district metallogeny, the evolution of geological province, and exploration methods* (pp. 983-1006). Geological Association of Canada, Mineral Deposits Division.

Martínez Cortizas, A., García-Rodeja, E., Pontevedra Pombal, X., Nóvoa Muñoz, J. C., Weiss, D., and Cheburkin, A. 2002. Atmospheric Pb deposition in Spain during the last 4600 years recorded by two ombrotrophic peat bogs and implications for the use of peat as archive. *The Science of the Total Environment,* 292: 33-44.

Martínez Cortizas, A., García-Rodeja Gayoso, E., and Weiss, D. 2002. Peat bog archives of atmospheric metal deposition. *The Science of the Total Environment,* 292(1-2): 1-5. doi:10.1016/S0048-9697(02)00024-4.

McClenaghan, M. B. 1996. Géochimie et minéralogie (minéraux indicateurs) des dépôts d'origine glaviaire sous-jacents à des kimberlites à Kirkland Lake (Ontario). In A. N. LeCheminant, D. G. Richardson, R.N.W. DiLabio, and K. A. Richardson (eds.), *La recherche de diamants au Canada* (pp. 219-224). Comission géologique du Canada.

McClenaghan, M. B., and Kjarsgaard, B. A. 2007. Indicator mineral and surficial geochemical exploration methods for kimberlite in glaciated terrain; examples from Canada. In W. D. Goodfellow (ed.), *Mineral deposits of Canada: A synthesis of major deposit-types, district metallogeny, the evolution of geological province, and exploration methods* (pp. 983-1006). Geological Association of Canada, Mineral Deposits Division.

McClenaghan, M. B., Thorleifson, L. H., and DiLabio, R. N. W. 2000. Till geochemical and indicator mineral methods in mineral exploration. *Ore Geology Reviews,* 16(3-4): 145-166.

Mil-Homens, M., Branco, V., Lopes, C., Vale, C., Abrantes, F., Boer, W., and Vicente, M. 2009. Using factor analysis to characterise historical trends of trace metal contamination in a sediment core from the Tagus prodelta, Portugal. *Water, Air, and Soil Pollution,* 197(1-4): 277-287. doi:10.1007/s11270-008-9810-0

Mitchell, Roger H. 1986. *Kimberlites: Mineralogy, Geochemistry, and Petrology*.: Plenum Press, New York, 442 p.

Murdoch University. 2009. *Notes on QQ-Plots – Introductory notes to accompany qplot puzzles.* Retrieved November 21, 2011, from http://www.cms.murdoch.edu.au/areas/maths/statsnotes/samplestats/qqplot.html

Olid, C., Garcia-Orellana, J., Martínez-Cortizas, A., Masqué, P., Peiteado-Varela, E., and Sanchez-Cabeza, J. 2010. Multiple site study of recent atmospheric metal (Pb, Zn and Cu) deposition in the NW Iberian Peninsula using peat cores. *Science of the Total Environment,* 408(22): 5540-5549. doi:10.1016/j.scitotenv.2010.07.058

Ontario Ministry of Northern Development, Mines and Forestry. 2011. *Northern Ontario – A profile*. Retrieved November 21, 2011, from http://www.mndm.gov.on.ca/northern_development/documents/northern_ontario_e.pdf

Power, M., Belcourt, G. and Rockel, E. 2004. Geophysical methods for kimberlite exploration in northern Canada. *The Leading Edge* (November), 1124-1129.

Prasanna, M.V., Chidabaram, S. and Srinivasamoorthy, K. 2010. Statistical analysis of the hydrogeochemical evolution of groundwater in hard and sedimentary aquifers system of Gadilam river basin, South India. *Journal of King Saud University (Science)*, 22:133-145.

Reimann, C., and Filzmoser, P. 1999. Normal and lognormal data distribution in geochemistry: Death of a myth. Consequences for the statistical treatment of geochemical and envrionmental data. *Environmental Geology,* 39: 1001-1014.

Reimann, C., Filzmoser, P., and Garrett, R. G. 2002. Factor analysis applied to regional geochemical data: Problems and possibilities. *Applied Geochemistry,* 17: 185-206.

Reis, A.P., Silva, E.f., Sousa, A.J., Patinha, C., Martins, E., Guimaraes, C., Azevedo, M.R. and Nogueira, P. 2009. Geochemical associations and their spatial patterns of variation in soil data from the Marrancos gold-tungsten deposit: a pilot analysis. Geochemistry: Exploration, Environment Analysis, 9:319-340.

Richardson, K. A. 1996. Partie 3: Utilisation des levés géophysiques et des systèmes d'information géographiques (SIG). In A. N. LeCheminant, D. G. Richardson, R. N. W. DiLabio, and K. A. Richardson (eds.), *La recherche de diamants au Canada* (pp. 231-234). Comission géologique du Canada.

Rudnick, R. L., and Gao, S. 2003. 3.01 – Composition of the continental crust. In The Crust, Heinrich D. Holland and Karl K. Turekian (eds.), *Treatise on Geochemistry* (pp. 1-64). Oxford: Pergamon.

Rummel, R. J. 1970. *Applied Factor Analysis*.: Northwestern University Press, Evanston, 617 p.

Sader, J. A., Hattori, K. H., Kong, J. M., Hamilton, S. M., and Brauneder, K. 2010. Geochemical responses in peat groundwater over Attawapiskat kimberlites, James Bay Lowlands, Canada and their application to diamond exploration. *Geochemistry: Exploration, Environment, Analysis,* 11: 193-210.

Sader, J. A., Hattori, K., Hamilton, S., and Brauneder, K. 2011. Metal binding to dissolved organic matter and adsorption to ferrihydrite in shallow peat groundwaters: Application to diamond exploration in the James Bay Lowlands, Canada. *Applied Geochemistry,* 261649-1664.

Shotyk, W. 1988. Review of the inorganic geochemistry of peats and peatland waters. *Earth Science Reviews,* 25(2): 95-176.

Shotyk, W., Goodsite, M. E., Roos-Barraclough, F., Givelet, N., Le Roux, G., Weiss, D., . . . Lohse, C. 2005. Accumulation rates and predominant atmospheric sources of natural and anthropogenic Hg and Pb on the Faroe Islands. *Geochimica et Cosmochimica Acta,* 69: 1-17.

Shotyk, W., Nesbitt, W. H., and Fyfe, W. S. 1990. The behaviour of major and trace elements in complete vertical peat profiles from three sphagnum bogs. *International Journal of Coal Geology,* 15(3): 163-190.

Sibrell, P. L., Chambers, M. A., Deaguero, A. L., Wildeman, T. R., and Reisman, D. J. 2007. An innovative carbonate coprecipitation process for the removal of zinc and manganese from mining impacted waters. *Environmental Engineering Science,* 24: 881-896.

Sjörs, H. 1959. Bogs and fens in the Hudson Bay Lowlands. *Arctic,* 12(1): 2-19.

Spijker, J., Vriend, S. P., and van Gaans, P.F.M. 2005. Natural and anthropogenic patterns of covariance and spatial variability of minor and trace elements in agricultural topsoil. *Geoderma,* 127(1-2): 24-35.

Stanley, C. R. 2006. Numerical transformation of geochemical data: 1. Maximizing geochemical contrast to facilitate information extraction and improve data presentation. *Geochemistry: Exploration, Environment, Analysis,* 6: 69-78.

Swan, A.R.H., and Sandilands, M. 1995. *Introduction to Geological Data Analysis.* Blackwell Science, Boston, 446 p.

Tripathi, V. S. 1979. Factor analysis in geochemical exploration. *Journal of Geochemical Exploration,* 11: 263-275.

van Helvoort, P. J., Filzmoser, P., and van Gaans, P.F.M. 2005. Sequential factor analysis as a new approach to multivariate analysis of heterogeneous geochemical datasets: An application to a bulk chemical characterization of fluvial deposits (Rhine-Meuse delta, The Netherlands). *Applied Geochemistry,* 20: 2233-2251.

Webb, K. J., et al. 2004. Geology of the Victor kimberlite, Attawapiskat, Northern Ontario, Canada: cross-cutting and nested craters. *Lithos,* 76: 29-50

Appendix A: 0.2m BGS dataset

Appendix A: 0.2m BGS dataset

Analytical method :			ICP-MS	ICP-MS	ICP-MS	ICP-MS	ICP-MS	ICP-MS	ICP-MS	ICP-MS	ICP-MS
Element/parameter :			Al	Ba	Ca	Cd	Ce	Co	Cr	Cs	Fe
Units :			ppb	ppb	ppb	ppb	ppb	ppb	ppb	ppb	ppb
Detection limits :			0.1	0.03	200	0.002	0.0002	0.006	0.004	0.0003	0.4
Sample code	Site	Sample number									
06-A01	A	A1	116.6	669.68	1010	0.058	0.11750	0.048	0.508	0.0057	155.3
06-A02	A	A2	74.7	739.35	772	0.080	0.12730	0.052	1.276	0.0038	110.8
06-A03	A	A3	83.9	533.48	667	0.048	0.12000	0.044	0.465	0.0037	141.0
06-A04	A	A4	85.1	481.42	638	0.052	0.13400	0.037	0.438	0.0035	151.6
06-A05	A	A5	76.6	553.76	716	0.058	0.11820	0.039	0.389	0.0043	126.7
06-A06	A	A6	81.2	506.43	892	0.058	0.10700	0.040	0.441	0.0041	117.7
06-A07	A	A7	94.0	617.70	799	0.082	0.11500	0.042	0.437	0.0035	157.6
06-A08	A	A8	74.3	501.14	905	0.055	0.10580	0.077	0.432	0.0083	123.6
06-A09	A	A9	60.1	394.67	846	0.099	0.08630	0.049	0.407	0.0058	194.8
06-A10	A	A10	92.8	625.03	986	0.074	0.12180	0.052	0.619	0.0069	185.5
06-A11	A	A11	78.7	649.91	1011	0.091	0.12050	0.054	0.653	0.0041	233.4
06-A12	A	A12	91.8	626.23	751	0.070	0.13850	0.053	0.758	0.0042	170.7
06-A13	A	A13	88.3	621.49	887	0.085	0.11990	0.057	0.676	0.0034	180.7
06-A14	A	A14	77.6	596.82	923	0.149	0.10130	0.048	0.650	0.0031	211.4
06-A15	A	A15	84.0	521.32	1176	0.064	0.08760	0.041	0.452	0.0034	193.5
06-A16	A	A16	108.7	694.76	2078	0.080	0.13450	0.068	1.117	0.0078	264.6
06-A17	A	A17	78.3	589.39	1628	0.081	0.10110	0.077	0.724	0.0040	236.3
06-A18	A	A18	90.1	891.80	1710	0.077	0.14230	0.084	1.958	0.0055	342.6
06-A19	A	A19	86.1	613.00	1446	0.097	0.12600	0.052	0.513	0.0086	262.1
06-A20	A	A20	62.2	766.52	2150	0.076	0.09090	0.056	1.179	0.0030	237.4
06-A21	A	A21	68.1	597.75	2227	0.100	0.09480	0.066	0.522	0.0041	258.1
06G-01	G	G1	75.3	280.64	3681	0.043	0.06610	0.034	0.225	0.0020	195.3
06G-02	G	G2	68.9	252.44	1721	0.043	0.06660	0.041	0.261	0.0021	157.0
06G-03	G	G3	112.4	256.87	2600	0.082	0.09510	0.044	0.398	0.0025	234.0
06G-04	G	G4	88.4	349.18	2948	0.076	0.07260	0.061	0.843	0.0035	173.9
06G-05	G	G5	98.0	2.46	2351	0.090	0.07540	0.064	0.374	0.0274	152.4
06G-06	G	G6	85.2	309.76	1804	0.227	0.08280	0.056	0.324	0.0051	224.7
06G-07	G	G7	76.4	521.28	1835	0.129	0.08910	0.068	1.059	0.0041	201.3
06G-08	G	G8	68.6	292.16	1550	0.048	0.07380	0.042	0.289	0.0122	163.6
06G-09	G	G9	66.1	403.70	1434	0.045	0.06150	0.045	0.680	0.0042	143.6
06G-10	G	G10	58.4	263.41	1992	0.028	0.06260	0.031	0.236	0.0017	221.9
06G-11	G	G11	60.4	229.99	1464	0.062	0.06520	0.036	0.319	0.0024	189.2
06G-12	G	G12	43.4	248.83	5420	0.031	0.04770	0.030	0.408	0.0020	788.7

Appendix A: 0.2m BGS dataset

Analytical method :			ICP-MS	ICP-MS	ICP-MS	ICP-MS	ICP-MS	ICP-MS	ICP-MS	ICP-MS	ICP-MS
Element/parameter :			Ga	Li	Mg	Mn	Mo	Ni	Pb	Rb	Sb
Units :			ppb	ppb	ppb	ppb	ppb	ppb	ppb	ppb	ppb
Detection limits :			0.001	0.02	50	0.08	0.005	0.08	0.002	0.07	0.003
Sample code	Site	Sample number									
06-A01	A	A1	0.072	0.22	180	1.30	0.074	0.30	0.605	0.33	0.042
06-A02	A	A2	0.061	0.17	135	1.24	0.092	0.34	0.851	0.25	0.061
06-A03	A	A3	0.062	0.14	135	1.47	0.058	0.40	0.762	0.22	0.048
06-A04	A	A4	0.060	0.14	137	1.70	0.073	0.27	0.761	0.21	0.041
06-A05	A	A5	0.054	0.13	124	4.29	0.066	0.40	0.779	0.22	0.041
06-A06	A	A6	0.062	0.15	136	1.48	0.172	0.45	0.856	0.23	0.046
06-A07	A	A7	0.063	0.17	152	1.21	0.055	0.28	0.866	0.24	0.038
06-A08	A	A8	0.048	0.18	135	3.33	0.147	1.27	0.708	0.29	0.040
06-A09	A	A9	0.047	0.15	142	3.21	0.222	0.59	0.574	0.23	0.118
06-A10	A	A10	0.054	0.15	129	1.92	0.059	0.36	0.780	0.24	0.048
06-A11	A	A11	0.050	0.16	152	2.42	0.086	0.50	1.061	0.31	0.058
06-A12	A	A12	0.060	0.16	168	1.13	0.240	0.35	0.921	0.26	0.044
06-A13	A	A13	0.059	0.19	211	2.65	0.236	0.57	1.019	0.27	0.049
06-A14	A	A14	0.048	0.22	222	0.86	0.054	0.24	0.654	0.21	0.039
06-A15	A	A15	0.052	0.21	186	0.68	0.040	0.31	0.516	0.23	0.034
06-A16	A	A16	0.046	0.27	259	1.39	0.075	5.47	1.300	0.32	0.107
06-A17	A	A17	0.041	0.21	178	0.90	0.070	0.58	0.764	0.24	0.046
06-A18	A	A18	0.046	0.25	248	2.67	0.102	1.33	1.230	0.31	0.078
06-A19	A	A19	0.047	0.19	165	1.45	0.059	0.51	0.970	0.22	0.040
06-A20	A	A20	0.029	0.24	238	1.78	0.075	0.37	0.805	0.18	0.048
06-A21	A	A21	0.034	0.24	237	3.72	0.052	0.68	0.688	0.22	0.062
06G-01	G	G1	0.026	0.41	388	1.72	0.023	0.19	0.492	0.20	0.028
06G-02	G	G2	0.035	0.37	319	4.42	0.032	0.34	0.604	0.15	0.038
06G-03	G	G3	0.037	0.51	462	6.09	0.029	0.27	0.310	0.20	0.038
06G-04	G	G4	0.027	0.52	536	1.69	0.041	0.23	0.274	0.27	0.033
06G-05	G	G5	0.032	0.41	382	3.19	0.047	0.79	0.382	0.80	0.123
06G-06	G	G6	0.034	0.29	286	3.93	0.056	0.74	0.723	0.26	0.054
06G-07	G	G7	0.033	0.34	264	1.57	0.061	0.28	0.308	0.16	0.031
06G-08	G	G8	0.036	0.27	263	11.94	0.029	3.14	0.658	0.29	0.034
06G-09	G	G9	0.026	0.28	258	1.76	0.046	0.23	0.214	0.17	0.024
06G-10	G	G10	0.029	0.39	385	1.45	0.019	0.24	0.710	0.20	0.030
06G-11	G	G11	0.030	0.35	296	1.04	0.044	0.44	0.764	0.18	0.042
06G-12	G	G12	0.012	0.84	599	2.04	0.035	0.18	0.284	0.11	0.024

Appendix A: 0.2m BGS dataset

Analytical method :			ICP-MS	ICP-MS	ICP-MS	ICP-MS	ICP-MS	ICP-MS	ICP-MS	ICP-MS	ICP-MS
Element/parameter :			Sn	Sr	Th	Ti	Tl	U	V	Y	Zn
Units :			ppb	ppb	ppb	ppb	ppb	ppb	ppb	ppb	ppb
Detection limits :			0.004	2	0.001	0.001	0.0002	0.001	0.03	0.003	0.100
Sample code	Site	Sample number									
06-A01	A	A1	0.116	5	0.012	2.806	0.0040	0.0058	0.19	0.152	544.9
06-A02	A	A2	0.076	5	0.009	1.607	0.0046	0.0050	0.21	0.189	562.6
06-A03	A	A3	0.038	4	0.010	1.567	0.0042	0.0045	0.17	0.142	473.4
06-A04	A	A4	0.033	3	0.012	1.884	0.0047	0.0043	0.17	0.137	337.7
06-A05	A	A5	0.039	4	0.009	1.625	0.0028	0.0047	0.19	0.140	470.0
06-A06	A	A6	0.041	3	0.012	1.749	0.0043	0.0052	0.22	0.114	359.8
06-A07	A	A7	0.044	4	0.012	1.800	0.0043	0.0051	0.20	0.120	460.8
06-A08	A	A8	0.046	4	0.014	1.767	0.0052	0.0062	0.17	0.107	430.0
06-A09	A	A9	0.115	3	0.008	1.537	0.0028	0.0035	0.24	0.102	218.7
06-A10	A	A10	0.051	4	0.012	2.189	0.0032	0.0064	0.19	0.152	474.0
06-A11	A	A11	0.037	5	0.012	1.468	0.0040	0.0048	0.23	0.157	506.7
06-A12	A	A12	0.088	4	0.012	2.013	0.0064	0.0059	0.28	0.165	503.2
06-A13	A	A13	0.035	4	0.010	1.698	0.0062	0.0054	0.25	0.162	483.7
06-A14	A	A14	0.040	4	0.009	1.672	0.0038	0.0041	0.18	0.117	413.4
06-A15	A	A15	0.024	4	0.011	2.080	0.0040	0.0049	0.15	0.096	422.8
06-A16	A	A16	0.187	7	0.010	2.387	0.0044	0.0052	0.20	0.173	548.4
06-A17	A	A17	0.029	5	0.009	1.540	0.0038	0.0042	0.18	0.143	478.2
06-A18	A	A18	0.044	7	0.010	1.766	0.0049	0.0049	0.26	0.221	557.5
06-A19	A	A19	0.032	5	0.011	1.792	0.0036	0.0047	0.21	0.158	461.4
06-A20	A	A20	0.020	6	0.008	1.315	0.0031	0.0037	0.17	0.149	495.6
06-A21	A	A21	0.038	6	0.008	1.579	0.0029	0.0041	0.17	0.126	461.0
06G-01	G	G1	0.785	7	0.008	1.818	0.0031	0.0034	0.17	0.040	133.7
06G-02	G	G2	0.122	5	0.008	1.562	0.0044	0.0027	0.14	0.041	171.0
06G-03	G	G3	0.101	7	0.009	2.018	0.0050	0.0036	0.15	0.049	168.9
06G-04	G	G4	0.090	8	0.010	2.053	0.0042	0.0042	0.16	0.055	313.3
06G-05	G	G5	0.160	5	0.012	2.539	0.0098	0.0037	0.21	0.029	13.4
06G-06	G	G6	0.077	5	0.012	2.027	0.0040	0.0040	0.16	0.051	168.0
06G-07	G	G7	0.067	7	0.010	2.004	0.0040	0.0052	0.15	0.072	515.3
06G-08	G	G8	0.114	4	0.009	1.552	0.0054	0.0032	0.16	0.047	197.4
06G-09	G	G9	0.199	6	0.011	2.163	0.0035	0.0046	0.13	0.055	344.8
06G-10	G	G10	0.145	5	0.007	1.246	0.0047	0.0027	0.15	0.040	197.4
06G-11	G	G11	0.116	4	0.010	1.686	0.0054	0.0029	0.17	0.041	111.9
06G-12	G	G12	0.040	10	0.004	1.365	0.0031	0.0017	0.09	0.032	167.0

Appendix A: 0.2m BGS dataset

Analytical method :			ICP-AES	ICP-AES	ICP-AES			
Element/parameter :			Na	Si	K	pH	ORP	Eh
Units :			ppm	ppm	ppm		mV	mV
Detection limits :			0.2	0.05	1			
Sample code	Site	Sample number						
06-A01	A	A1	3.527	0.409	1.431	3.81	346.0	553.0
06-A02	A	A2	5.030	0.216	0.500	3.79	349.7	556.7
06-A03	A	A3	3.024	0.174	1.211	3.76	321.6	528.6
06-A04	A	A4	2.588	0.185	1.057	3.84	284.7	491.7
06-A05	A	A5	2.957	0.219	1.343	3.79	288.0	495.0
06-A06	A	A6	2.546	0.214	1.718	3.85	303.3	510.3
06-A07	A	A7	2.748	0.244	1.255	3.82	306.7	513.7
06-A08	A	A8	2.852	0.525	1.299	3.83	294.0	501.0
06-A09	A	A9	2.199	0.390	0.500	3.85	315.1	522.1
06-A10	A	A10	3.355	0.343	1.806	3.85	306.9	513.9
06-A11	A	A11	3.921	0.184	1.321	3.91	301.0	508.0
06-A12	A	A12	4.022	0.246	2.004	3.80	320.1	527.1
06-A13	A	A13	3.070	0.092	1.255	3.73	317.8	524.8
06-A14	A	A14	3.079	0.491	1.321	3.73	300.9	507.9
06-A15	A	A15	2.530	0.448	1.497	3.81	301.0	508.0
06-A16	A	A16	4.802	0.475	1.475	3.81	280.5	487.5
06-A17	A	A17	3.502	0.415	1.255	3.98	269.4	476.4
06-A18	A	A18	6.690	0.232	0.500	3.99	301.8	508.8
06-A19	A	A19	2.878	0.237	1.189	3.98	305.5	512.5
06-A20	A	A20	4.902	0.557	1.365	4.14	286.0	493.0
06-A21	A	A21	2.907	0.994	0.500	4.03	294.3	501.3
06G-01	G	G1	5.170	1.198	1.343	4.60	213.0	420.0
06G-02	G	G2	5.020	0.471	0.500	4.14	274.3	481.3
06G-03	G	G3	6.570	0.962	0.500	3.62	282.1	489.1
06G-04	G	G4	8.940	0.789	1.696	4.41	260.3	467.3
06G-05	G	G5	5.560	0.846	1.079	4.16	293.3	500.3
06G-06	G	G6	4.257	0.415	0.500	4.19	279.3	486.3
06G-07	G	G7	7.810	0.559	1.475	4.02	321.4	528.4
06G-08	G	G8	4.529	0.318	0.500	4.75	299.7	506.7
06G-09	G	G9	6.310	0.322	1.277	4.06	333.7	540.7
06G-10	G	G10	5.690	0.543	0.500	4.18	309.5	516.5
06G-11	G	G11	4.014	0.464	0.500	4.10	307.0	514.0
06G-12	G	G12	5.210	1.255	1.079	5.08	211.7	418.7

Appendix A: 0.2m BGS dataset

Analytical method :			ICP-MS	ICP-MS	ICP-MS	ICP-MS	ICP-MS	ICP-MS	ICP-MS	ICP-MS	ICP-MS
Element/parameter :			Al	Ba	Ca	Cd	Ce	Co	Cr	Cs	Fe
Units :			ppb	ppb	ppb	ppb	ppb	ppb	ppb	ppb	ppb
Detection limits :			0.1	0.03	200	0.002	0.0002	0.006	0.004	0.0003	0.4
Sample code	Site	Sample number									
06G-13	G	G13	23.1	168.30	10491	0.026	0.02510	0.062	0.290	0.0015	963.4
06G-14	G	G14	12.9	209.57	10275	0.036	0.02720	0.033	0.254	0.0016	262.4
06G-15	G	G15	9.9	174.88	13511	0.042	0.02320	0.042	0.351	0.0019	232.8
06G-16	G	G16	10.1	143.20	13090	0.051	0.01620	0.058	0.156	0.0013	639.9
06G-17	G	G17	9.8	207.11	9837	0.024	0.02100	0.032	0.999	0.0013	257.5
06Y-01	Y	6Y1	68.9	237.12	788	0.050	0.05850	0.032	0.214	0.0018	130.8
06Y-02	Y	6Y2	71.1	405.03	1172	0.053	0.06870	0.049	0.354	0.0028	204.2
06Y-03	Y	6Y3	92.6	502.98	1582	0.038	0.09050	0.060	0.535	0.0024	399.8
06Y-04	Y	6Y4	26.1	333.32	15998	0.047	0.03670	0.056	0.740	0.0017	50.0
06Y-05	Y	6Y5	53.4	176.32	2538	0.045	0.04070	0.023	0.188	0.0053	24.9
06Y-06	Y	6Y6	20.9	97.64	9434	0.176	0.05570	0.048	0.270	0.0026	26.1
06Y-07	Y	6Y7	134.8	144.84	1656	0.049	0.10530	0.042	0.219	0.0028	131.7
06Y-08	Y	6Y8	114.0	182.32	1458	0.066	0.13350	0.305	0.252	0.0037	526.5
06Y-09	Y	6Y9	138.1	1260.00	2085	0.075	0.24240	0.090	1.836	0.0083	168.9
06Y-10	Y	6Y10	98.5	212.92	1762	0.077	0.09040	0.085	0.318	0.0057	147.8
06Y-11	Y	6Y11	41.2	161.56	29158	0.044	0.04640	0.205	0.398	0.0011	1800.0
06Y-12	Y	6Y12	21.8	164.02	11748	0.036	0.02650	0.221	0.278	0.0014	438.6
06Y-14	Y	6Y14	111.7	287.44	1181	0.067	0.10810	0.062	0.418	0.0024	175.0
06Y-15	Y	6Y15	98.6	331.31	1253	0.154	0.10880	0.048	0.263	0.0149	221.7
06Y-17	Y	6Y17	96.4	437.16	1115	0.128	0.11920	0.054	0.537	0.0064	265.5

Appendix A: 0.2m BGS dataset

Analytical method :			ICP-MS	ICP-MS	ICP-MS	ICP-MS	ICP-MS	ICP-MS	ICP-MS	ICP-MS	ICP-MS
Element/parameter :			Ga	Li	Mg	Mn	Mo	Ni	Pb	Rb	Sb
Units :			ppb	ppb	ppb	ppb	ppb	ppb	ppb	ppb	ppb
Detection limits :			0.001	0.02	50	0.08	0.005	0.08	0.002	0.07	0.003
Sample code	Site	Sample number									
06G-13	G	G13	0.010	0.70	1021	5.83	0.068	0.26	0.288	0.11	0.025
06G-14	G	G14	0.007	0.43	916	5.19	0.046	0.28	0.412	0.08	0.032
06G-15	G	G15	0.006	0.48	1188	5.13	0.047	0.44	1.288	0.14	0.045
06G-16	G	G16	0.007	0.54	1340	4.13	0.038	0.45	0.276	0.00	0.053
06G-17	G	G17	0.005	0.49	1081	1.49	0.109	0.52	0.113	0.00	0.016
06Y-01	Y	6Y1	0.034	0.15	166	5.16	0.025	0.16	0.363	0.12	0.033
06Y-02	Y	6Y2	0.030	0.15	156	1.42	0.046	0.32	0.418	0.16	0.029
06Y-03	Y	6Y3	0.046	0.16	119	0.92	0.054	0.19	0.431	0.11	0.035
06Y-04	Y	6Y4	0.009	0.16	408	9.85	0.065	0.23	0.301	0.04	0.026
06Y-05	Y	6Y5	0.024	0.13	91	0.37	0.024	0.25	0.277	0.12	0.017
06Y-06	Y	6Y6	0.008	0.13	234	2.28	0.026	0.62	1.680	0.10	0.056
06Y-07	Y	6Y7	0.044	0.16	239	0.71	0.042	0.21	0.232	0.18	0.031
06Y-08	Y	6Y8	0.045	0.14	517	1.32	0.052	1.10	0.399	0.16	0.031
06Y-09	Y	6Y9	0.067	0.20	196	1.52	0.178	0.57	1.192	0.31	0.056
06Y-10	Y	6Y10	0.036	0.20	205	1.32	0.045	1.00	0.564	0.22	0.031
06Y-11	Y	6Y11	0.018	0.90	1783	35.14	0.840	0.60	0.321	0.04	0.026
06Y-12	Y	6Y12	0.022	0.16	384	160.00	0.286	0.28	0.194	0.04	0.020
06Y-14	Y	6Y14	0.047	0.16	199	1.16	0.060	0.42	0.606	0.16	0.045
06Y-15	Y	6Y15	0.055	0.14	171	2.23	0.080	0.59	0.788	0.28	0.048
06Y-17	Y	6Y17	0.065	0.16	139	1.47	0.075	0.93	1.010	0.34	0.060

Appendix A: 0.2m BGS dataset

Analytical method :			ICP-MS	ICP-MS	ICP-MS	ICP-MS	ICP-MS	ICP-MS	ICP-MS	ICP-MS	ICP-MS
Element/parameter :			Sn	Sr	Th	Ti	Tl	U	V	Y	Zn
Units :			ppb	ppb	ppb	ppb	ppb	ppb	ppb	ppb	ppb
Detection limits :			0.004	2	0.001	0.001	0.0002	0.001	0.03	0.003	0.100
Sample code	Site	Sample number									
06G-13	G	G13	0.042	15	0.002	0.860	0.0022	0.0012	0.08	0.019	195.2
06G-14	G	G14	0.031	14	0.002	0.700	0.0018	0.0011	0.08	0.021	252.1
06G-15	G	G15	0.032	18	0.002	0.922	0.0013	0.0013	0.05	0.018	227.8
06G-16	G	G16	0.024	20	0.001	0.863	0.0009	0.0011	0.05	0.015	207.2
06G-17	G	G17	0.005	14	0.001	0.705	0.0011	0.0007	0.05	0.020	207.6
06Y-01	Y	6Y1	0.118	3	0.008	1.322	0.0032	0.0023	0.14	0.037	122.8
06Y-02	Y	6Y2	0.074	4	0.009	1.857	0.0036	0.0044	0.16	0.048	288.3
06Y-03	Y	6Y3	0.048	6	0.013	2.219	0.0031	0.0050	0.25	0.059	363.1
06Y-04	Y	6Y4	0.016	15	0.004	0.800	0.0017	0.0026	0.10	0.034	243.7
06Y-05	Y	6Y5	0.031	4	0.010	1.800	0.0012	0.0037	0.15	0.025	121.7
06Y-06	Y	6Y6	0.049	8	0.004	0.972	0.0012	0.0021	0.11	0.019	92.6
06Y-07	Y	6Y7	0.080	4	0.015	3.024	0.0030	0.0047	0.20	0.047	92.0
06Y-08	Y	6Y8	0.070	4	0.014	2.919	0.0021	0.0048	0.24	0.056	90.6
06Y-09	Y	6Y9	0.072	9	0.019	4.420	0.0036	0.0125	0.42	0.320	960.8
06Y-10	Y	6Y10	0.063	3	0.013	3.111	0.0025	0.0053	0.20	0.046	133.4
06Y-11	Y	6Y11	0.032	26	0.006	2.039	0.0018	0.0031	0.21	0.043	241.0
06Y-12	Y	6Y12	0.027	10	0.002	0.879	0.0012	0.0013	0.07	0.024	233.5
06Y-14	Y	6Y14	0.069	4	0.013	2.772	0.0027	0.0058	0.28	0.058	185.4
06Y-15	Y	6Y15	0.117	3	0.012	2.160	0.0046	0.0034	0.22	0.056	78.0
06Y-17	Y	6Y17	0.196	3	0.014	2.790	0.0031	0.0039	0.33	0.089	153.2

Appendix A: 0.2m BGS dataset

Analytical method :			ICP-AES	ICP-AES	ICP-AES			
Element/parameter :			Na	Si	K	pH	ORP	Eh
Units :			ppm	ppm	ppm		mV	mV
Detection limits :			0.2	0.05	1			
Sample code	Site	Sample number						
06G-13	G	G13	6.940	0.603	1.012	5.85	125.7	332.7
06G-14	G	G14	4.047	0.697	0.500	6.03	175.7	382.7
06G-15	G	G15	4.156	0.884	0.500	6.26	159.1	366.1
06G-16	G	G16	3.993	1.205	0.500	5.96	186.7	393.7
06G-17	G	G17	3.754	1.097	0.500	6.17	152.6	359.6
06Y-01	Y	6Y1	1.746	0.261	2.137	3.94	299.1	506.1
06Y-02	Y	6Y2	3.033	0.742	1.431	3.99	297.3	504.3
06Y-03	Y	6Y3	3.389	0.369	1.850	3.91	313.8	520.8
06Y-04	Y	6Y4	2.882	0.321	1.057	6.02	218.9	425.9
06Y-05	Y	6Y5	1.905	0.185	0.500	4.72	300.9	507.9
06Y-06	Y	6Y6	1.658	0.296	0.500	5.55	250.4	457.4
06Y-07	Y	6Y7	1.322	0.335	0.500	3.93	343.4	550.4
06Y-08	Y	6Y8	1.532	0.701	0.500	3.99	301.4	508.4
06Y-09	Y	6Y9	8.210	0.492	1.586	3.92	345.2	552.2
06Y-10	Y	6Y10	1.721	0.601	1.299	4.00	341.0	548.0
06Y-11	Y	6Y11	2.563	1.761	0.500	6.04	157.8	364.8
06Y-12	Y	6Y12	2.207	0.654	0.500	5.79	187.4	394.4
06Y-14	Y	6Y14	2.437	0.450	0.500	3.92	311.3	518.3
06Y-15	Y	6Y15	1.436	0.298	0.500	3.90	311.4	518.4
06Y-17	Y	6Y17	2.127	0.337	2.071	3.85	340.4	547.4

Appendix B: 1.1m BGS dataset

Appendix B – 1.1m BGS dataset

Analytical method :			ICP-MS	ICP-MS	ICP_AES	ICP-MS	ICP-MS	ICP-MS	ICP-MS	ICP-MS	ICP_AES
Element/parameter :			Al	Ba	Ca	Cd	Ce	Co	Cr	Cs	Fe
Units :			ppb	ppb	ppb	ppb	ppb	ppb	ppb	ppb	ppb
Detection limits :			5	0.02	70	0.01	0.002	0.005	0.02	0.0005	10
Sample code	Site	Sample number									
07-Y-01	Y7	7Y1	82	2.80	7010.6	0.05	0.059	0.129	0.34	0.0215	404.1
07-Y-02	Y7	7Y2	87	2.62	7875.0	0.04	0.069	0.388	0.11	0.0352	252.2
07-Y-03	Y7	7Y3	78	2.69	56832.4	0.04	0.068	0.183	0.15	0.0087	26.1
07-Y-04	Y7	7Y4	33	3.11	9266.9	0.02	0.150	0.243	0.10	0.0010	254.1
07-Y-06	Y7	7Y6	78	3.04	5846.6	0.10	0.097	0.400	0.20	0.0122	168.6
07-Y-07	Y7	7Y7	89	3.26	23641.1	0.14	0.109	0.164	0.26	0.0031	353.0
07-Y-08	Y7	7Y8	176	58.06	20817.5	0.04	2.386	5.412	4.79	0.0038	532.1
07-Y-09	Y7	7Y9	146	8.65	5049.5	0.19	0.123	0.308	0.21	0.0251	107.6
07-Y-10	Y7	7Y10	92	2.41	61837.7	0.15	0.077	0.096	0.18	0.0107	3524.4
07-Y-11	Y7	7Y11	11	8.57	14067.1	0.08	0.075	0.239	0.24	0.0130	4318.9
07-Y-12	Y7	7Y12	15	6.41	2455.0	0.04	0.017	0.429	0.09	0.0046	127.3
07-Y-13	Y7	7Y13	73	1.71	3163.7	0.07	0.063	0.148	0.18	0.0131	138.8
07-Y-14A	Y7	7Y14	84	2.11	3014.5	0.14	0.065	0.100	0.39	0.0168	127.7
07-Y-15	Y7	7Y15	105	2.00	5860.0	0.15	0.102	0.154	0.34	0.0134	415.7
07-Y-16	Y7	7Y16	109	3.05	9318.7	0.17	0.132	0.178	0.46	0.0154	1324.0
07-Y-17	Y7	7Y17	79	2.92	56927.3	0.11	0.100	0.166	0.29	0.0202	31.6
07-Z-07	Z	Z7Z	56	3.66	6946.1	0.03	0.058	0.210	0.08	0.0166	498.4
07-Z-09	Z	7Z9	62	3.32	8955.6	0.14	0.076	0.082	0.23	0.0291	603.9
07-Z-11	Z	7Z11	65	3.29	2683.5	0.06	0.070	0.121	0.13	0.0079	244.4
07-Z-13	Z	7Z13	55	7.80	2252.0	0.25	0.078	0.199	1.10	0.0283	137.6
07-Z-15	Z	7Z15	64	6.31	20440.3	0.23	0.099	0.175	0.41	0.0041	490.3
07-Z-17	Z	7Z17	82	20.72	35327.8	0.26	0.123	0.306	0.25	0.0192	217.6
07-Z-19	Z	7Z19.	11	49.97	17546.4	0.19	0.077	0.426	0.25	0.0418	221.8
07-Z-21	Z	7Z21	8	18.49	25889.3	0.19	0.033	0.218	0.11	0.0347	933.7
07-Z-23	Z	7Z23	5	12.83	35891.1	0.04	0.017	0.395	0.08	0.0364	1402.5
07-Z-25	Z	7Z25	5	15.89	20127.8	0.13	0.020	0.318	0.13	0.0320	783.7
07-Z-27	Z	7Z27	11	10.29	50261.3	0.06	0.027	0.391	0.12	0.0469	1975.2
07-Z-29	Z	7Z29	5	16.90	54743.4	0.05	0.009	0.353	0.05	0.0256	3104.5
07-Z-31	Z	7Z31	6	14.07	41443.7	0.09	0.016	0.261	0.06	0.0173	2334.7
07-Z-33	Z	7Z33	6	12.62	49064.8	0.02	0.018	0.252	0.07	0.0089	3019.9
07-Z-35	Z	7Z35	22	14.57	3486.1	1.49	0.054	0.288	0.08	0.0023	363.7
07-Z-53	Z	7Z53	68	2.37	2759.6	0.11	0.084	0.080	0.72	0.0419	147.7
07-Z-55	Z	7Z55	54	2.94	2873.6	0.19	0.063	0.075	0.39	0.0441	233.8
07-Z-59	Z	7Z59	36	1.88	2290.6	0.04	0.038	0.065	0.13	0.0124	141.6

Appendix B – 1.1m BGS dataset

Analytical method :			ICP-MS	ICP-MS	ICP_AES	ICP_AES	ICP-MS	ICP-MS	ICP-MS	ICP-MS	ICP-MS
Element/parameter :			Ga	Li	Mg	Mn	Mo	Ni	Pb	Rb	Sb
Units :			ppb	ppb	ppb	ppb	ppb	ppb	ppb	ppb	ppb
Detection limits :			0.002	0.01	6	2	0.01	0.1	0.05	0.005	0.01
Sample code	Site	Sample number									
07-Y-01	Y7	7Y1	0.020	0.13	388.6	20.5	0.06	0.4	0.52	0.894	0.08
07-Y-02	Y7	7Y2	0.025	0.17	333.7	2.8	0.04	0.6	0.66	1.334	0.04
07-Y-03	Y7	7Y3	0.014	0.17	926.0	65.1	0.05	0.5	0.53	0.217	0.04
07-Y-04	Y7	7Y4	0.028	0.26	928.9	10.5	0.05	1.5	0.10	0.296	0.04
07-Y-06	Y7	7Y6	0.017	0.16	691.8	31.8	0.06	0.6	1.28	0.471	0.09
07-Y-07	Y7	7Y7	0.021	0.12	11323.2	75.3	0.02	1.1	0.98	0.196	0.12
07-Y-08	Y7	7Y8	0.056	1.93	2039.2	33.1	0.05	65.7	0.17	0.588	0.04
07-Y-09	Y7	7Y9	0.036	0.22	381.4	14.9	0.02	0.9	0.59	1.117	0.03
07-Y-10	Y7	7Y10	0.016	0.11	2754.3	73.3	0.03	0.4	0.72	0.496	0.12
07-Y-11	Y7	7Y11	0.018	0.35	498.0	134.5	0.07	1.3	0.39	0.508	0.04
07-Y-12	Y7	7Y12	0.029	0.23	382.4	18.3	0.06	0.3	0.22	0.295	0.05
07-Y-13	Y7	7Y13	0.017	0.15	473.1	5.8	0.03	0.3	0.30	0.511	0.16
07-Y-14A	Y7	7Y14	0.020	0.12	470.7	4.9	0.08	0.9	0.47	0.805	0.25
07-Y-15	Y7	7Y15	0.022	0.16	480.4	33.4	0.05	0.6	0.40	0.615	0.26
07-Y-16	Y7	7Y16	0.028	0.18	445.3	23.2	0.05	1.1	0.81	0.660	0.09
07-Y-17	Y7	7Y17	0.018	0.27	926.2	64.6	0.07	0.4	0.32	0.681	0.06
07-Z-07	Z	Z7Z	0.013	0.42	386.5	5.8	0.02	0.4	0.43	0.407	0.03
07-Z-09	Z	7Z9	0.015	0.51	659.1	8.1	0.03	0.4	0.81	0.741	0.05
07-Z-11	Z	7Z11	0.014	0.44	794.6	7.9	0.05	0.4	0.47	0.143	0.04
07-Z-13	Z	7Z13	0.011	0.29	564.5	2.9	0.12	1.5	1.25	0.894	0.25
07-Z-15	Z	7Z15	0.015	0.22	3734.5	16.5	0.05	0.6	1.22	0.179	0.10
07-Z-17	Z	7Z17	0.026	2.26	5708.1	22.4	0.02	0.8	1.08	0.606	0.06
07-Z-19	Z	7Z19.	0.007	4.54	4864.7	4.4	0.10	0.9	0.39	2.968	0.12
07-Z-21	Z	7Z21	0.004	3.33	6712.6	19.9	0.04	0.2	0.65	2.345	0.02
07-Z-23	Z	7Z23	0.006	5.65	7109.0	28.5	0.03	0.1	0.17	2.545	0.07
07-Z-25	Z	7Z25	0.007	4.85	4842.0	51.2	0.04	0.1	0.22	2.152	0.06
07-Z-27	Z	7Z27	0.011	3.87	10834.9	70.9	0.04	0.2	0.16	3.772	0.06
07-Z-29	Z	7Z29	0.014	8.13	11501.3	97.3	0.03	0.1	0.09	1.753	0.02
07-Z-31	Z	7Z31	0.021	7.78	7855.9	36.9	0.04	0.1	0.17	1.388	0.02
07-Z-33	Z	7Z33	0.012	7.67	7800.4	78.6	0.03	0.1	0.13	0.881	0.02
07-Z-35	Z	7Z35	0.019	5.82	213.6	10.1	0.05	0.1	0.18	0.549	0.03
07-Z-53	Z	7Z53	0.015	0.32	298.3	5.5	0.03	0.3	1.15	1.233	0.08
07-Z-55	Z	7Z55	0.012	0.28	434.9	4.5	0.04	0.3	0.72	0.928	0.07
07-Z-59	Z	7Z59	0.008	0.30	268.5	8.0	0.02	0.2	0.22	0.121	0.06

Appendix B – 1.1m BGS dataset

Analytical method :			ICP-MS	ICP-MS	ICP-MS	ICP-MS	ICP-MS	ICP-MS	ICP-MS	ICP-MS	ICP-MS
Element/parameter :			Sn	Sr	Th	Ti	Tl	U	V	Y	Zn
Units :			ppb	ppb	ppb	ppb	ppb	ppb	ppb	ppb	ppb
Detection limits :			0.01	0.1	0.001	0.1	0.001	0.0002	0.003	0.0005	1
Sample code	Site	Sample number									
07-Y-01	Y7	7Y1	0.31	4.2	0.004	1.2	0.006	0.0020	0.163	0.0253	8.0
07-Y-02	Y7	7Y2	0.13	8.5	0.003	1.3	0.004	0.0026	0.136	0.0317	5.0
07-Y-03	Y7	7Y3	0.14	8.7	0.006	1.2	0.002	0.0018	0.125	0.0304	3.0
07-Y-04	Y7	7Y4	0.07	58.1	0.007	1.4	0.004	0.0344	0.399	0.1238	1.0
07-Y-06	Y7	7Y6	0.34	10.6	0.003	1.2	0.002	0.0035	0.141	0.0466	7.0
07-Y-07	Y7	7Y7	0.25	7.4	0.003	0.9	0.005	0.0021	0.253	0.0432	13.0
07-Y-08	Y7	7Y8	0.09	153.6	0.082	8.3	0.004	0.1339	1.110	0.3456	1.0
07-Y-09	Y7	7Y9	0.06	26.8	0.008	2.4	0.004	0.0055	0.208	0.0431	6.0
07-Y-10	Y7	7Y10	0.18	5.4	0.004	0.8	0.005	0.0022	0.205	0.0320	5.0
07-Y-11	Y7	7Y11	0.14	56.2	0.015	1.8	0.003	0.0064	0.283	0.0604	6.0
07-Y-12	Y7	7Y12	0.09	12.7	0.003	0.5	0.006	0.0013	0.059	0.0095	6.0
07-Y-13	Y7	7Y13	0.20	3.0	0.004	1.0	0.005	0.0022	0.100	0.0356	24.0
07-Y-14A	Y7	7Y14	0.55	3.8	0.004	1.2	0.005	0.0031	0.132	0.0263	7.0
07-Y-15	Y7	7Y15	0.69	4.2	0.004	1.3	0.004	0.0032	0.235	0.0357	7.0
07-Y-16	Y7	7Y16	0.46	6.2	0.008	1.6	0.006	0.0052	0.208	0.0411	10.0
07-Y-17	Y7	7Y17	0.32	8.5	0.008	2.0	0.004	0.0035	0.237	0.0370	7.0
07-Z-07	Z	Z7Z	0.09	26.9	0.002	0.9	0.003	0.0013	0.098	0.0216	2.0
07-Z-09	Z	7Z9	0.55	14.1	0.004	0.8	0.005	0.0026	0.106	0.0283	6.0
07-Z-11	Z	7Z11	0.33	16.4	0.003	0.9	0.002	0.0019	0.147	0.0261	2.0
07-Z-13	Z	7Z13	0.57	8.7	0.005	0.9	0.006	0.0041	0.141	0.0359	20.0
07-Z-15	Z	7Z15	0.32	9.5	0.008	1.1	0.004	0.0041	0.151	0.0317	7.0
07-Z-17	Z	7Z17	0.47	80.4	0.007	1.3	0.003	0.0061	0.164	0.0351	6.0
07-Z-19	Z	7Z19.	0.48	179.3	0.003	0.3	0.002	0.0029	0.106	0.0224	16.0
07-Z-21	Z	7Z21	0.19	96.1	0.002	0.1	0.002	0.0012	0.040	0.0116	4.0
07-Z-23	Z	7Z23	0.11	135.5	0.001	0.1	0.002	0.0009	0.047	0.0086	5.0
07-Z-25	Z	7Z25	0.08	149.8	0.002	0.2	0.002	0.0014	0.017	0.0088	4.0
07-Z-27	Z	7Z27	0.08	77.3	0.002	0.1	0.004	0.0014	0.060	0.0127	6.0
07-Z-29	Z	7Z29	0.06	215.3	0.001	0.1	0.002	0.0005	0.037	0.0104	1.0
07-Z-31	Z	7Z31	0.23	223.2	0.002	0.4	0.002	0.0010	0.021	0.0112	3.0
07-Z-33	Z	7Z33	0.27	133.5	0.003	0.1	0.002	0.0008	0.027	0.0104	2.0
07-Z-35	Z	7Z35	0.29	128.9	0.004	0.6	0.001	0.0020	0.142	0.0209	2.0
07-Z-53	Z	7Z53	0.99	6.3	0.007	0.8	0.004	0.0030	0.137	0.0310	9.0
07-Z-55	Z	7Z55	0.76	6.7	0.003	0.7	0.005	0.0024	0.113	0.0203	8.0
07-Z-59	Z	7Z59	0.12	8.2	0.003	0.4	0.002	0.0015	0.103	0.0128	3.0

Appendix B – 1.1m BGS dataset

Analytical method :			ICP-AES	ICP-AES	ICP-AES			
Element/parameter :			Na	Si	K	pH	ORP	Eh
Units :			ppb	ppb	ppb		mV	mV
Detection limits :			50	13	180			
Sample code	Site	Sample number						
07-Y-01	Y7	7Y1	444.6	1606.1	356.7	5.49	124.7	331.7
07-Y-02	Y7	7Y2	363.6	590.8	90.0	5.87	109.4	316.4
07-Y-03	Y7	7Y3	422.9	506.2	90.0	5.89	108.8	315.8
07-Y-04	Y7	7Y4	516.3	1862.2	90.0	7.71	53.3	260.3
07-Y-06	Y7	7Y6	393.9	1882.6	90.0	5.59	110.2	317.2
07-Y-07	Y7	7Y7	660.7	5355.5	90.0	5.77	108.9	315.9
07-Y-08	Y7	7Y8	473.4	2708.9	312.7	7.15	33.2	240.2
07-Y-09	Y7	7Y9	255.2	957.5	90.0	6.53	92.1	299.1
07-Y-10	Y7	7Y10	852.6	2783.6	90.0	6.21	109.0	316.0
07-Y-11	Y7	7Y11	325.5	1107.9	90.0	7.37	16.5	223.5
07-Y-12	Y7	7Y12	335.1	1262.0	245.9	6.83	51.2	258.2
07-Y-13	Y7	7Y13	325.8	1311.4	445.1	5.71	117.7	324.7
07-Y-14A	Y7	7Y14	247.7	1278.9	222.5	6.40	59.2	266.2
07-Y-15	Y7	7Y15	431.1	1456.4	190.7	6.11	95.5	302.5
07-Y-16	Y7	7Y16	503.3	1473.9	267.7	6.21	86.8	293.8
07-Y-17	Y7	7Y17	387.2	493.6	181.9	7.10	95.0	302.0
07-Z-07	Z	Z7Z	1140.5	2211.3	272.1	5.60	83.6	290.6
07-Z-09	Z	7Z9	753.6	797.7	90.0	5.27	120.2	327.2
07-Z-11	Z	7Z11	1055.9	1457.2	428.8	5.46	106.0	313.0
07-Z-13	Z	7Z13	345.4	628.9	90.0	5.27	118.4	325.4
07-Z-15	Z	7Z15	3315.7	5986.7	501.4	5.41	103.1	310.1
07-Z-17	Z	7Z17	12536.7	5668.5	2507.8	5.90	60.4	267.4
07-Z-19	Z	7Z19.	11401.7	4452.8	2621.5	6.15	-81.8	125.2
07-Z-21	Z	7Z21	20988.9	5043.6	2479.1	6.44	-16.7	190.3
07-Z-23	Z	7Z23	14069.1	5347.7	1780.0	6.06	17.4	224.4
07-Z-25	Z	7Z25	11015.1	4562.2	2650.1	5.74	34.7	241.7
07-Z-27	Z	7Z27	28549.8	7013.2	2222.6	5.77	31.5	238.5
07-Z-29	Z	7Z29	25512.0	5680.9	1630.4	5.90	25.3	232.3
07-Z-31	Z	7Z31	30586.1	5287.7	1031.9	6.21	-9.4	197.6
07-Z-33	Z	7Z33	25800.7	4940.0	808.4	6.39	-17.3	189.7
07-Z-35	Z	7Z35	1233.0	2529.6	334.0	5.93	-24.5	182.5
07-Z-53	Z	7Z53	448.8	1005.4	304.9	5.12	94.9	301.9
07-Z-55	Z	7Z55	428.5	2147.9	90.0	5.78	101.9	308.9
07-Z-59	Z	7Z59	298.8	927.9	90.0	4.72	100.0	307.0

Appendix B – 1.1m BGS dataset

Analytical method :			ICP-MS	ICP-MS	ICP_AES	ICP-MS	ICP-MS	ICP-MS	ICP-MS	ICP-MS	ICP_AES
Element/parameter :			Al	Ba	Ca	Cd	Ce	Co	Cr	Cs	Fe
Units :			ppb	ppb	ppb	ppb	ppb	ppb	ppb	ppb	ppb
Detection limits :			5	0.02	70	0.01	0.002	0.005	0.02	0.0005	10
Sample code	Site	Sample number									
07-Z-61	Z	7Z61	61	4.32	696.2	0.14	0.075	0.055	0.29	0.0260	84.8
07-Z-62	Z	7Z62	70	7.59	41700.2	0.04	0.045	0.038	1.14	0.0349	403.2
Z-07-12C	Z	7Z12C	11	127.74	2451.3	0.01	0.090	0.818	0.67	0.0579	206.5

Appendix B – 1.1m BGS dataset

Analytical method :			ICP-MS	ICP-MS	ICP_AES	ICP_AES	ICP-MS	ICP-MS	ICP-MS	ICP-MS	ICP-MS
Element/parameter :			Ga	Li	Mg	Mn	Mo	Ni	Pb	Rb	Sb
Units :			ppb	ppb	ppb	ppb	ppb	ppb	ppb	ppb	ppb
Detection limits :			0.002	0.01	6	2	0.01	0.1	0.05	0.005	0.01
Sample code	Site	Sample number									
07-Z-61	Z	7Z61	0.010	0.17	163.1	7.9	0.03	0.3	0.59	0.313	0.12
07-Z-62	Z	7Z62	0.018	0.31	34638.0	10.9	0.06	0.3	0.23	0.487	0.03
Z-07-12C	Z	7Z12C	0.014	41.65	155.5	4.4	1.41	28.5	0.16	3.599	0.09

Appendix B – 1.1m BGS dataset

Analytical method :			ICP-MS	ICP-MS	ICP-MS	ICP-MS	ICP-MS	ICP-MS	ICP-MS	ICP-MS	ICP-MS
Element/parameter :			Sn	Sr	Th	Ti	Tl	U	V	Y	Zn
Units :			ppb	ppb	ppb	ppb	ppb	ppb	ppb	ppb	ppb
Detection limits :			0.01	0.1	0.001	0.1	0.001	0.0002	0.003	0.0005	1
Sample code	Site	Sample number									
07-Z-61	Z	7Z61	1.00	6.2	0.005	0.7	0.003	0.0032	0.175	0.0243	5.0
07-Z-62	Z	7Z62	0.43	4.1	0.008	2.6	0.003	0.0033	0.200	0.0144	3.0
Z-07-12C	Z	7Z12C	0.02	535.0	0.001	1.1	0.001	0.0785	2.458	0.0208	3.0

Appendix B – 1.1m BGS dataset

Analytical method :			ICP-AES	ICP-AES	ICP-AES			
Element/parameter :			Na	Si	K	pH	ORP	Eh
Units :			ppb	ppb	ppb		mV	mV
Detection limits :			50	13	180			
Sample code	Site	Sample number						
07-Z-61	Z	7Z61	326.7	466.3	90.0	4.85	102.1	309.1
07-Z-62	Z	7Z62	117766.1	6217.6	9470.3	4.26	-6.8	200.2
Z-07-12C	Z	7Z12C	365.1	907.6	90.0	7.51	-139.1	67.9

Appendix C: Normal QQ plots for the 0.2m dataset – raw data

Appendix C: Normal QQ plots for the 0.2m dataset – raw data

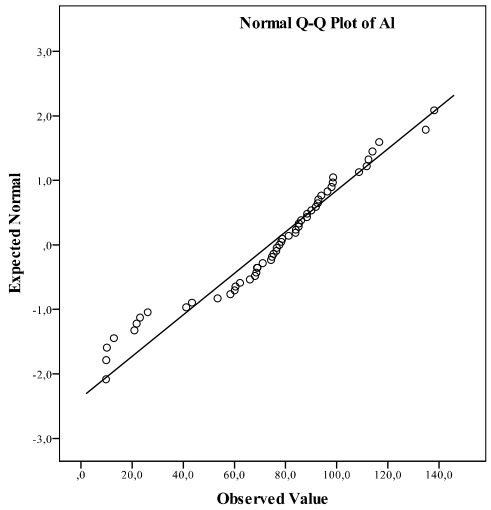

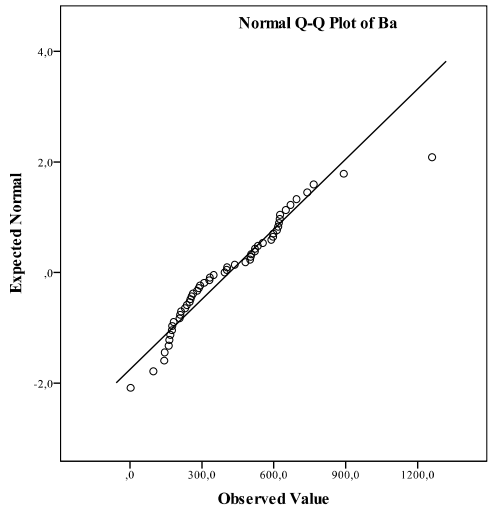

Appendix C: Normal QQ plots for the 0.2m dataset – raw data

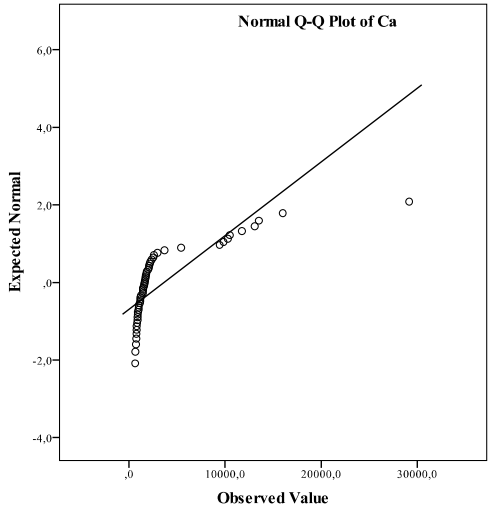

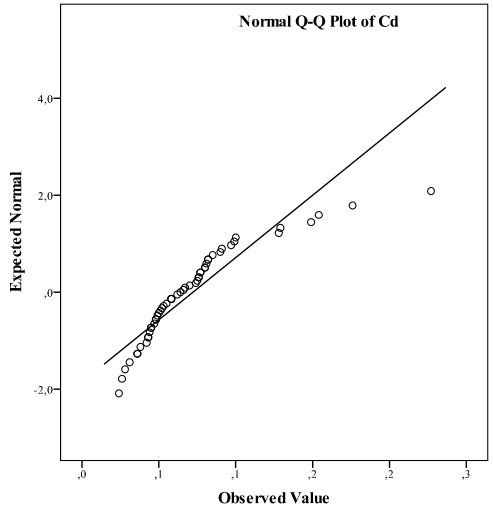

Appendix C: Normal QQ plots for the 0.2m dataset – raw data

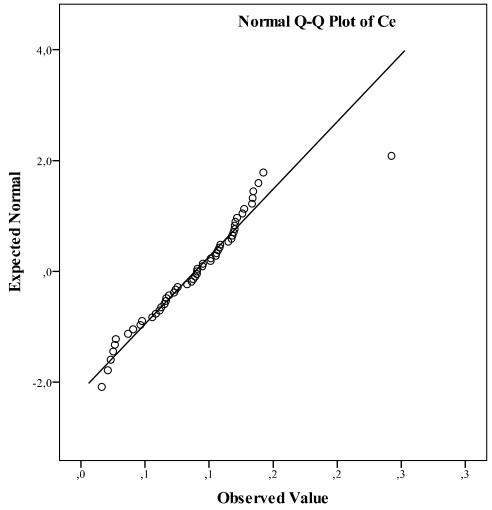

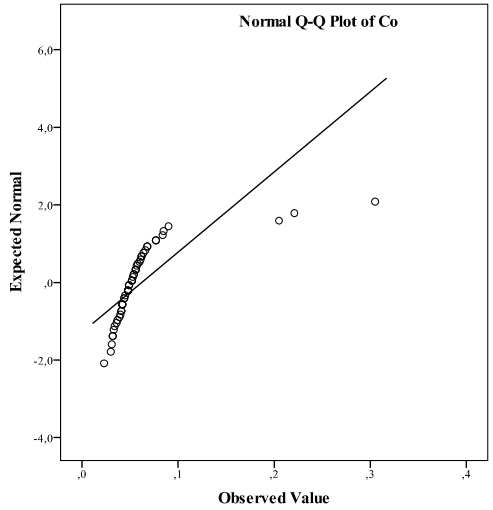

Appendix C: Normal QQ plots for the 0.2m dataset – raw data

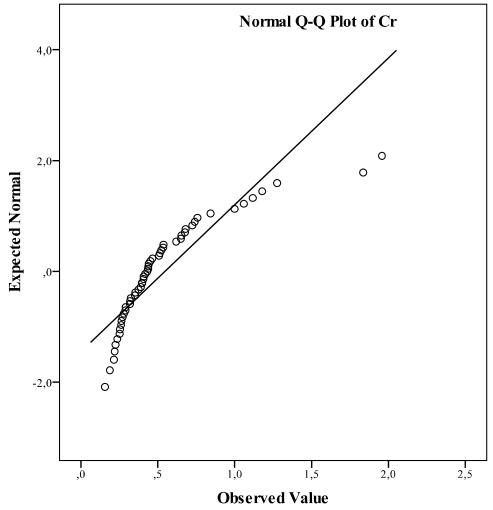

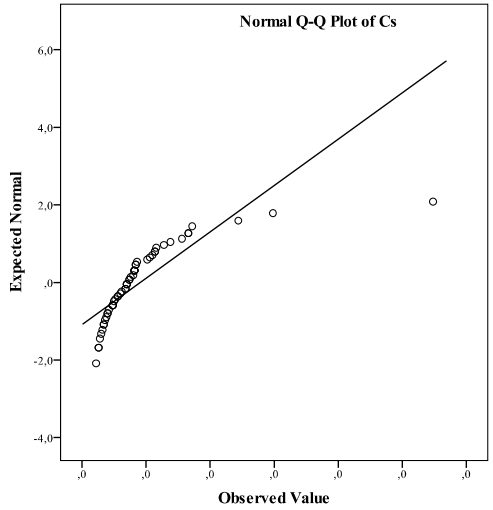

Appendix C: Normal QQ plots for the 0.2m dataset – raw data

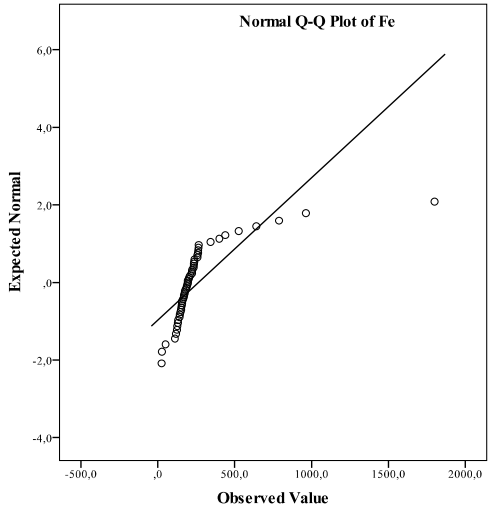

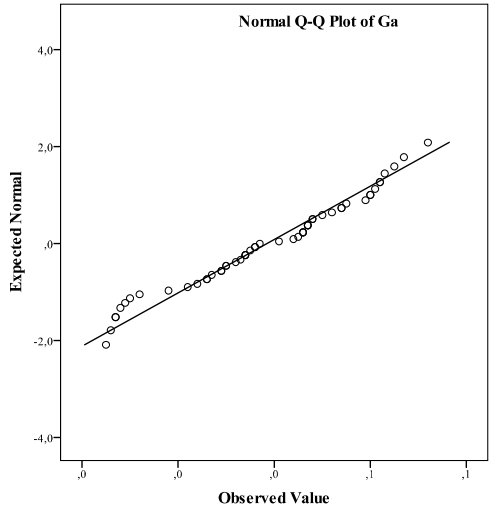

Appendix C: Normal QQ plots for the 0.2m dataset – raw data

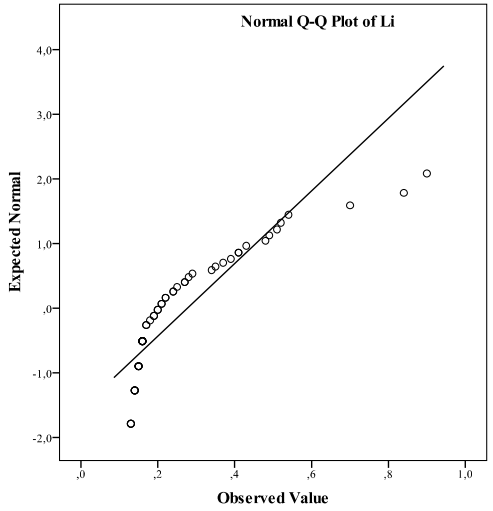

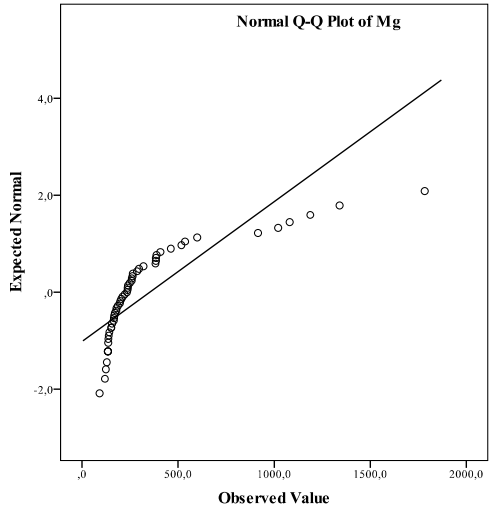

Appendix C: Normal QQ plots for the 0.2m dataset – raw data

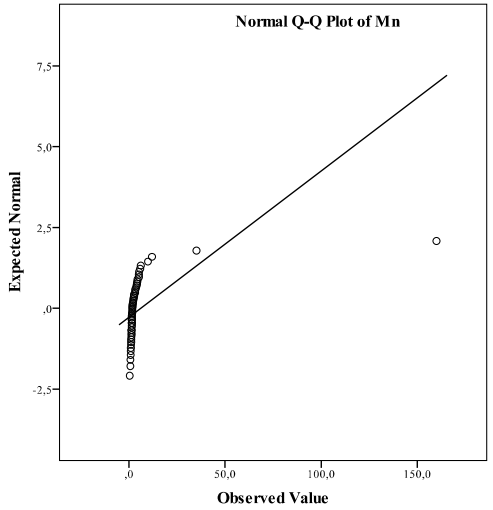

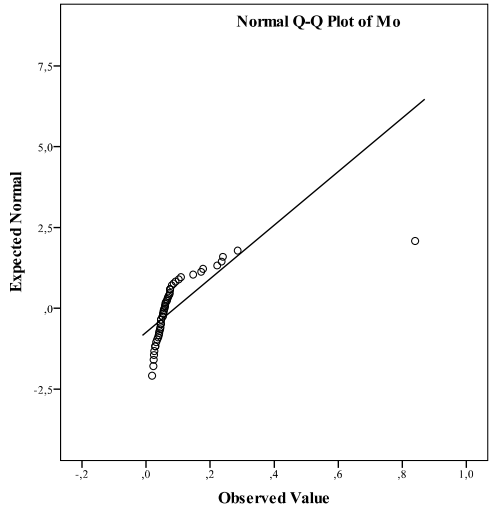

Appendix C: Normal QQ plots for the 0.2m dataset – raw data

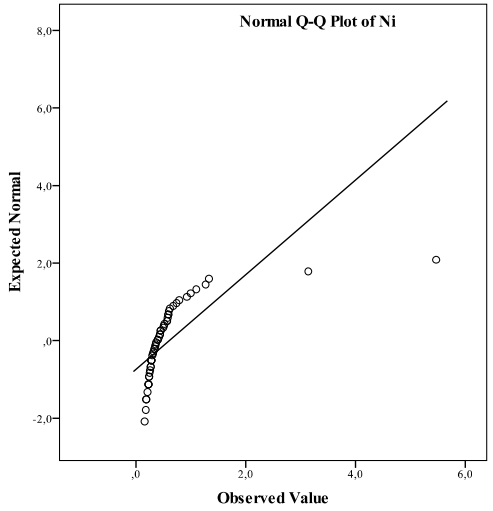

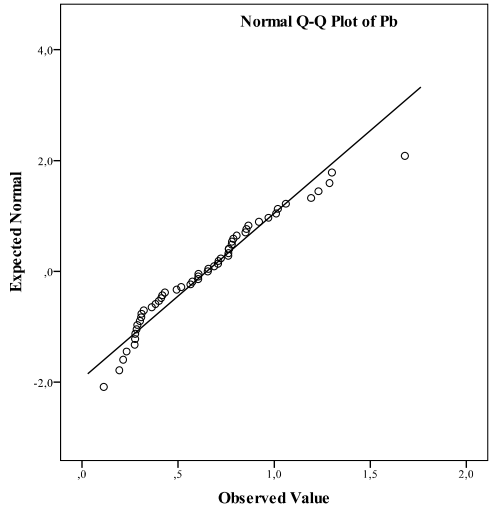

Appendix C: Normal QQ plots for the 0.2m dataset – raw data

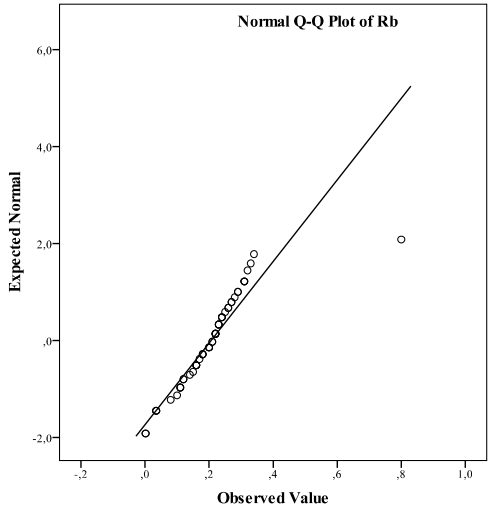

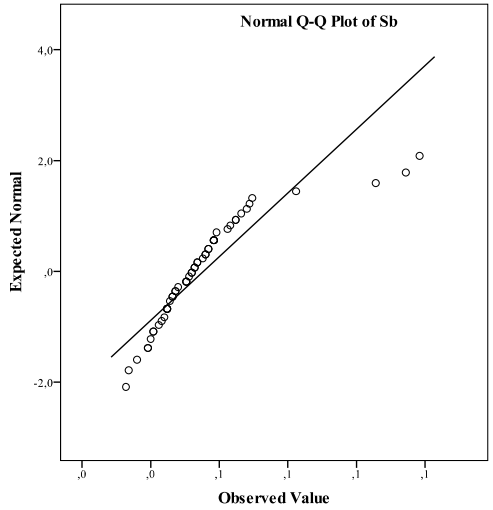

Appendix C: Normal QQ plots for the 0.2m dataset – raw data

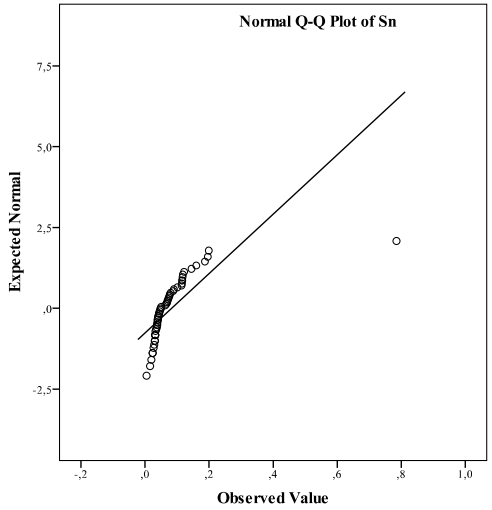

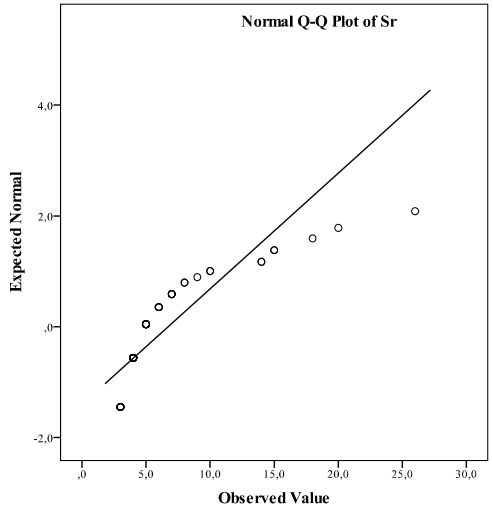

Appendix C: Normal QQ plots for the 0.2m dataset – raw data

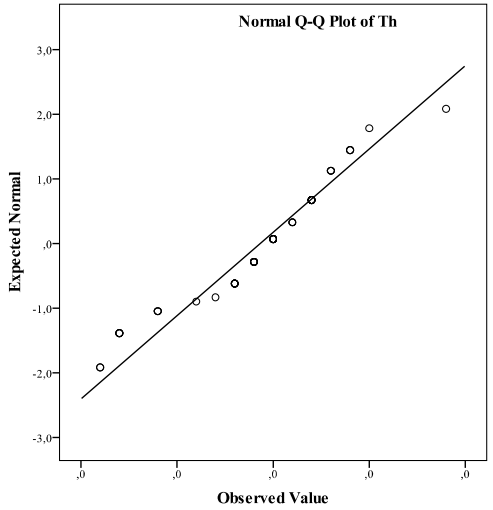

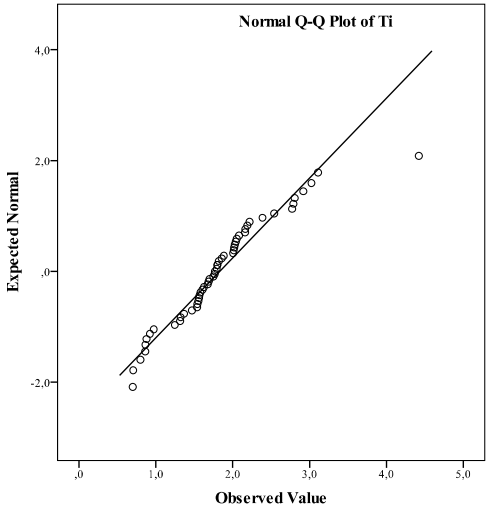

Appendix C: Normal QQ plots for the 0.2m dataset – raw data

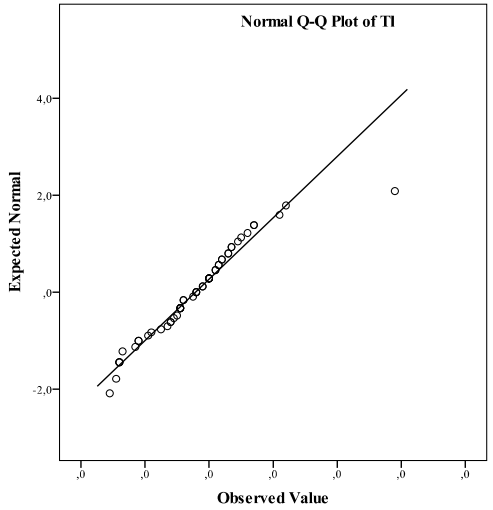

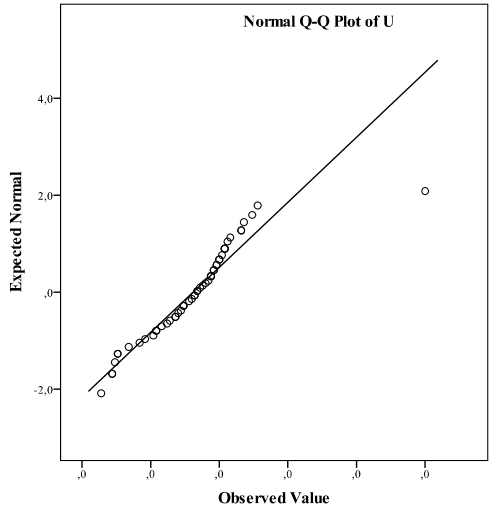

Appendix C: Normal QQ plots for the 0.2m dataset – raw data

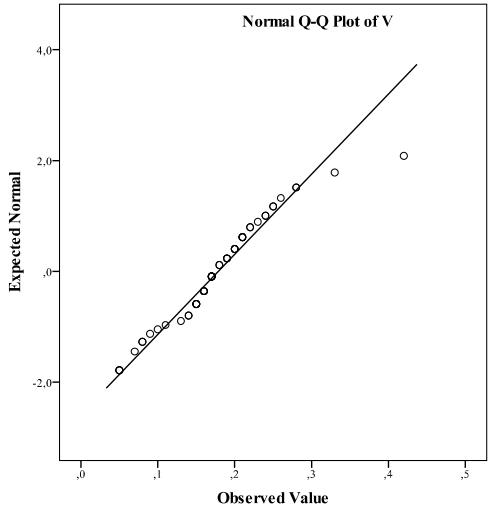

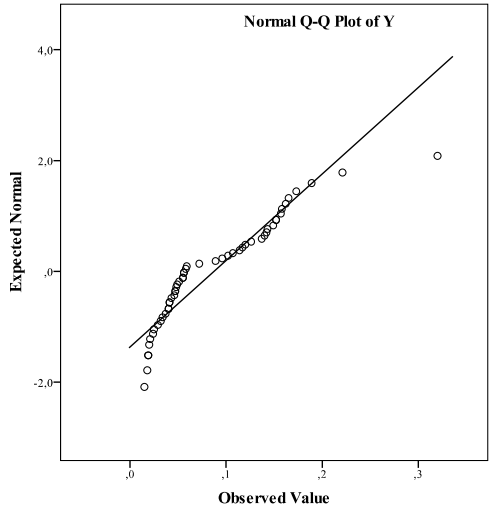

Appendix C: Normal QQ plots for the 0.2m dataset – raw data

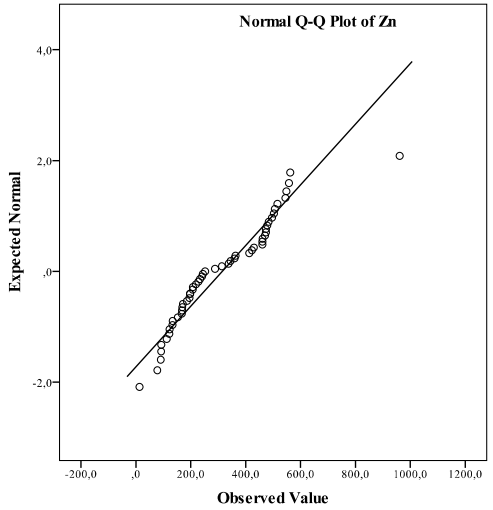

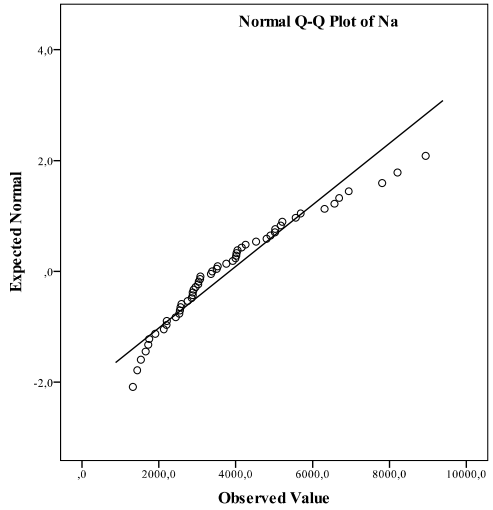

Appendix C: Normal QQ plots for the 0.2m dataset – raw data

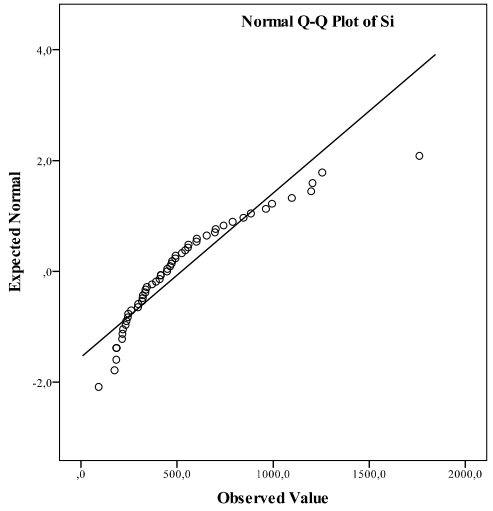

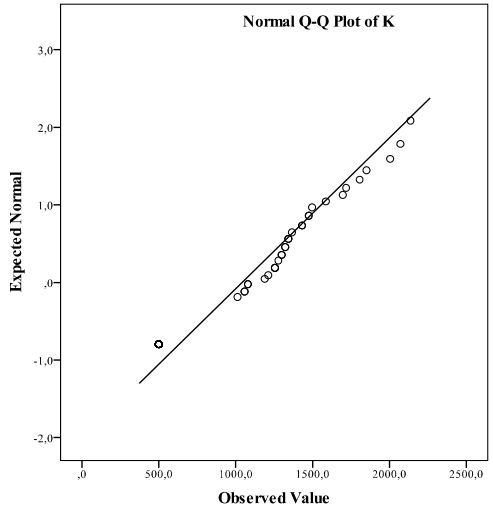

Appendix D: Normal QQ plots for the 1.1m BGS dataset – raw data

Appendix D: Normal QQ plots for the 1.1m BGS dataset – raw data

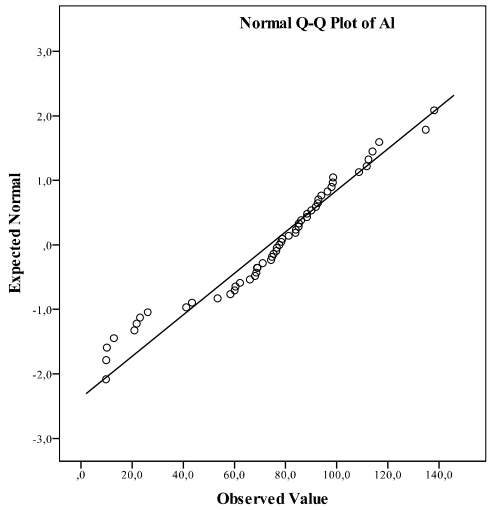

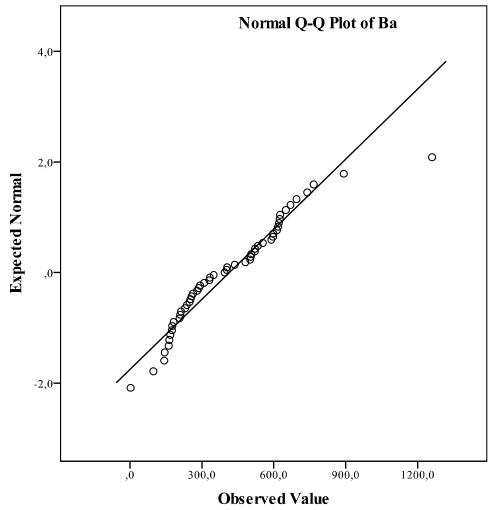

Appendix D: Normal QQ plots for the 1.1m BGS dataset – raw data

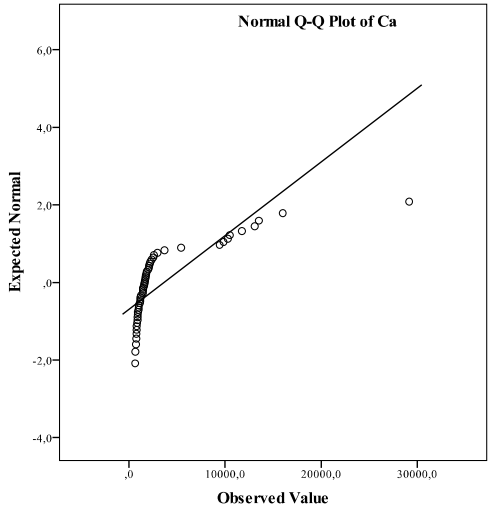

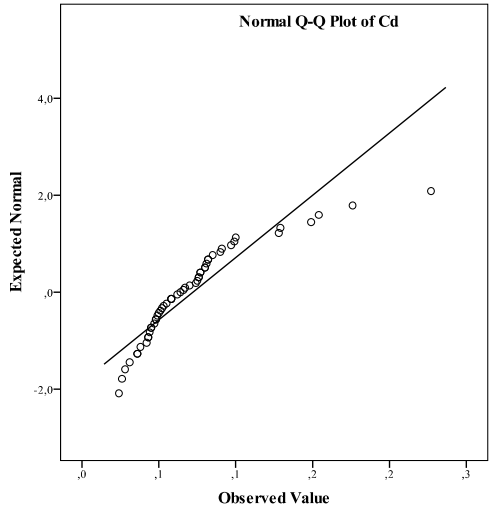

Appendix D: Normal QQ plots for the 1.1m BGS dataset – raw data

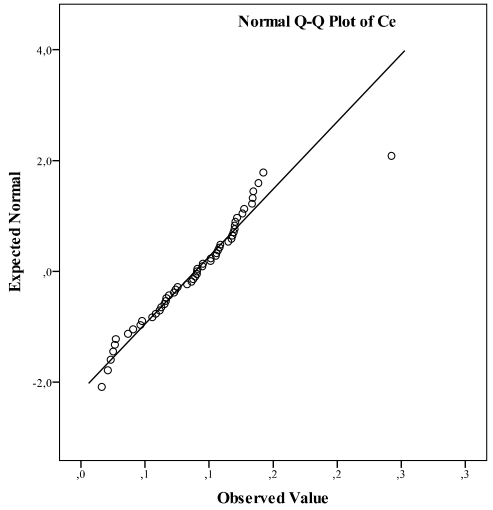

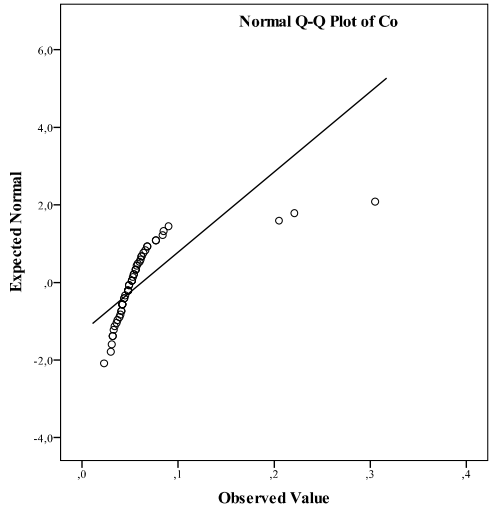

Appendix D: Normal QQ plots for the 1.1m BGS dataset – raw data

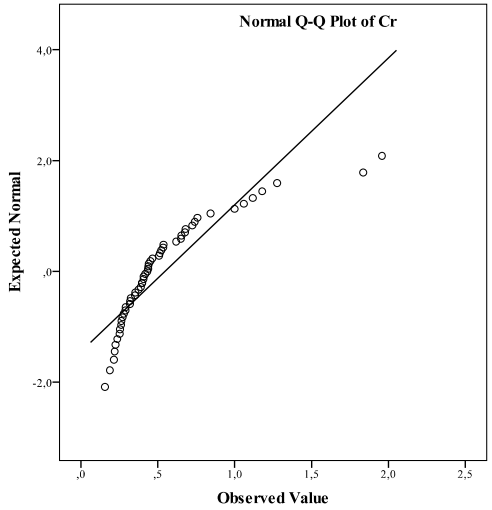

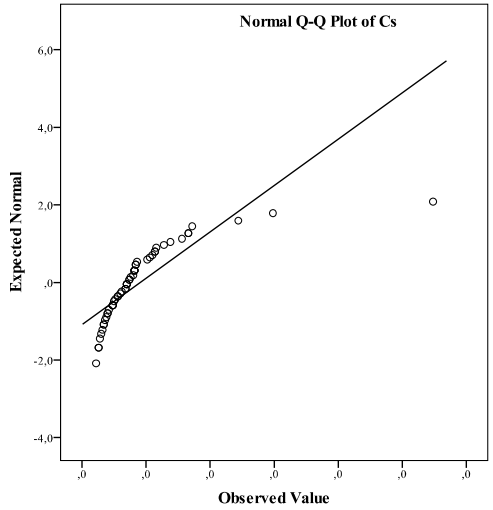

Appendix D: Normal QQ plots for the 1.1m BGS dataset – raw data

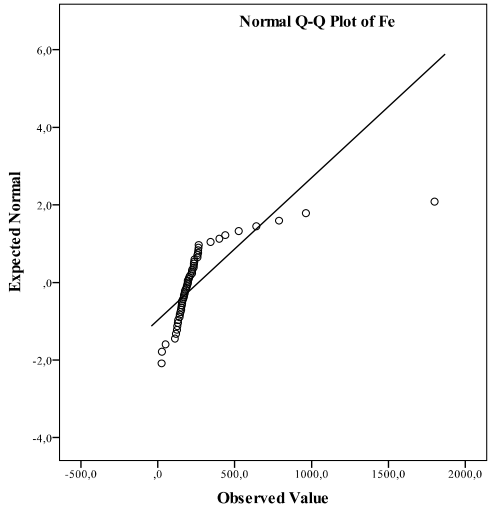

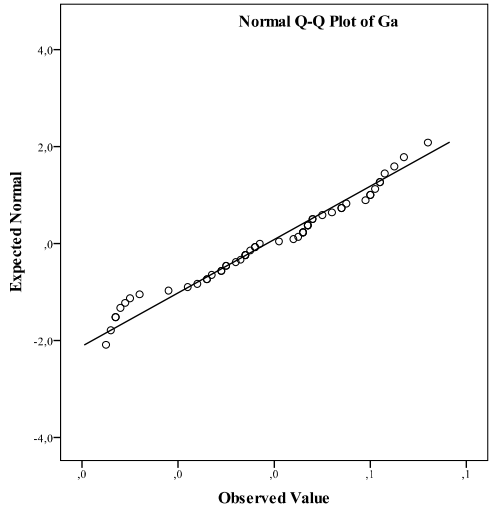

Appendix D: Normal QQ plots for the 1.1m BGS dataset – raw data

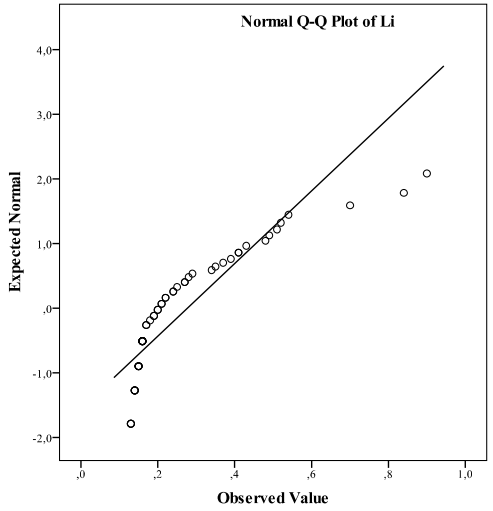

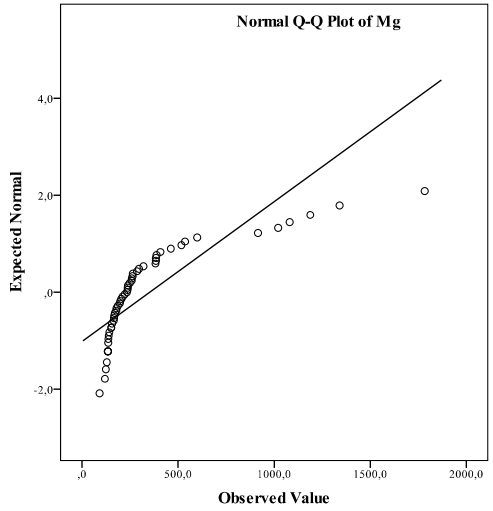

Appendix D: Normal QQ plots for the 1.1m BGS dataset – raw data

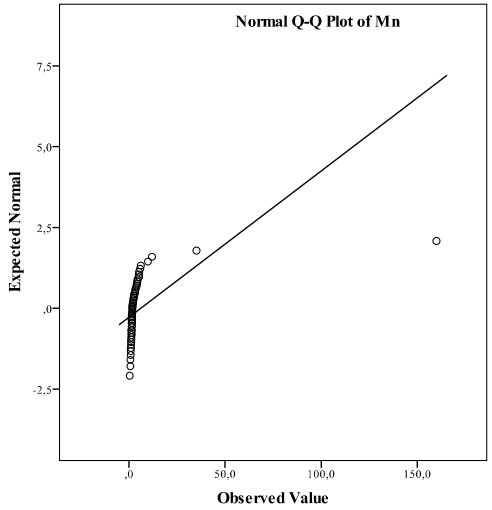

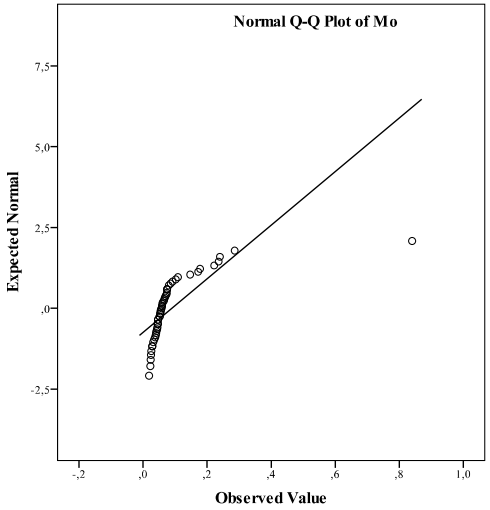

Appendix D: Normal QQ plots for the 1.1m BGS dataset – raw data

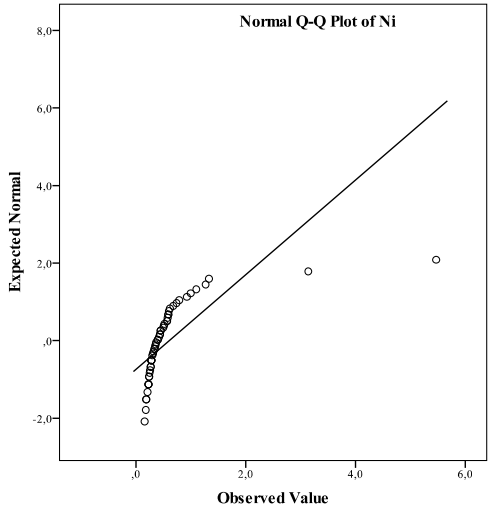

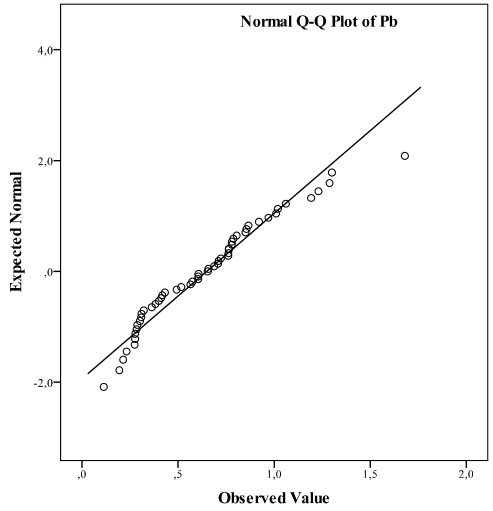

Appendix D: Normal QQ plots for the 1.1m BGS dataset – raw data

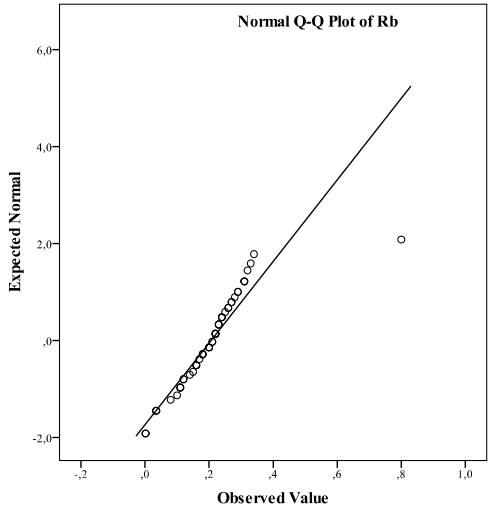

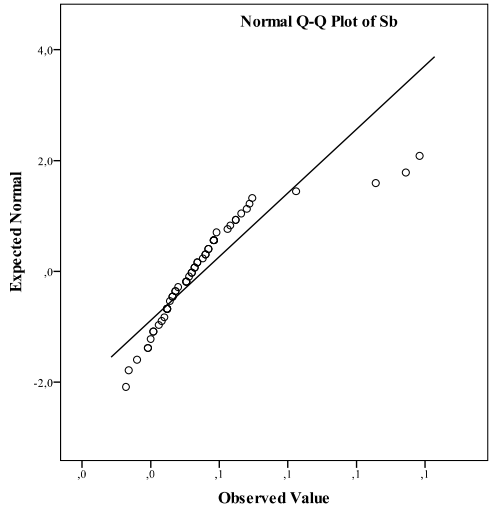

Appendix D: Normal QQ plots for the 1.1m BGS dataset – raw data

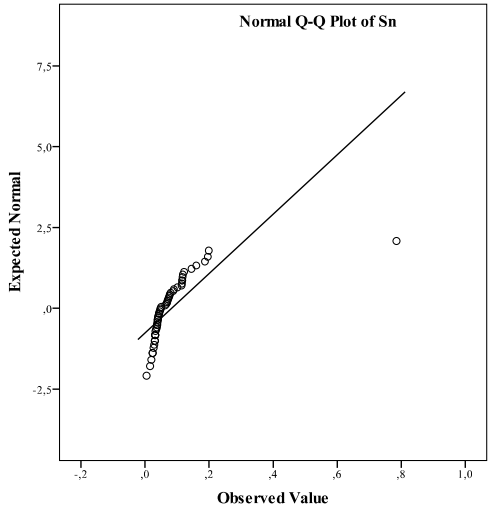

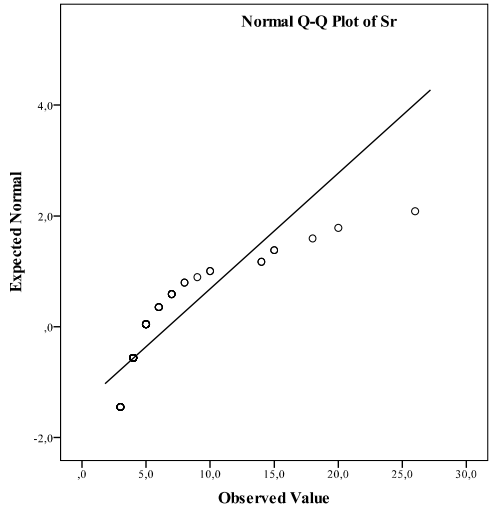

Appendix D: Normal QQ plots for the 1.1m BGS dataset – raw data

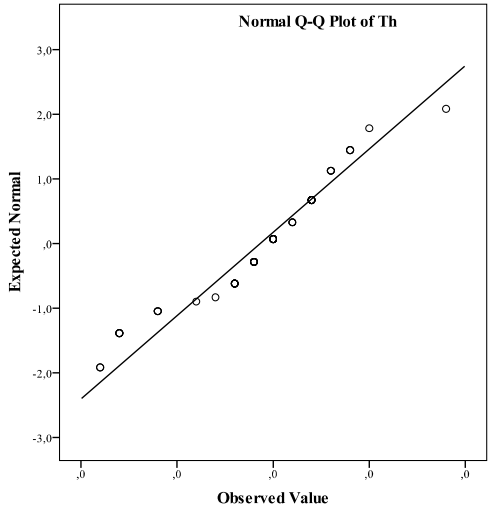

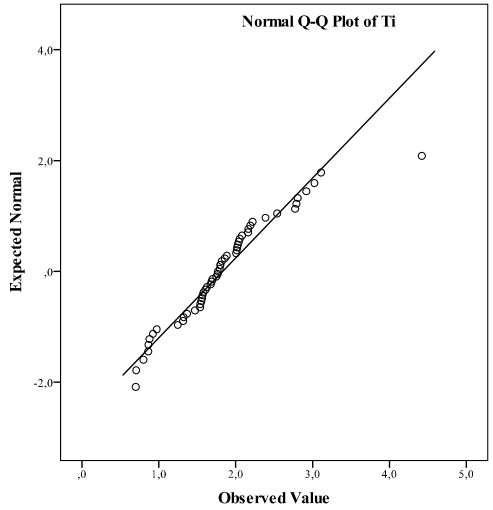

Appendix D: Normal QQ plots for the 1.1m BGS dataset – raw data

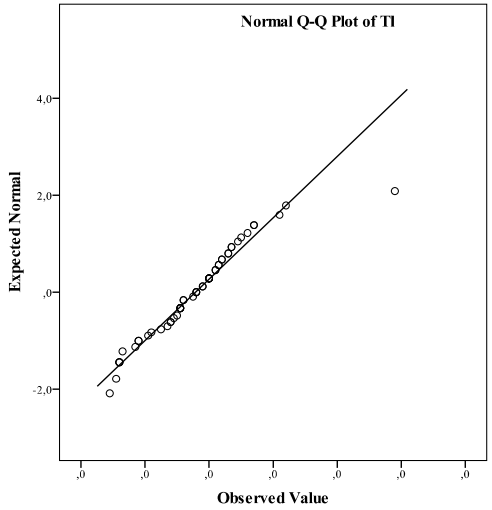

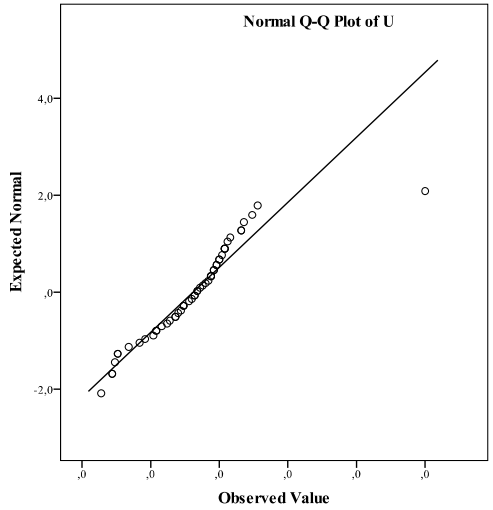

Appendix D: Normal QQ plots for the 1.1m BGS dataset – raw data

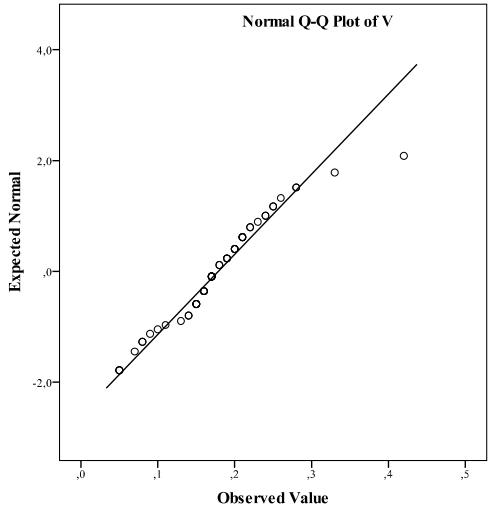

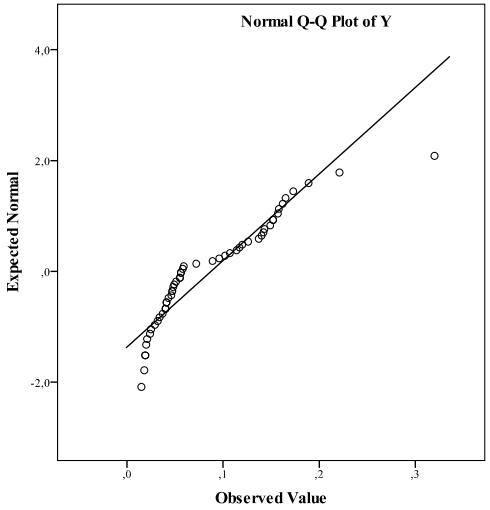

Appendix D: Normal QQ plots for the 1.1m BGS dataset – raw data

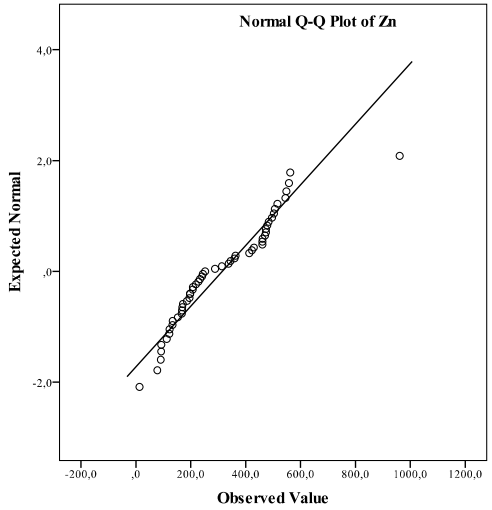

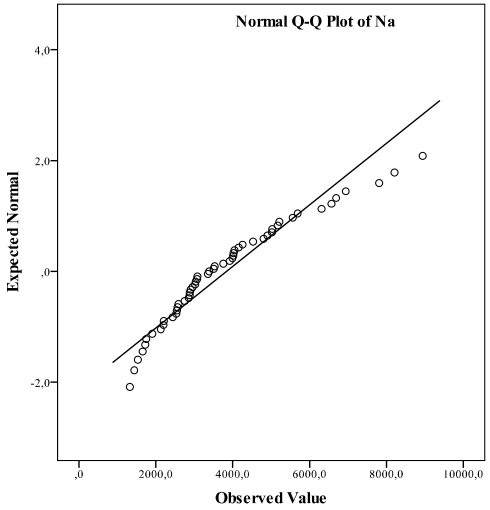

Appendix D: Normal QQ plots for the 1.1m BGS dataset – raw data

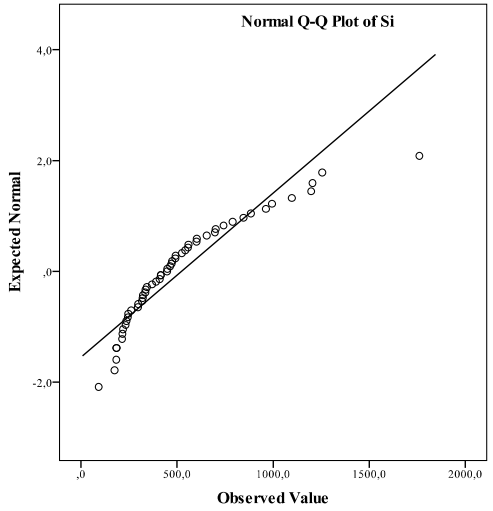

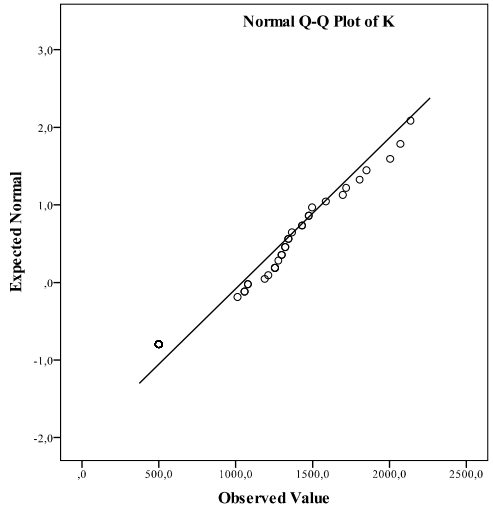

Appendix E: Normal QQ plots for the 0.2m BGS dataset – processed data

Appendix E: Normal QQ plots for the 0.2m BGS dataset – processed data

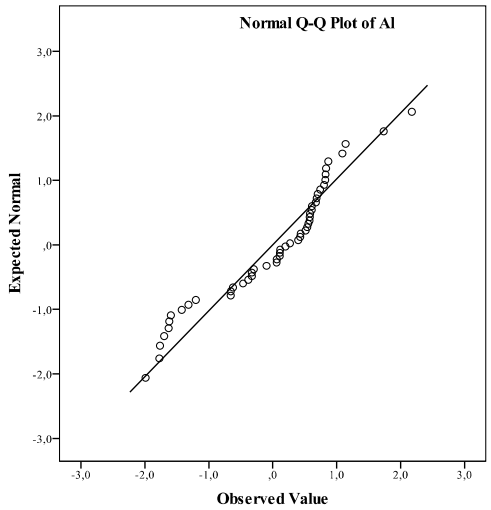

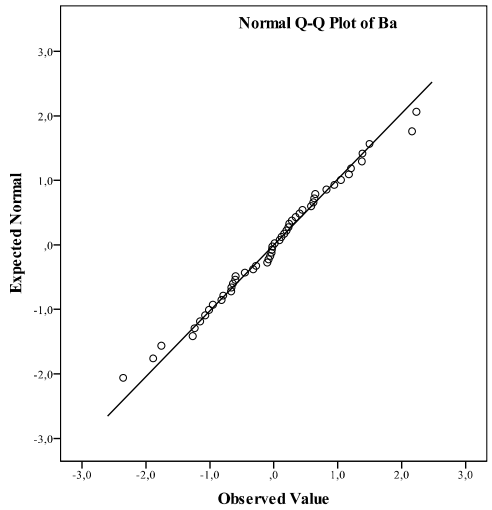

Appendix E: Normal QQ plots for the 0.2m BGS dataset – processed data

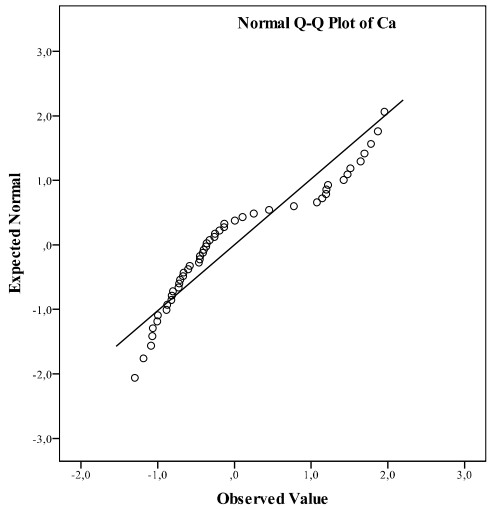

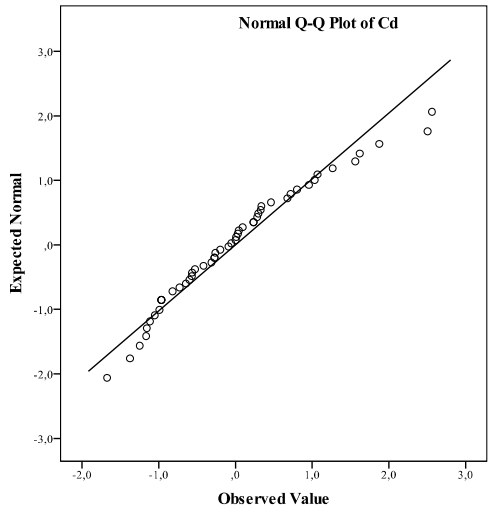

Appendix E: Normal QQ plots for the 0.2m BGS dataset – processed data

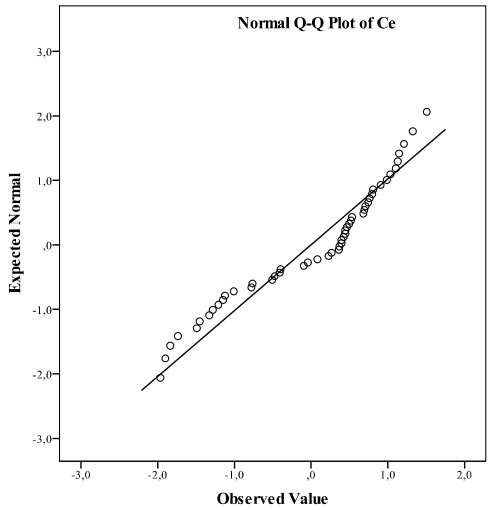

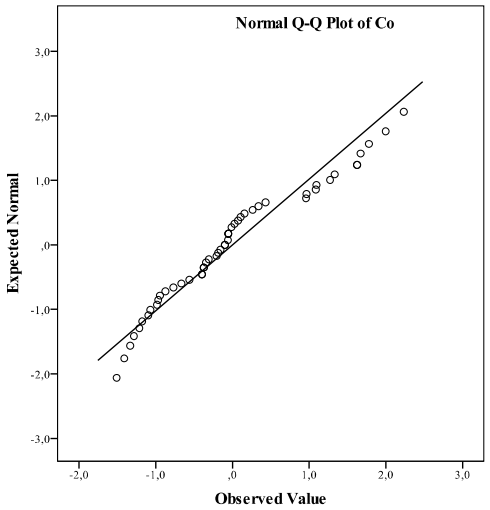

Appendix E: Normal QQ plots for the 0.2m BGS dataset – processed data

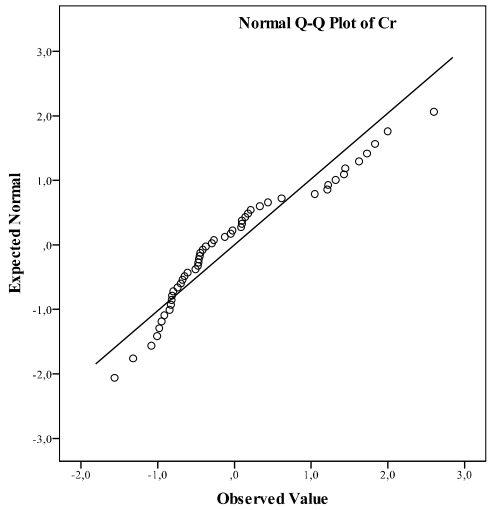

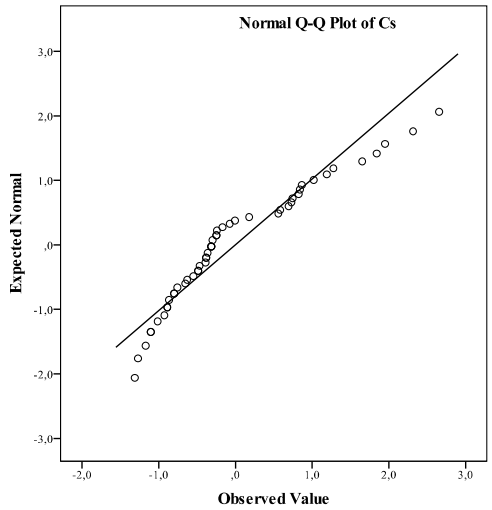

Appendix E: Normal QQ plots for the 0.2m BGS dataset – processed data

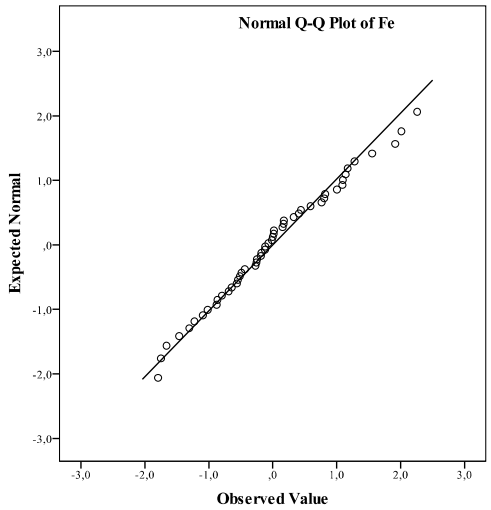

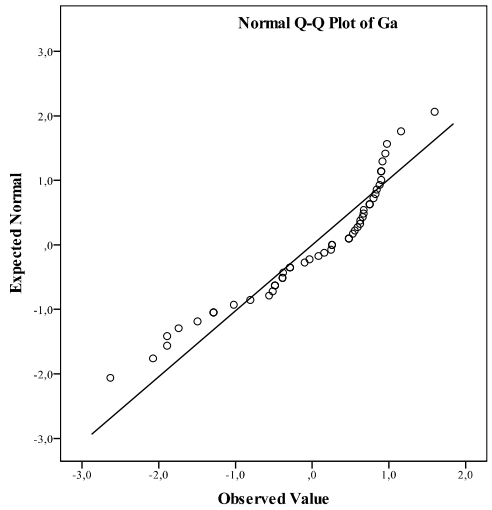

Appendix E: Normal QQ plots for the 0.2m BGS dataset – processed data

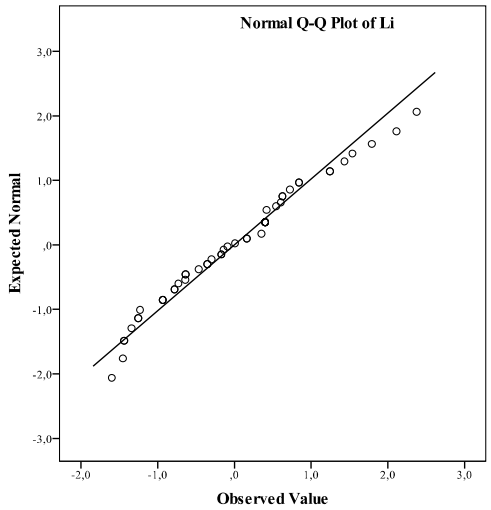

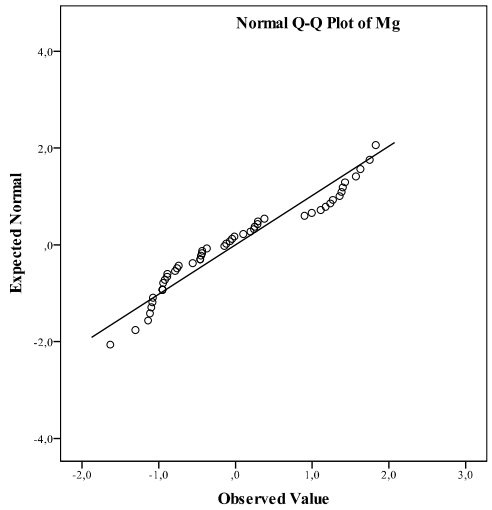

Appendix E: Normal QQ plots for the 0.2m BGS dataset – processed data

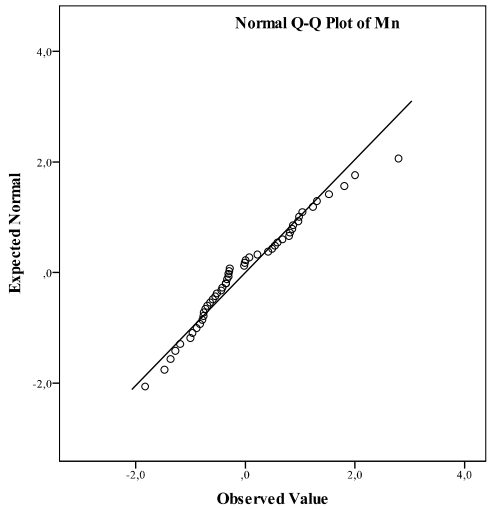

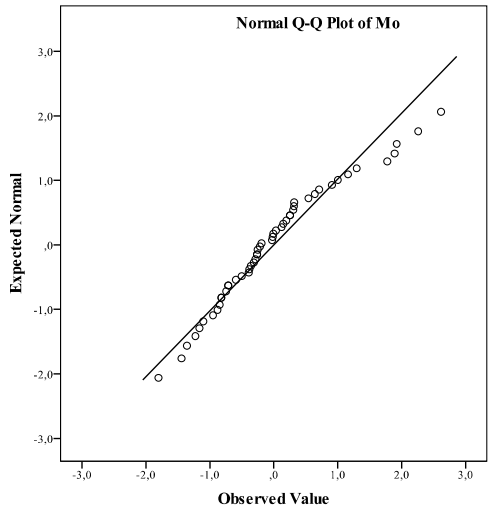

Appendix E: Normal QQ plots for the 0.2m BGS dataset – processed data

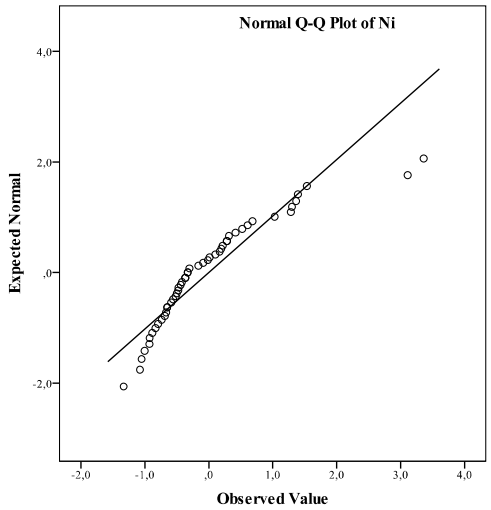

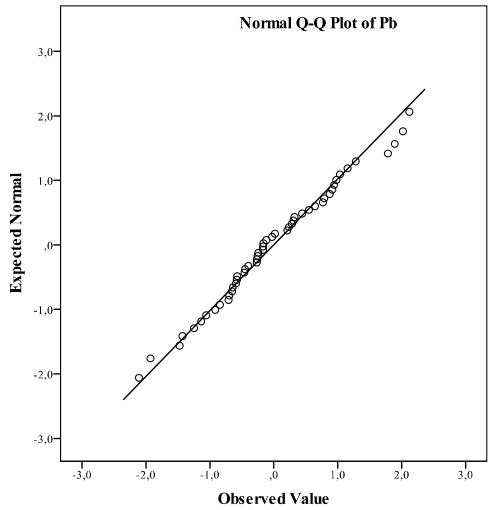

Appendix E: Normal QQ plots for the 0.2m BGS dataset – processed data

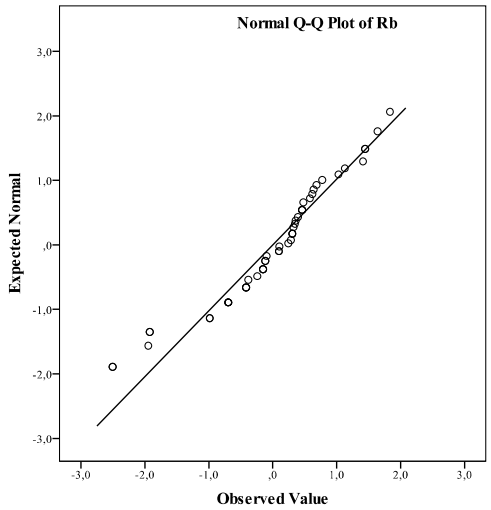

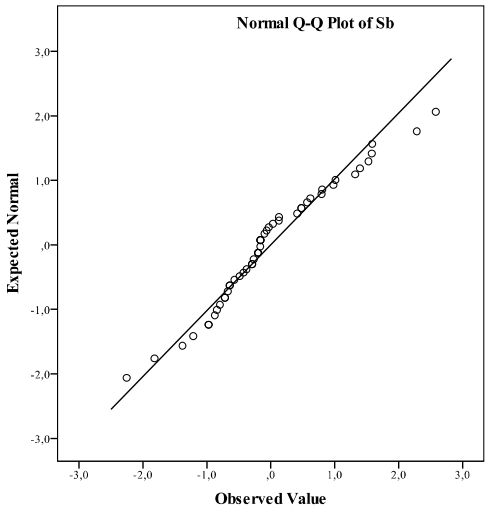

Appendix E: Normal QQ plots for the 0.2m BGS dataset – processed data

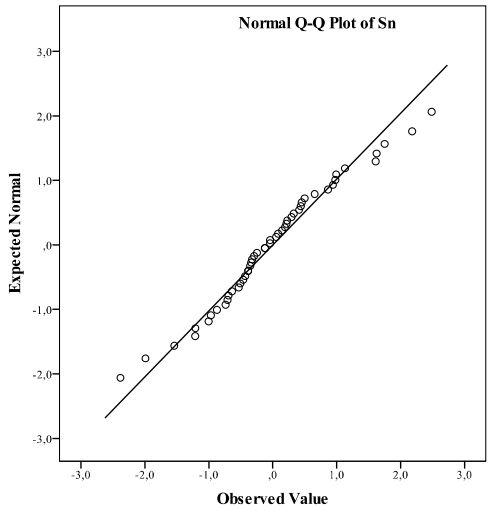

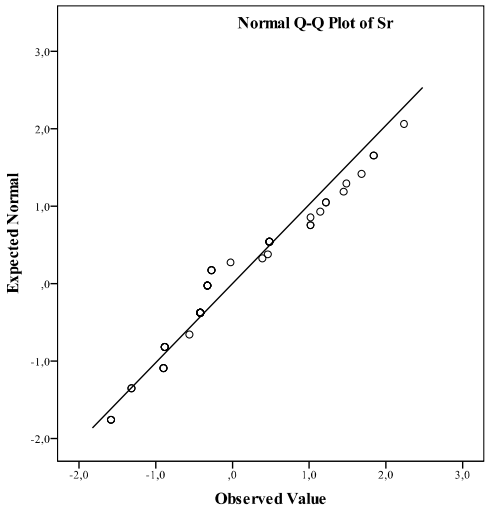

Appendix E: Normal QQ plots for the 0.2m BGS dataset – processed data

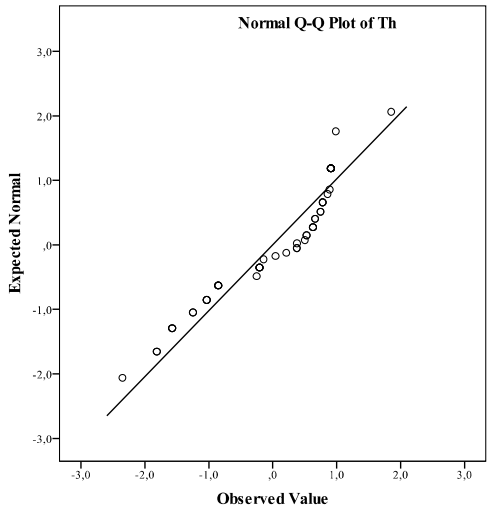

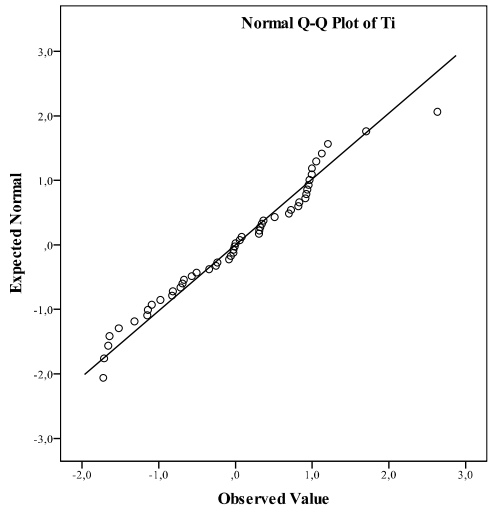

Appendix E: Normal QQ plots for the 0.2m BGS dataset – processed data

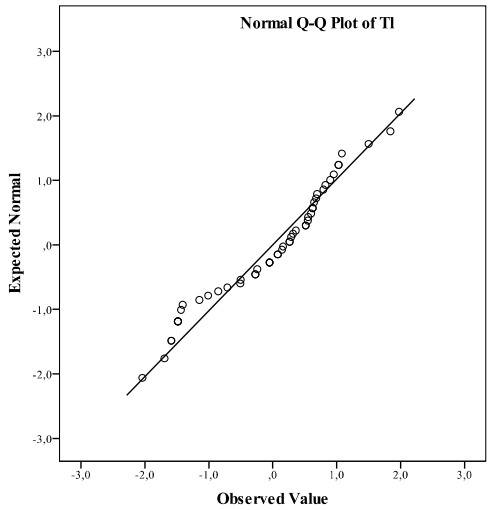

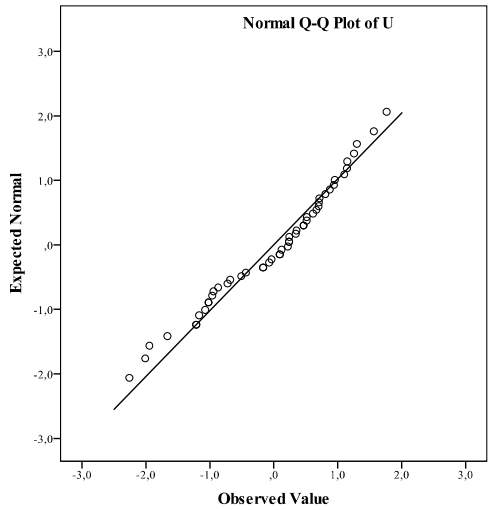

Appendix E: Normal QQ plots for the 0.2m BGS dataset – processed data

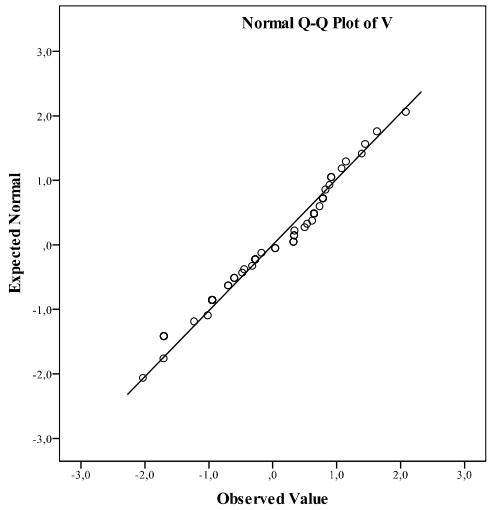

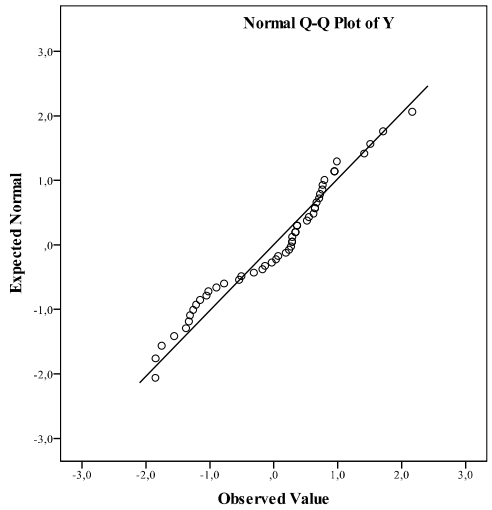

Appendix E: Normal QQ plots for the 0.2m BGS dataset – processed data

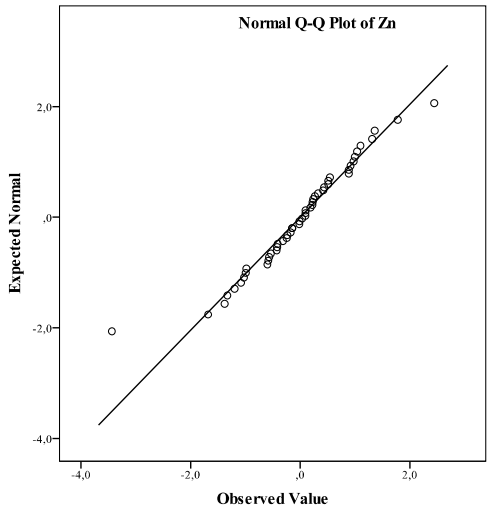

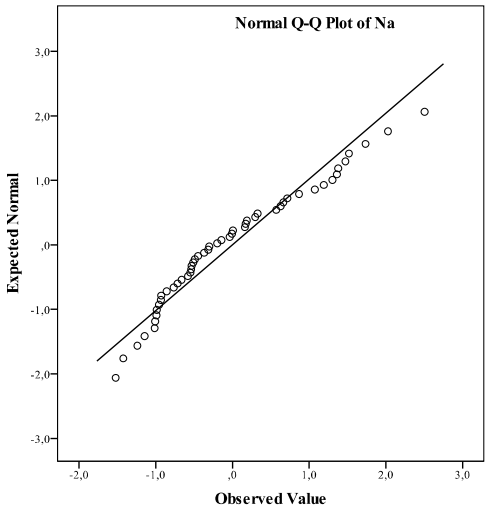

Appendix E: Normal QQ plots for the 0.2m BGS dataset – processed data

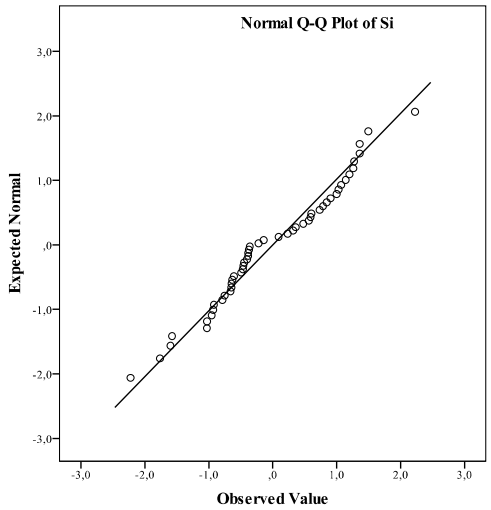

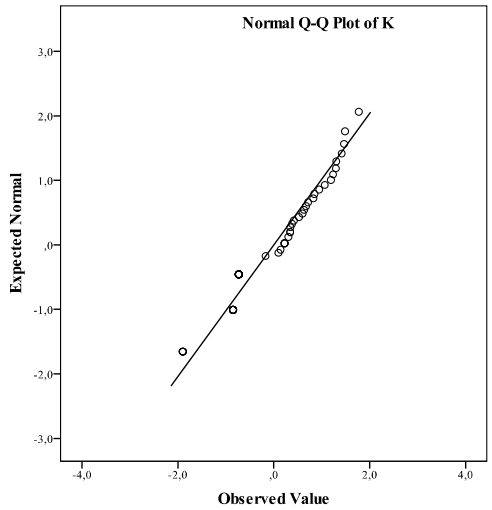

Appendix F: Normal QQ plots for the 1.1m BGS dataset – processed data

Appendix F: Normal QQ plots for the 1.1m BGS dataset – processed data

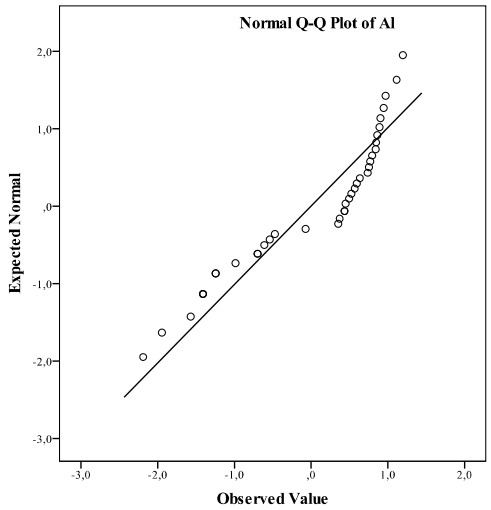

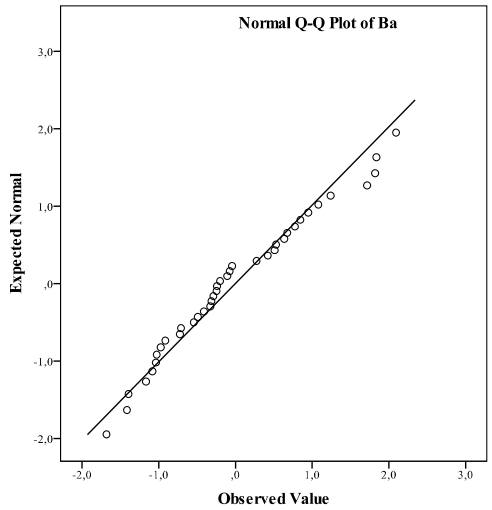

Appendix F: Normal QQ plots for the 1.1m BGS dataset – processed data

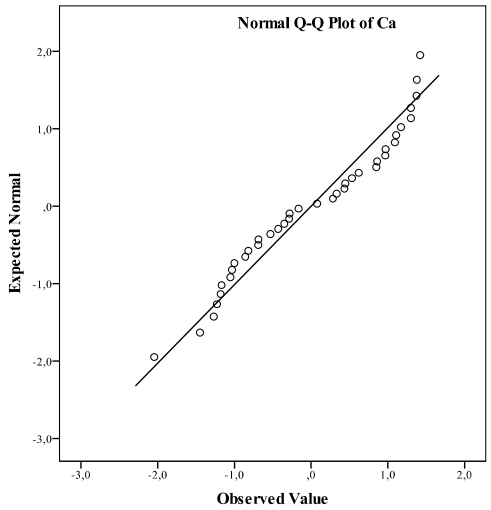

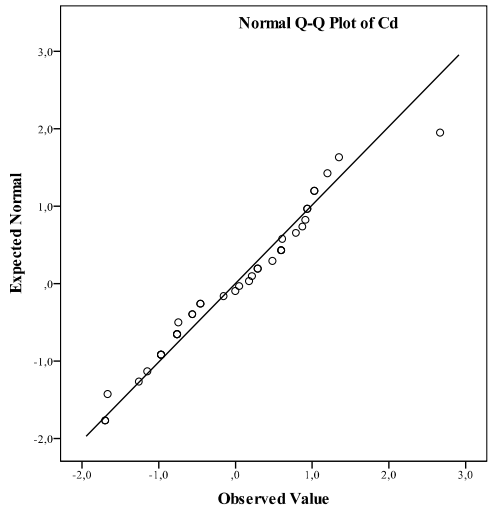

Appendix F: Normal QQ plots for the 1.1m BGS dataset – processed data

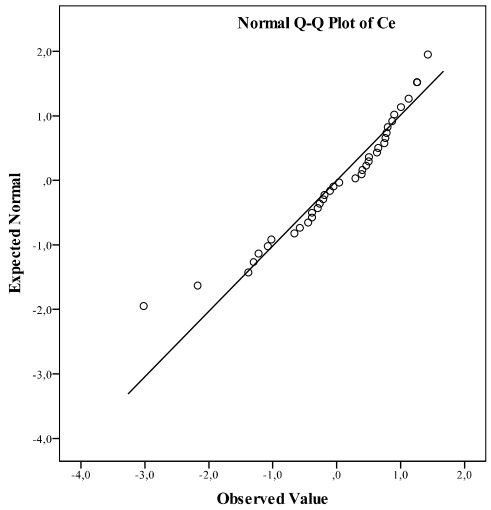

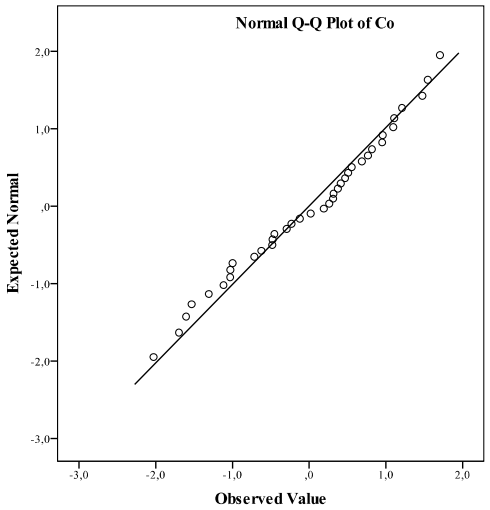

Appendix F: Normal QQ plots for the 1.1m BGS dataset – processed data

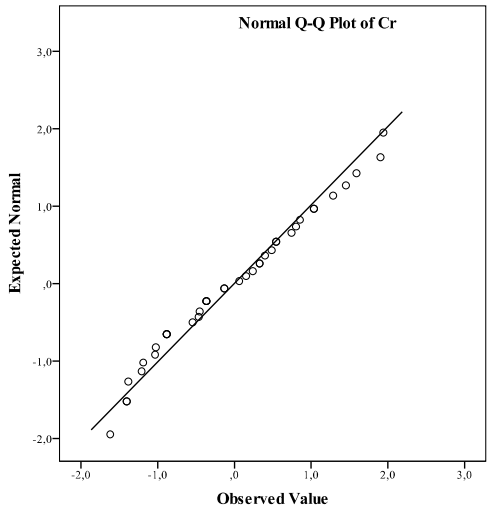

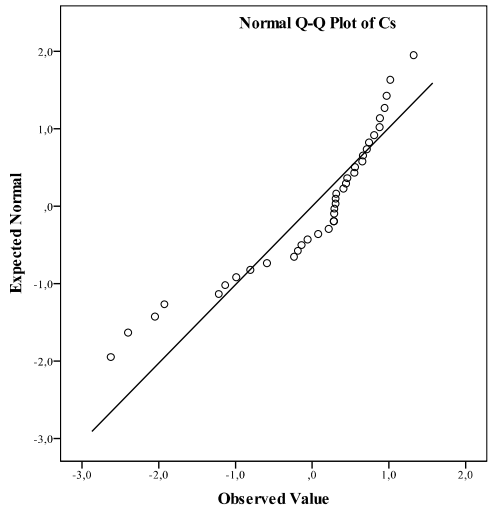

Appendix F: Normal QQ plots for the 1.1m BGS dataset – processed data

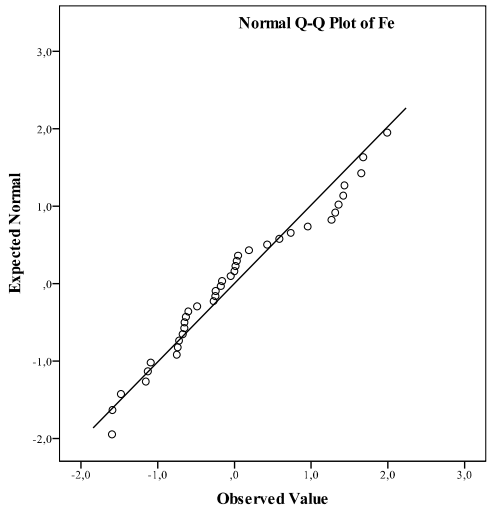

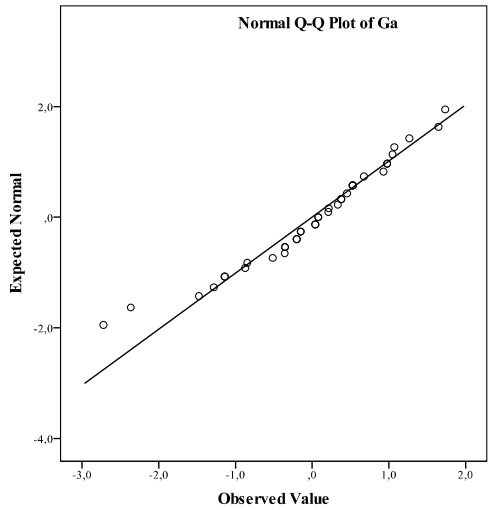

Appendix F: Normal QQ plots for the 1.1m BGS dataset – processed data

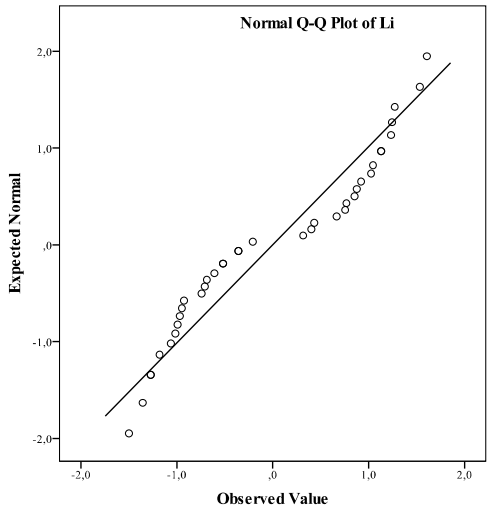

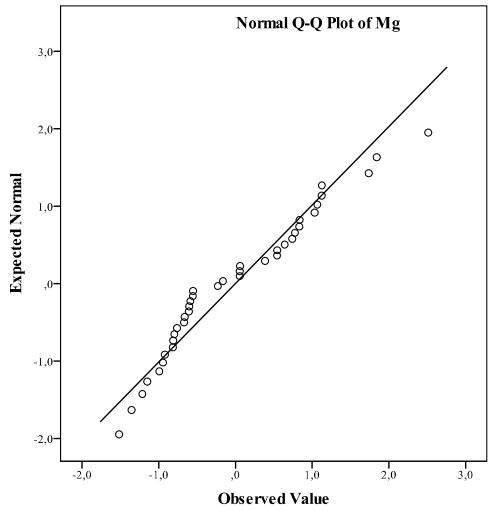

Appendix F: Normal QQ plots for the 1.1m BGS dataset – processed data

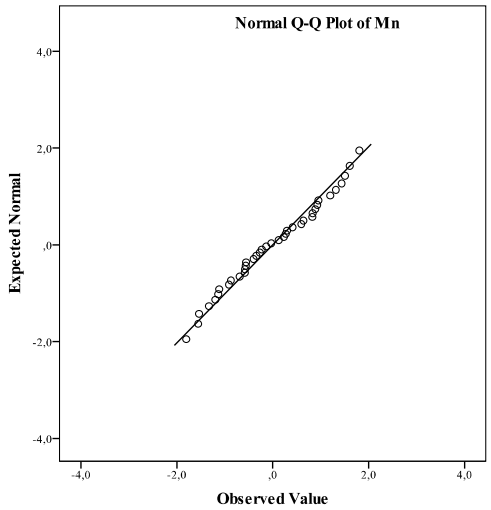

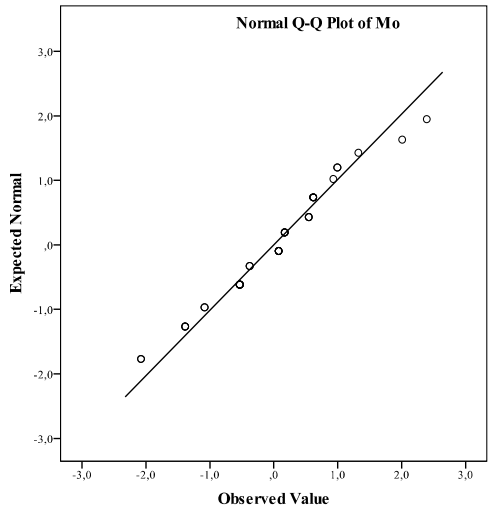

Appendix F: Normal QQ plots for the 1.1m BGS dataset – processed data

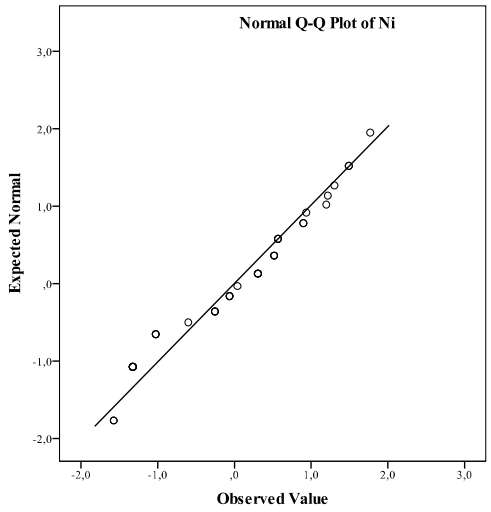

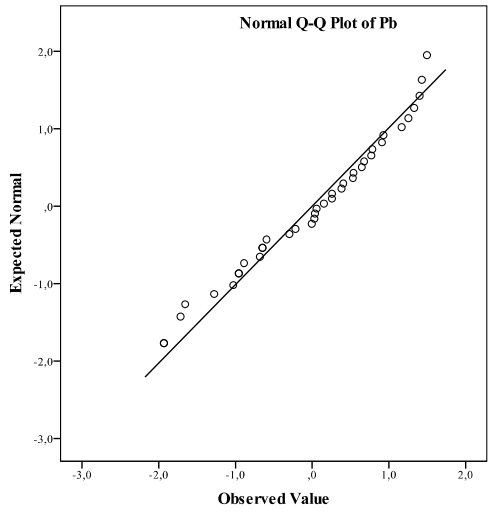

Appendix F: Normal QQ plots for the 1.1m BGS dataset – processed data

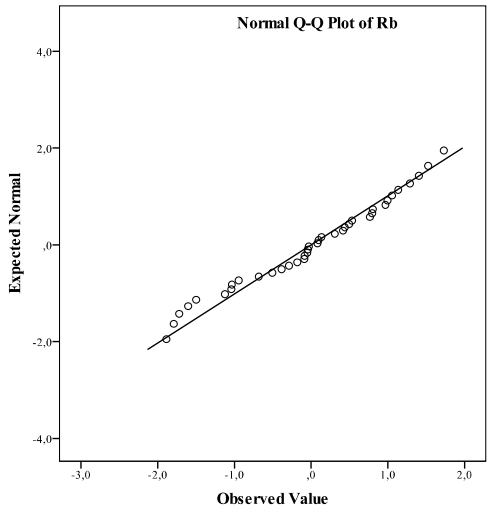

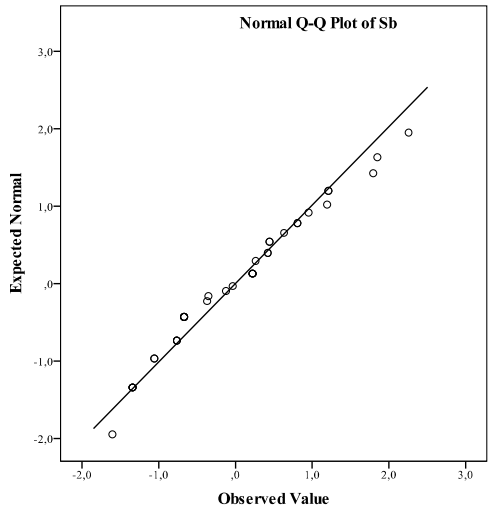

Appendix F: Normal QQ plots for the 1.1m BGS dataset – processed data

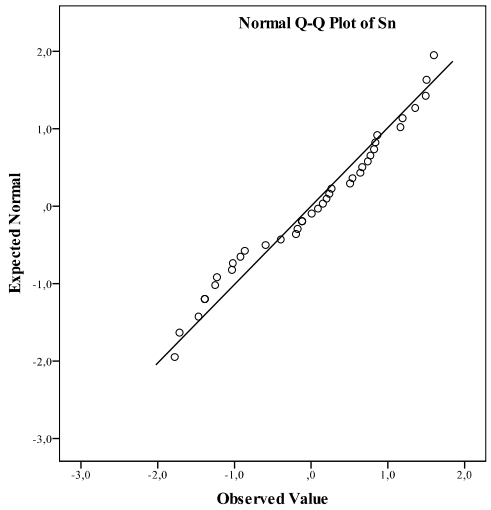

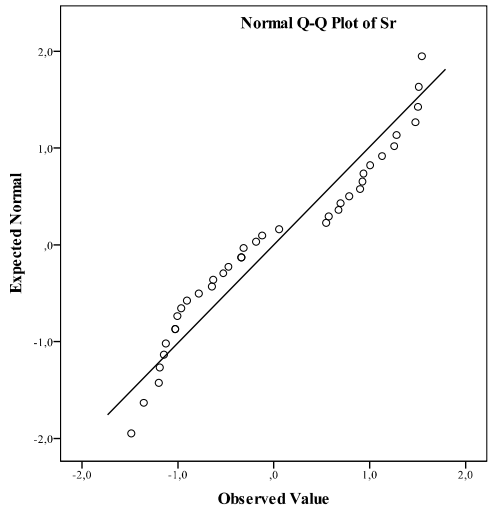

Appendix F: Normal QQ plots for the 1.1m BGS dataset – processed data

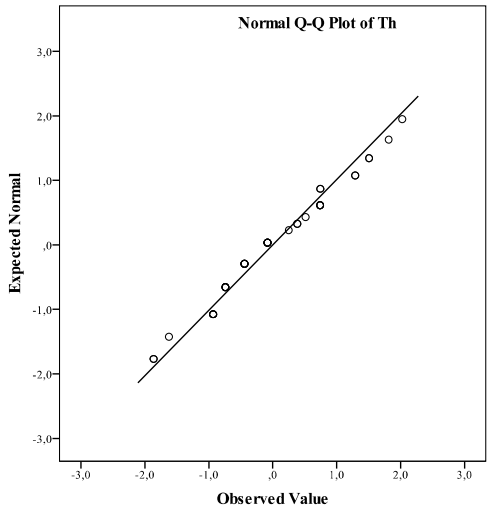

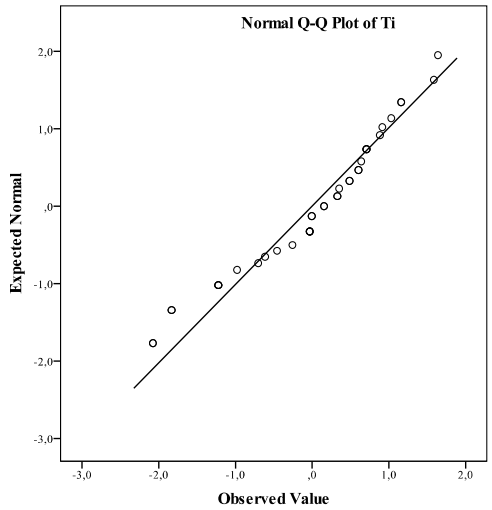

Appendix F: Normal QQ plots for the 1.1m BGS dataset – processed data

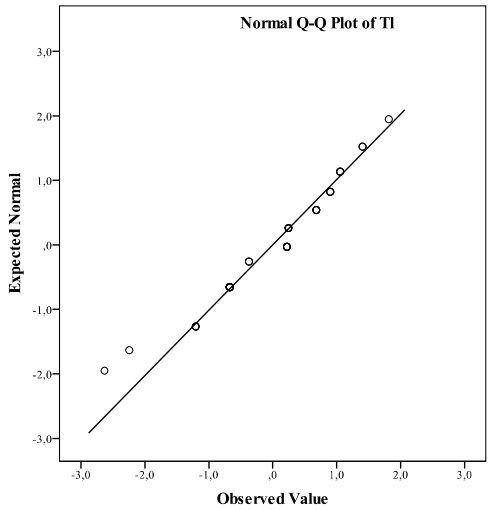

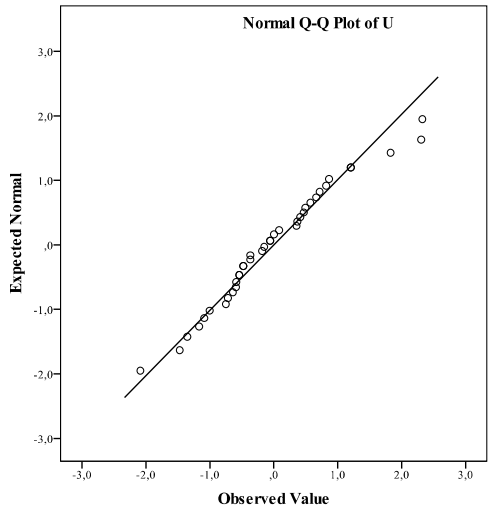

Appendix F: Normal QQ plots for the 1.1m BGS dataset – processed data

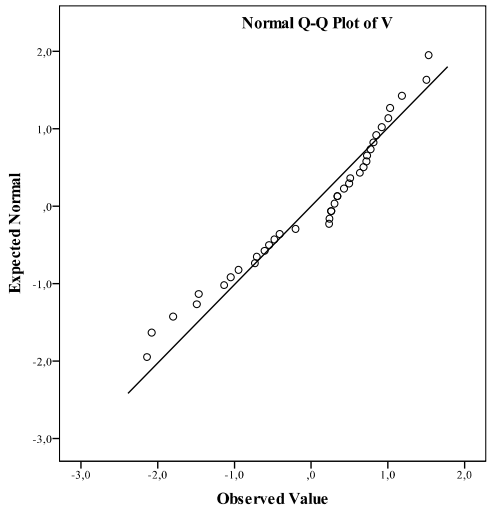

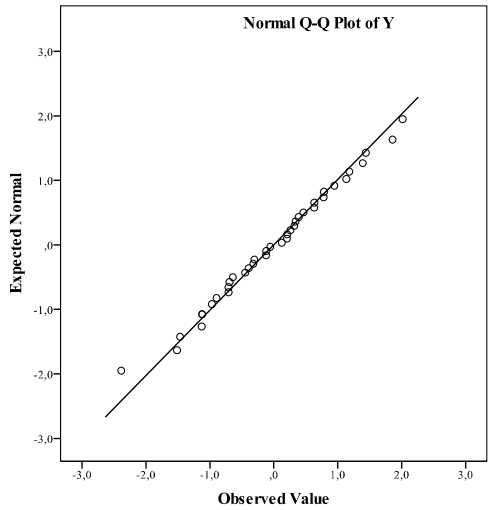

Appendix F: Normal QQ plots for the 1.1m BGS dataset – processed data

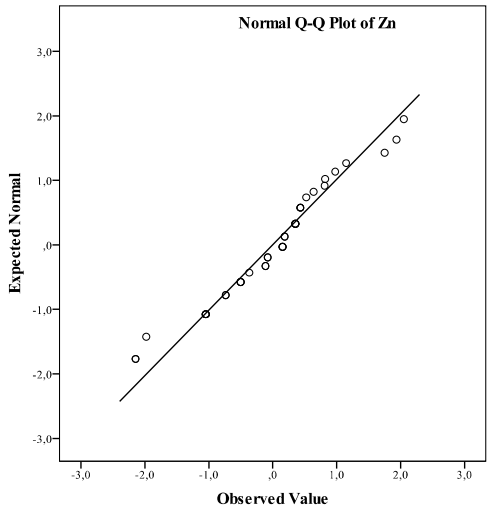

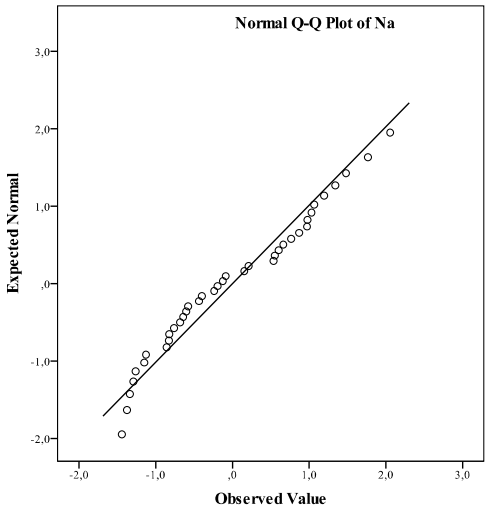

Appendix F: Normal QQ plots for the 1.1m BGS dataset – processed data